U N I K A S S E L
V E R S I T Ä T

Institut für Werkstofftechnik
Metallische Werkstoffe
Prof. Dr.-Ing. Thomas Niendorf

Process-microstructure-property relationships in Ni- and Fe-based alloys processed by AM

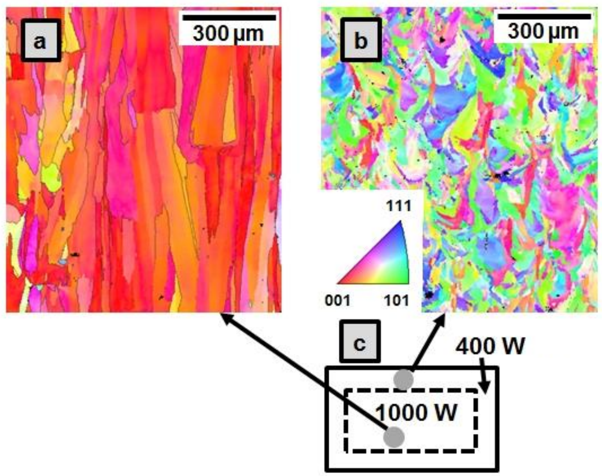

Alloys for Additive Manufacturing Workshop
MPIE Düsseldorf

Prof. Dr.-Ing. Thomas Niendorf
July 2016

Emmy Noether-Programm
DFG Deutsche Forschungsgemeinschaft

Research Partners

Metals Group

Institute of Materials Engineering

Materials Science & Engineering, Institute I

Agenda

1. Stainless steel 316L
2. Ni-based alloy IN 718
3. High-Mn Fe-based alloys

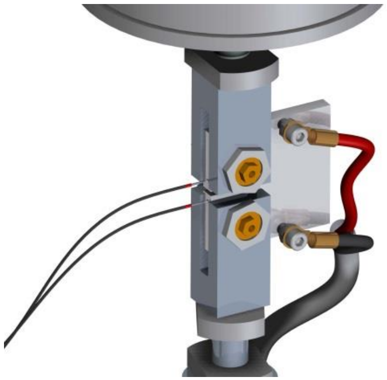

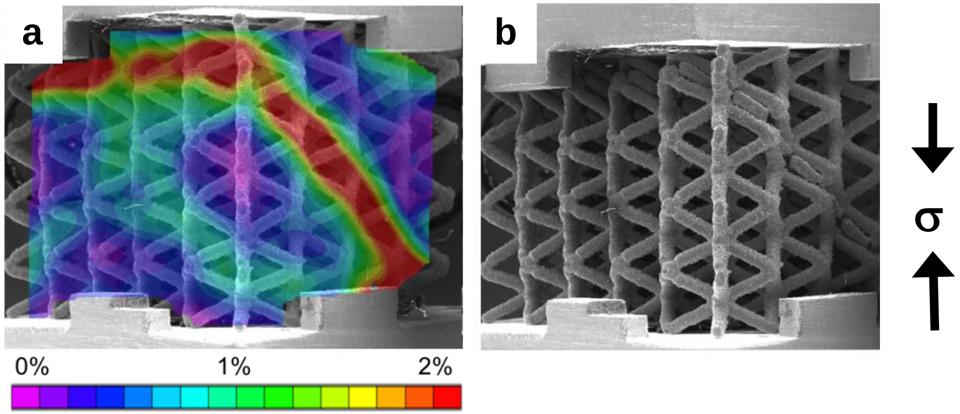

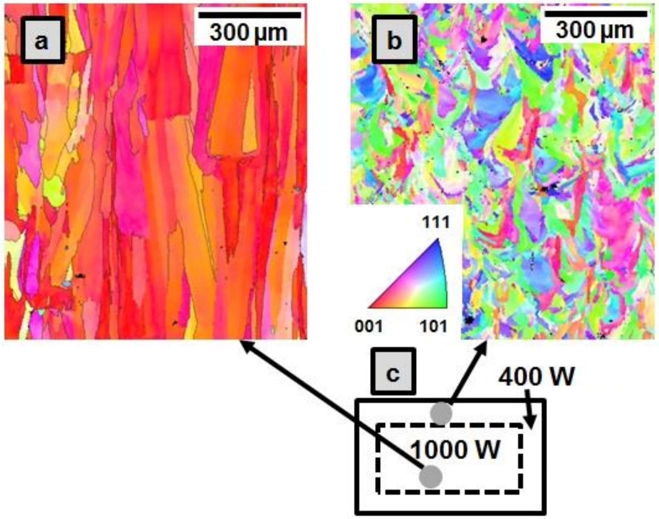

Agenda

1. Stainless steel 316L

2. Ni-based alloy IN 718

3. High-Mn Fe-based alloys

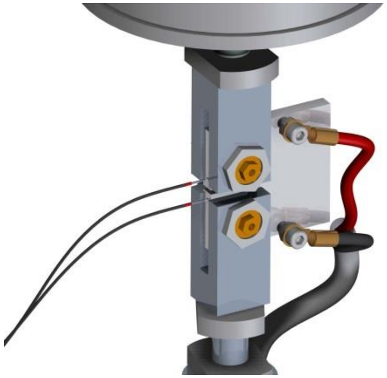

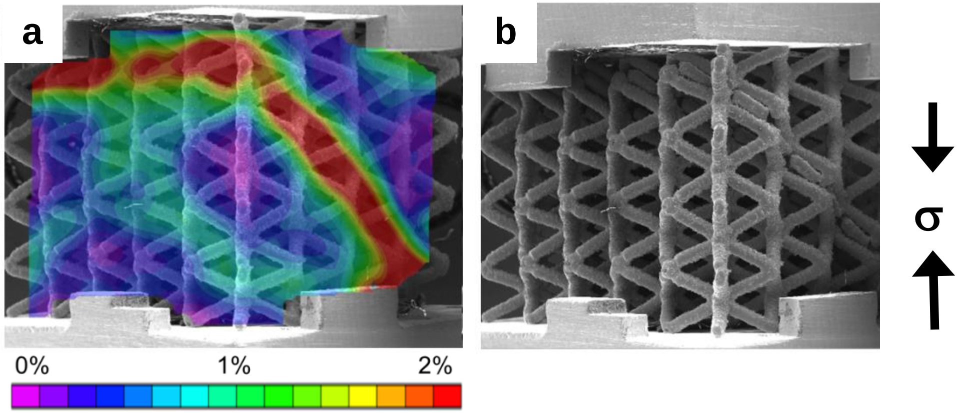

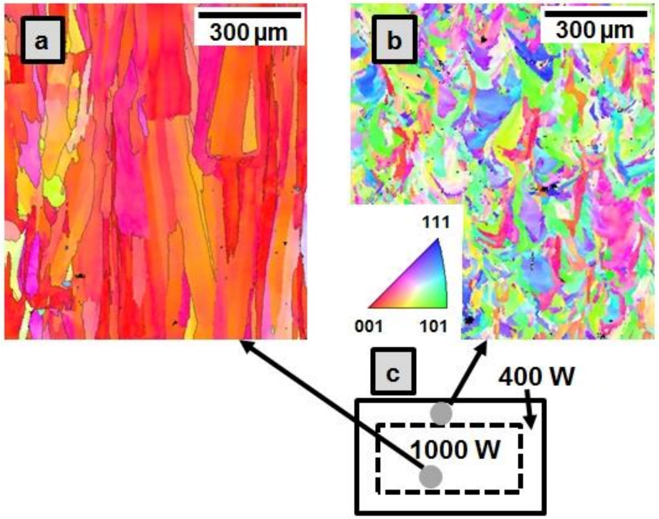

Stainless steel 316L

Melting system: ***SLM 250^{HL} (SLM Solutions)***
- ***400W fibre laser***
- ***Argon atmosphere***

Tested material: ***Stainless steel 316L***
- ***Layer thickness: 30µm***
- ***Average particle size: 40µm***
- ***Platform temperature: 100°C***

Treatment	1 (as-built)	2 (650°C)	3 (HIP)
Temperature [°C]	20	650	1150 (1000 bar)
Time [h]	-	2	4
Atmosphere	-	Argon	Argon

Microstructure

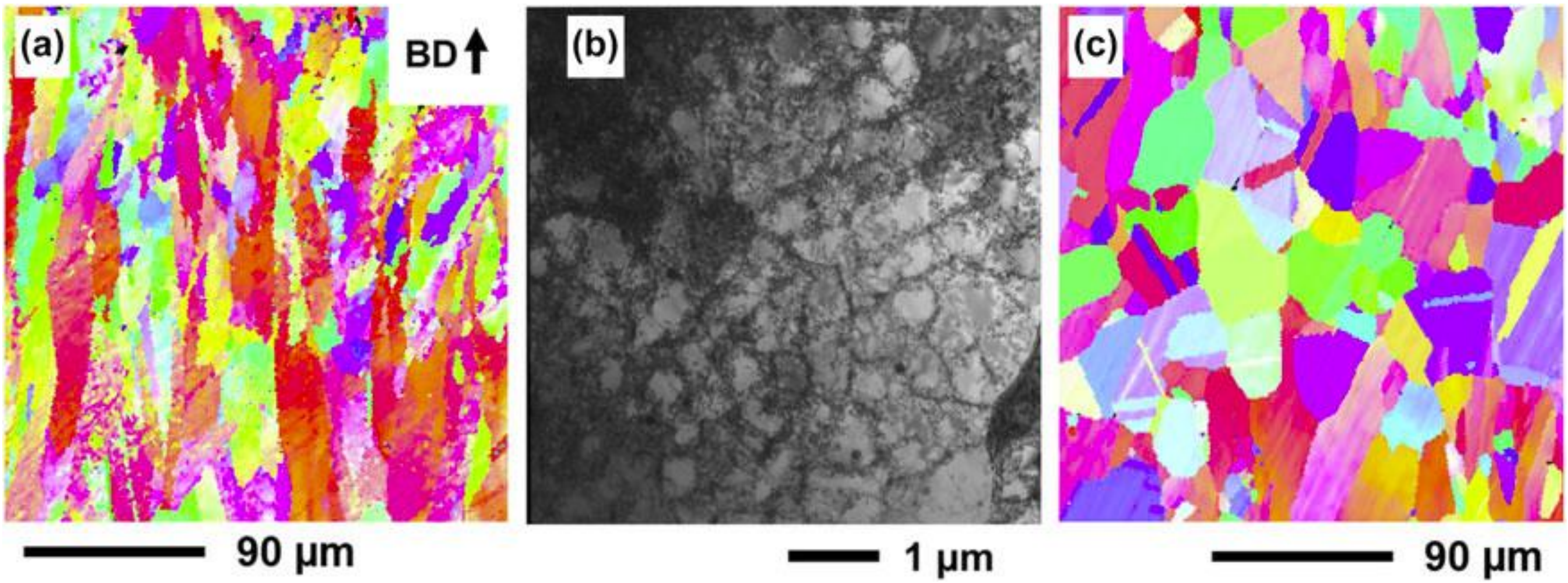

EBSD IPF | TEM | EBSD IPF

As-built | HIP

 S. Leuders, et al., J. Mater. Res. 29, 2014, 1911-1919.

Stainless steel 316L

Tensile tests:

- *in accordance with ISO6892-1:2009*
- *as-built surface*
- *displacement controlled (5mm/min)*
- *tests performed on testing machine Instron 5569*
- *at ambient conditions*

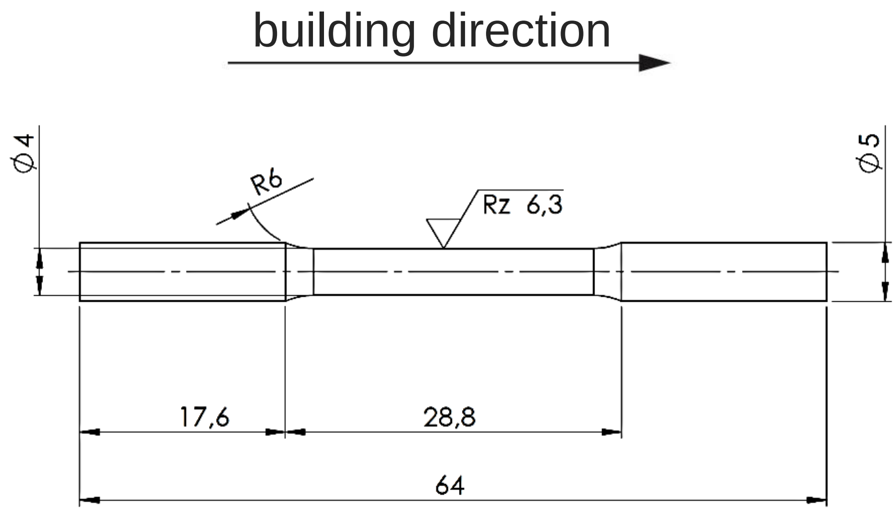

condition	UTS / MPa	YS / MPa	ε_f / %
as-built/SLM surface	565 ±5 MPa	462 ±5 MPa	53.7 ±2.6 %
650 °C/turned surface	595 ±5 MPa	443 ±5 MPa	48.6 ±2.6 %
traditionally processed	530-680	220	≈ 40

A. Riemer et al., Eng. Fract. Mech. 120, 2014, 15-25.

Tensile tests

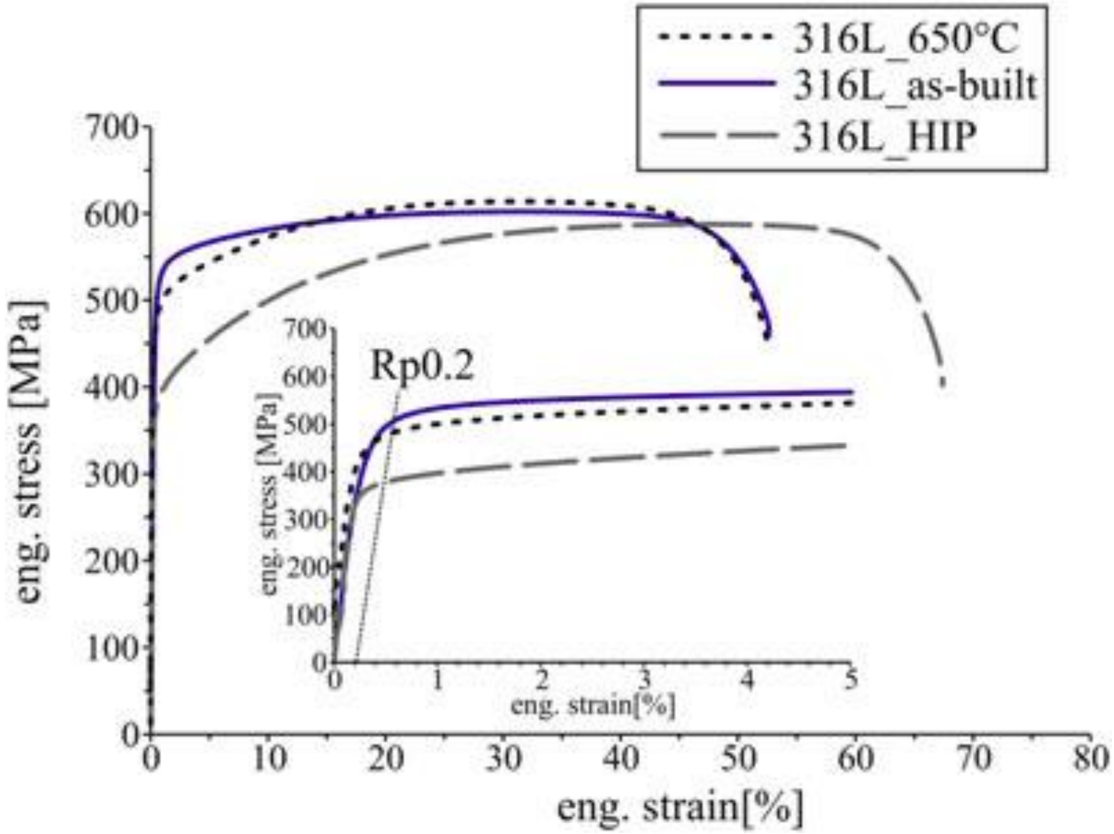

Fatigue tests:

- *in accordance with* ASTM E466-07
- *as-built and turned surface*
- *force controlled*
- *Frequency: 40 Hz*
- *Stress ratio: R = -1*

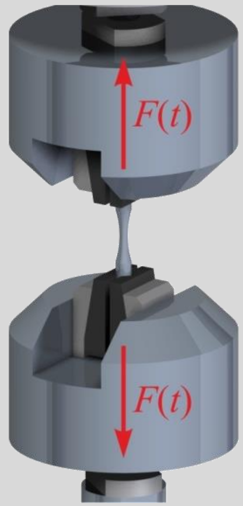

condition	fatigue limit $\bar{\sigma}$ [MPa]
as-built/SLM surface	108
as-built/turned surface	267
650 °C/turned surface	294
HIPed/turned surface	317
traditionally processed	240-381

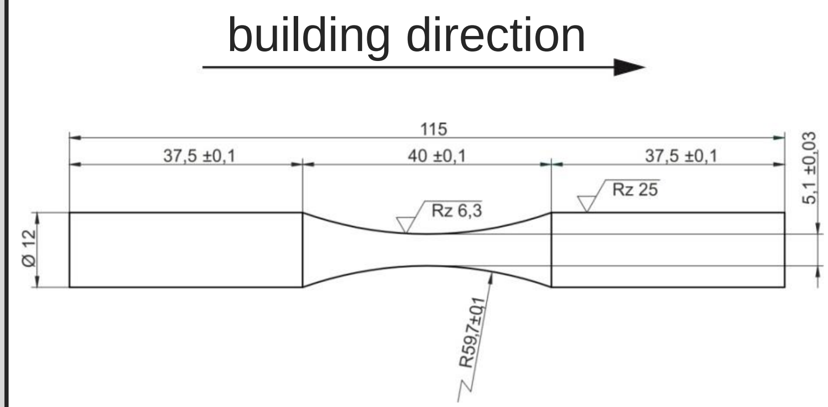

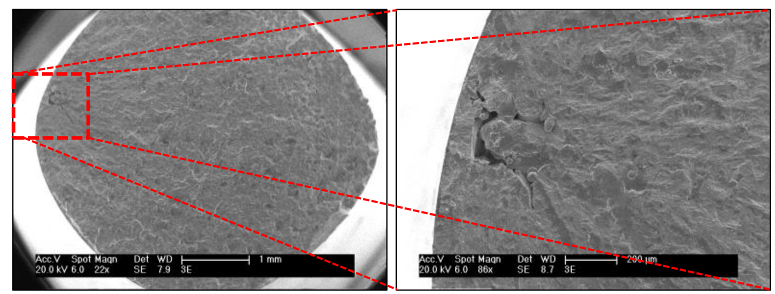

Woehler type S-N-curves

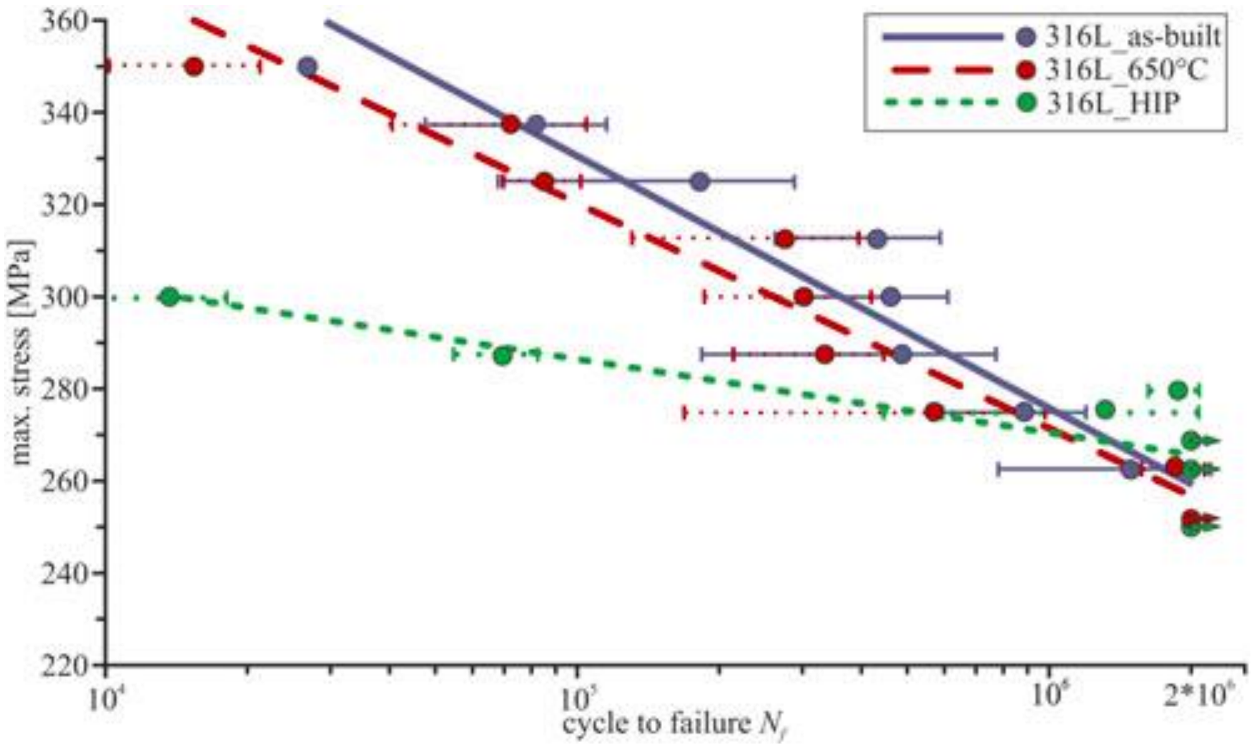

UNIKASSEL VERSITÄT

Fracture mechanics tests: *Comparison of threshold values*

- *Effect of post-treatments*
- *Effect of crack growth direction*

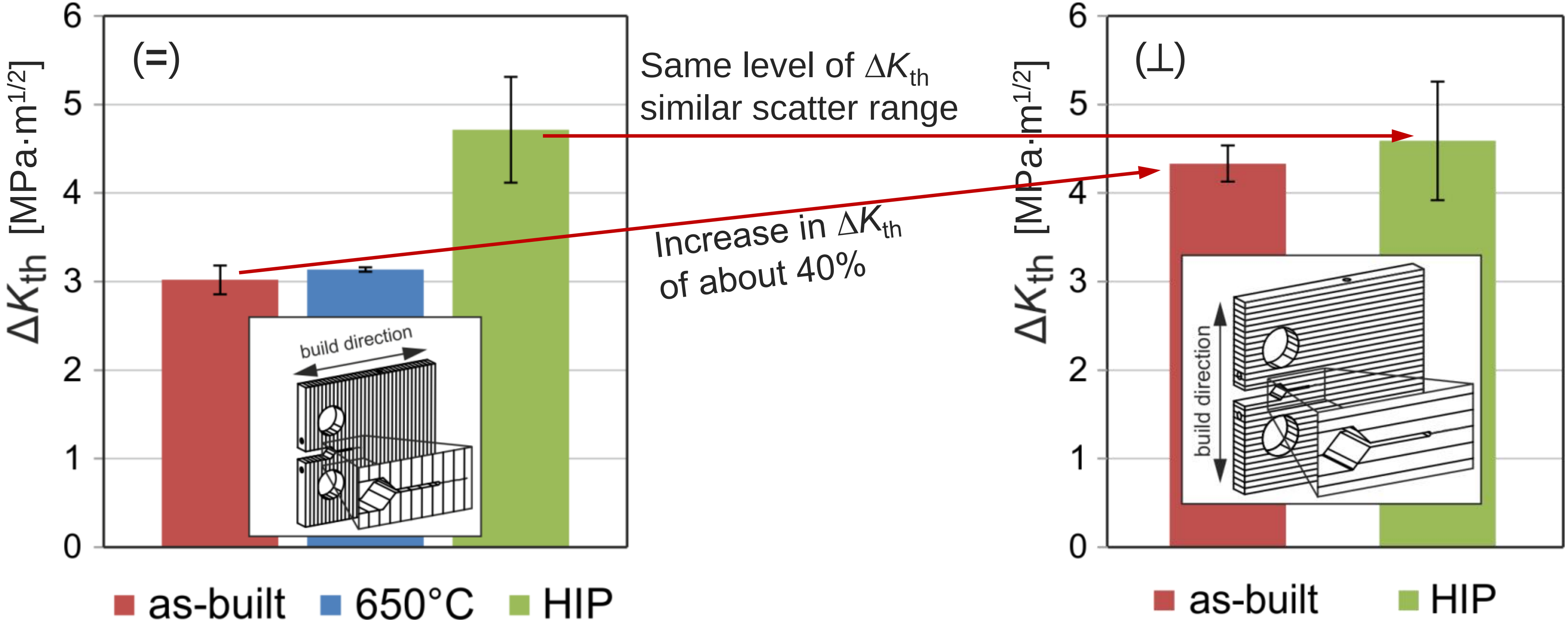

A. Riemer et al., Eng. Fract. Mech. 120, 2014, 15-25.

UNI KASSEL VERSITÄT

X-Ray diffraction:

Residual stresses for
- 3 directions
- sample surface, 100µm and 200µm depth
- average error of data is about 25 MPa

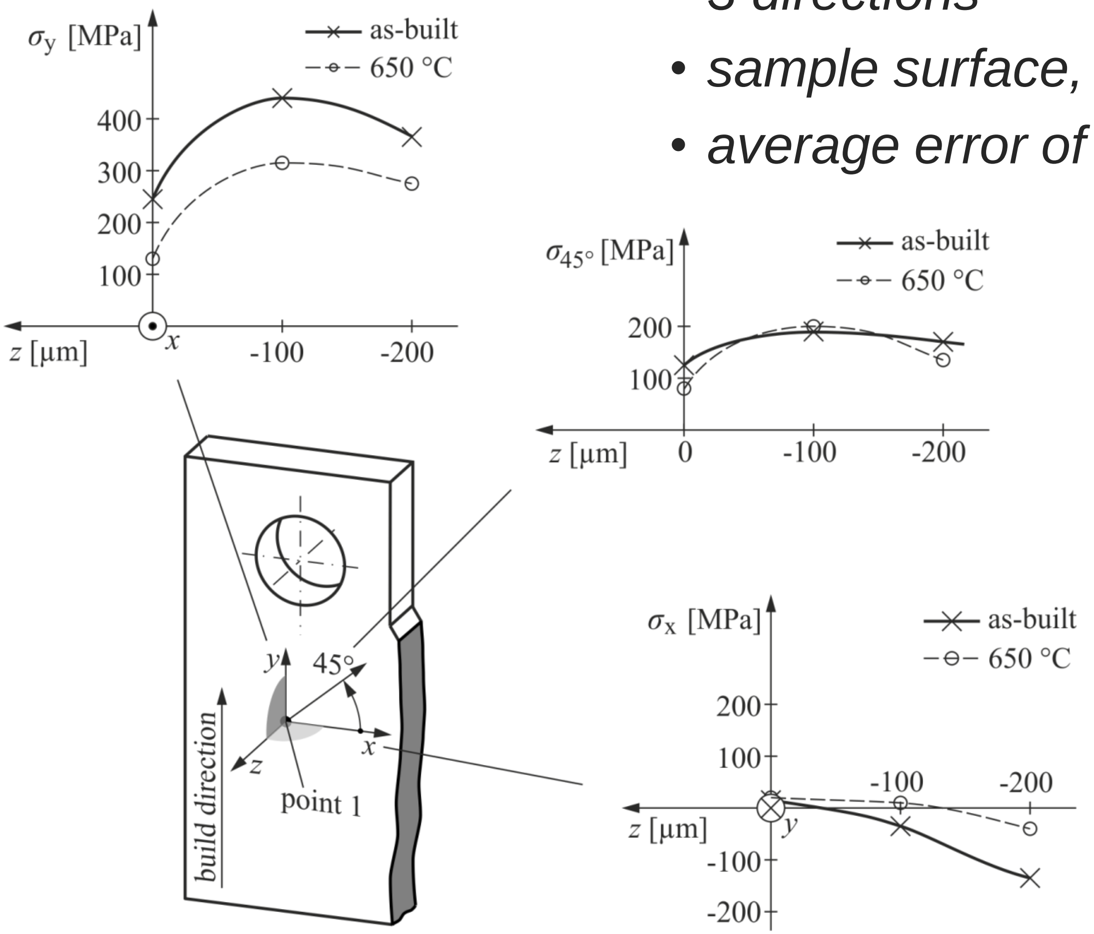

- ➢ No significant internal stresses for x-direction
- ➢ Highest internal stresses for y-direction (building direction)
- ➢ Highest value in a depth of 100µm for y-direction => shell-core re-melting
- ➢ y-direction: decrease after heat treatment

Stainless steel 316L

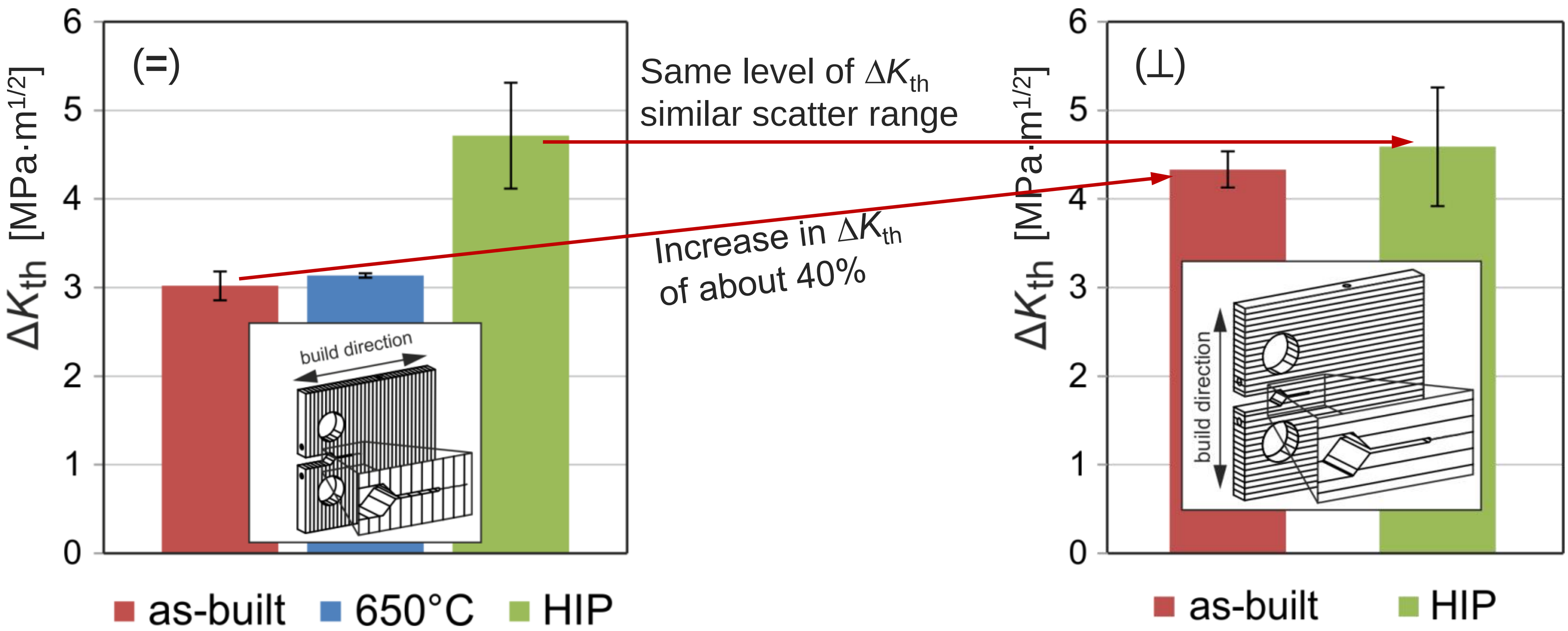

Higher threshold value for (⊥)-direction despite highest internal stresses in building direction superposed with testing load

=> small effect of internal stresses on crack growth

Stainless steel 316L

Microstructure: *Similar microstructure for as-built and 650°C*

- *elongated grains in building direction*
- *strongly textured*

HIP condition exhibits

- coarse grains, almost equiaxed
- absence of strong texture

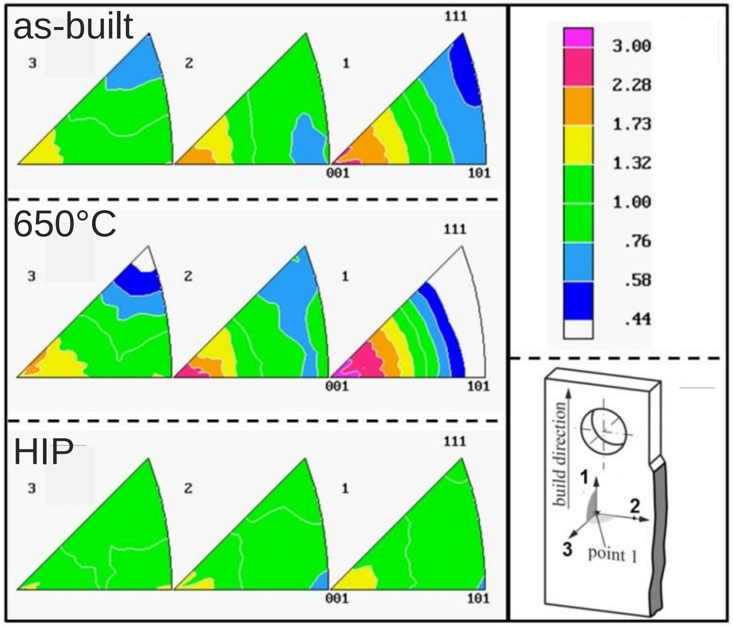

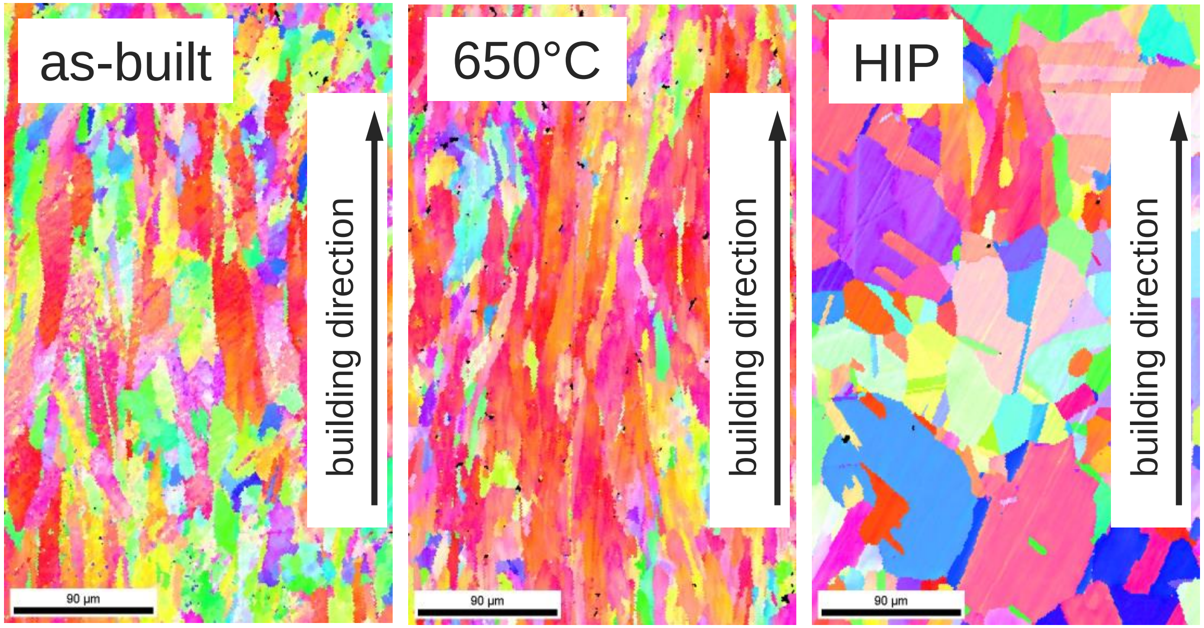

UNI KASSEL VERSITÄT

as-built & 650°C

- *Grains are elongated in the building direction*
- *Lower crack growth resistance along stretched grains => Lower threshold values*
- *For crack growth normal to building direction the boundaries are closer and act as barrier => higher threshold value*

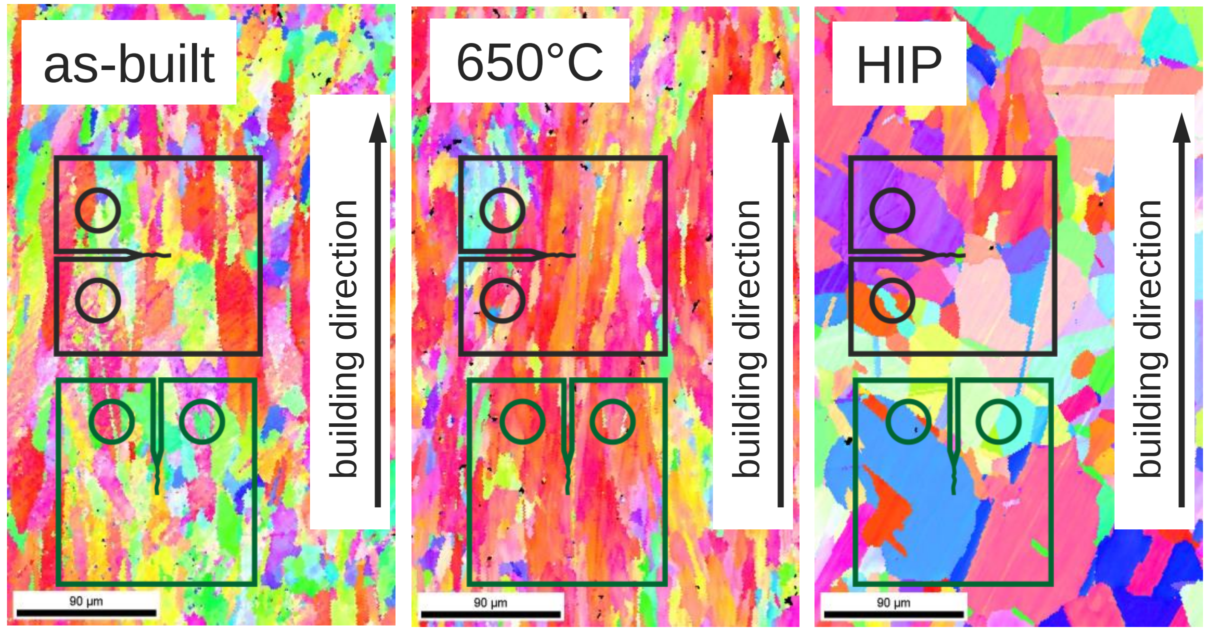

	as-built	650°C	HIP
Threshold (⊥) [MPa·m$^{1/2}$]	4.3	-	4.7
Threshold (=) [MPa·m$^{1/2}$]	3	3	4.6

HIP

- *Absence of preferred grain orientation leads to similar thresholds*
- *Increase in thresholds due to elevated grain size*
- *Grain boundary as barrier*
- *crack growth at low load levels stops dependent on the microstructure present in front of the crack tip =>higher scatter*

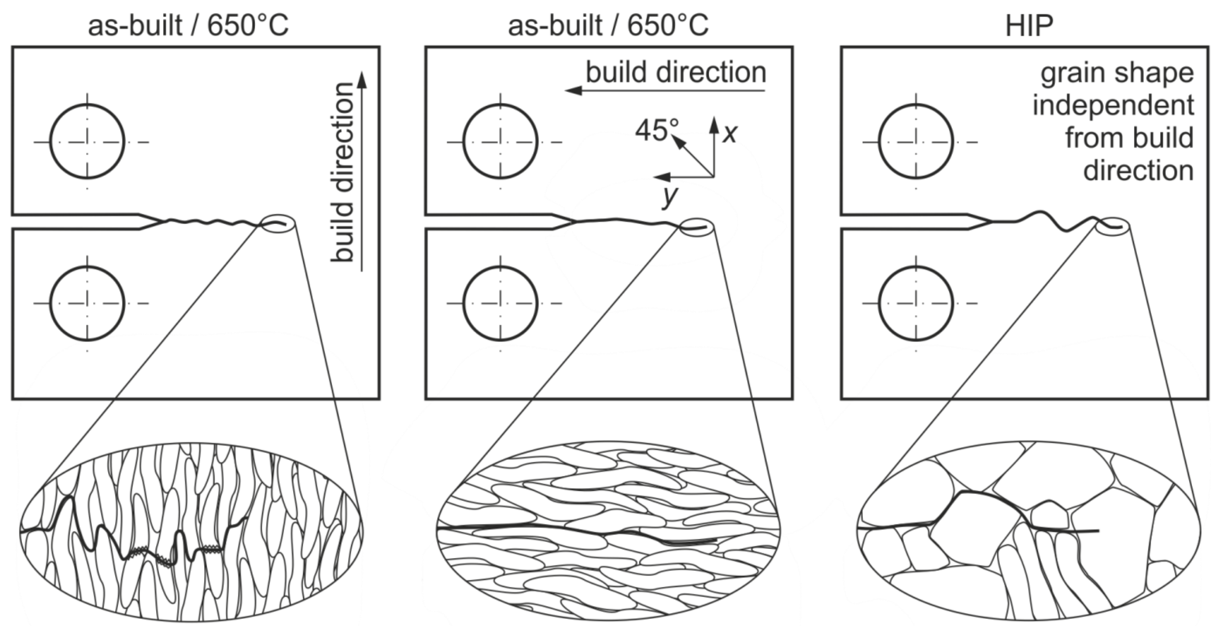

	as-built	650°C	HIP
Threshold (⊥) [MPa·m$^{1/2}$]	4.3	-	4.7
Threshold (=) [MPa·m$^{1/2}$]	3	3	4.6

Agenda

1. Stainless steel 316L

2. Ni-based alloy IN 718

3. High-Mn Fe-based alloys

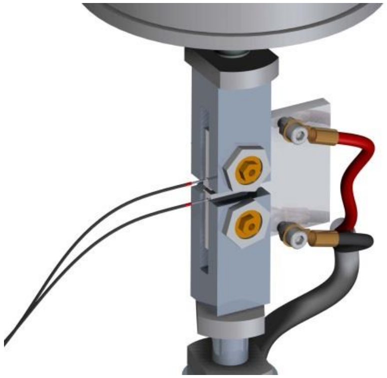

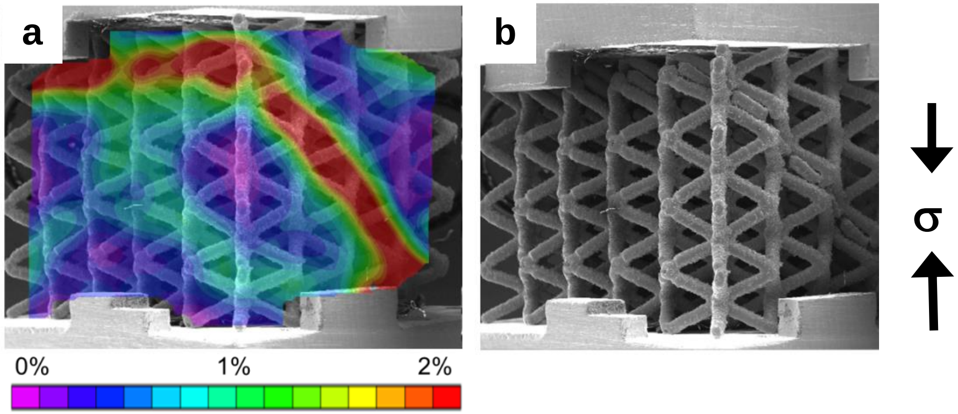

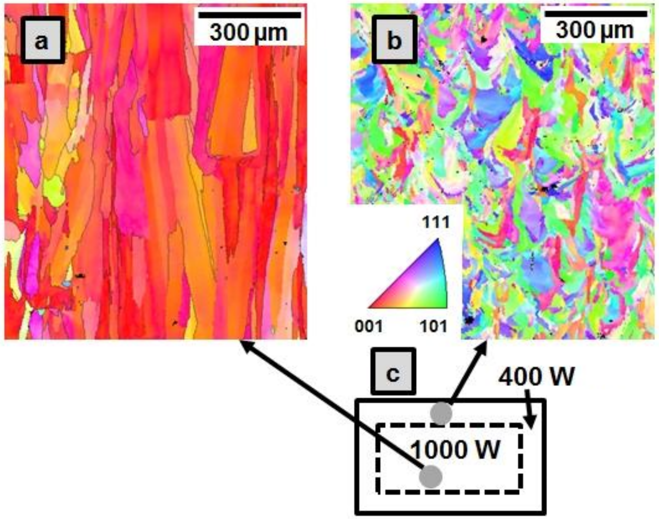

Microstructure design

What kind of microstructure can be obtained?

- Employed for processing of samples

→ SLM-280[HL] → 400W / 1000W laser sources

→ layer thickness up to 150 µm

→ shell/core structures

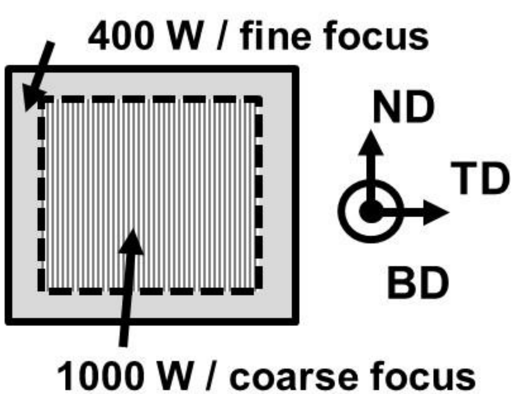

Microstructure design

Microstructure/ grain shape

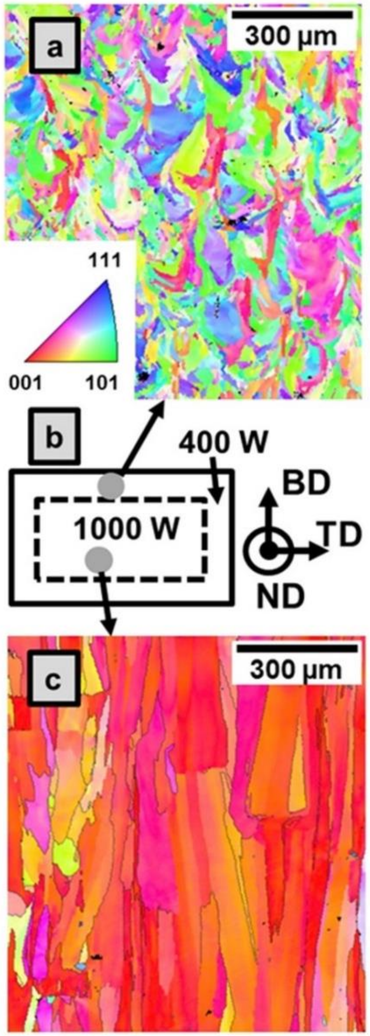

T. Niendorf et al., Metall. Mater. Trans. B 44, 2013, 794-796.

Microstructure design

Microstructure/ grain shape

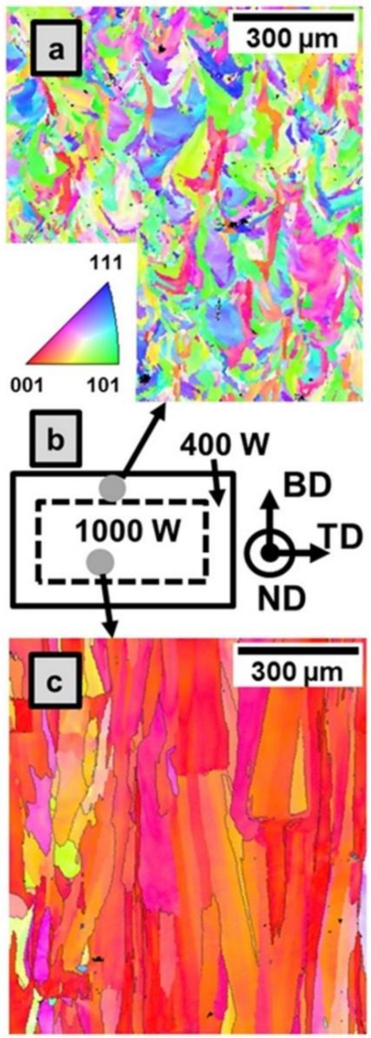

Anisotropy/ texture

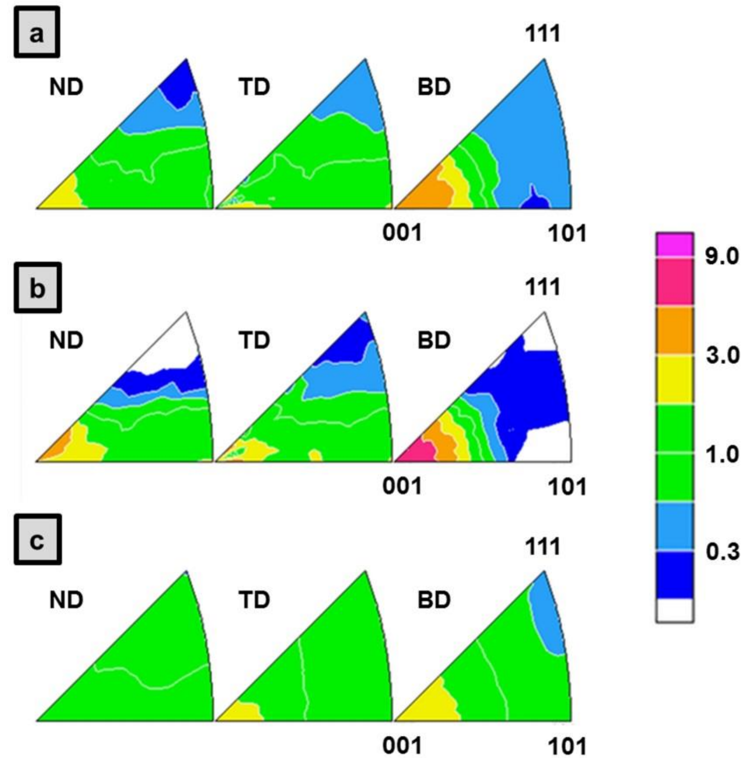

Microstructure design

What kind of microstructure can be obtained?

- Microstructurally tailored
- Load-adapted design

Functionally graded by microstructure design

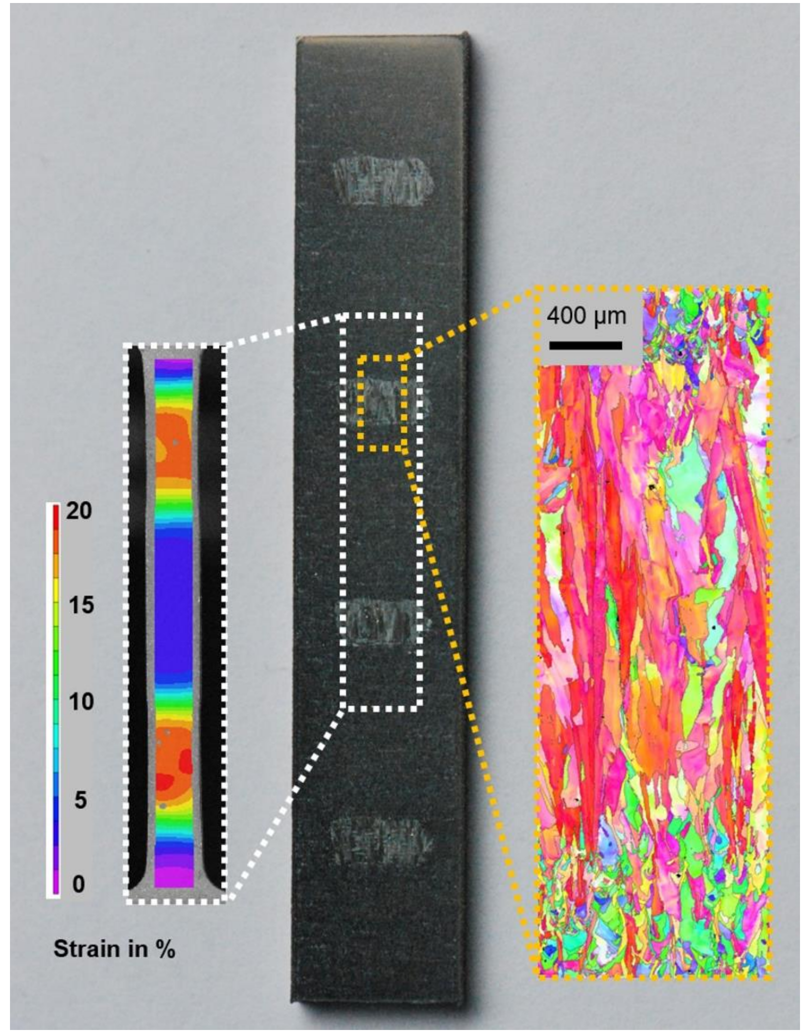

Similar microstructure evolution for other alloys:
> Solidification in cubic phase
> No phase transformation upon cooling

➔ Ni-based alloys

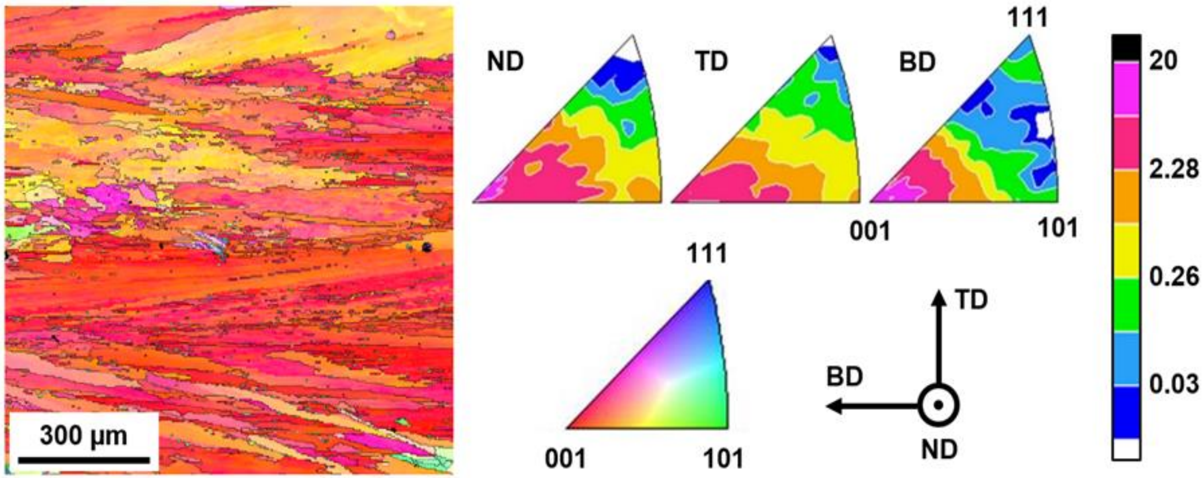

Microstructure design

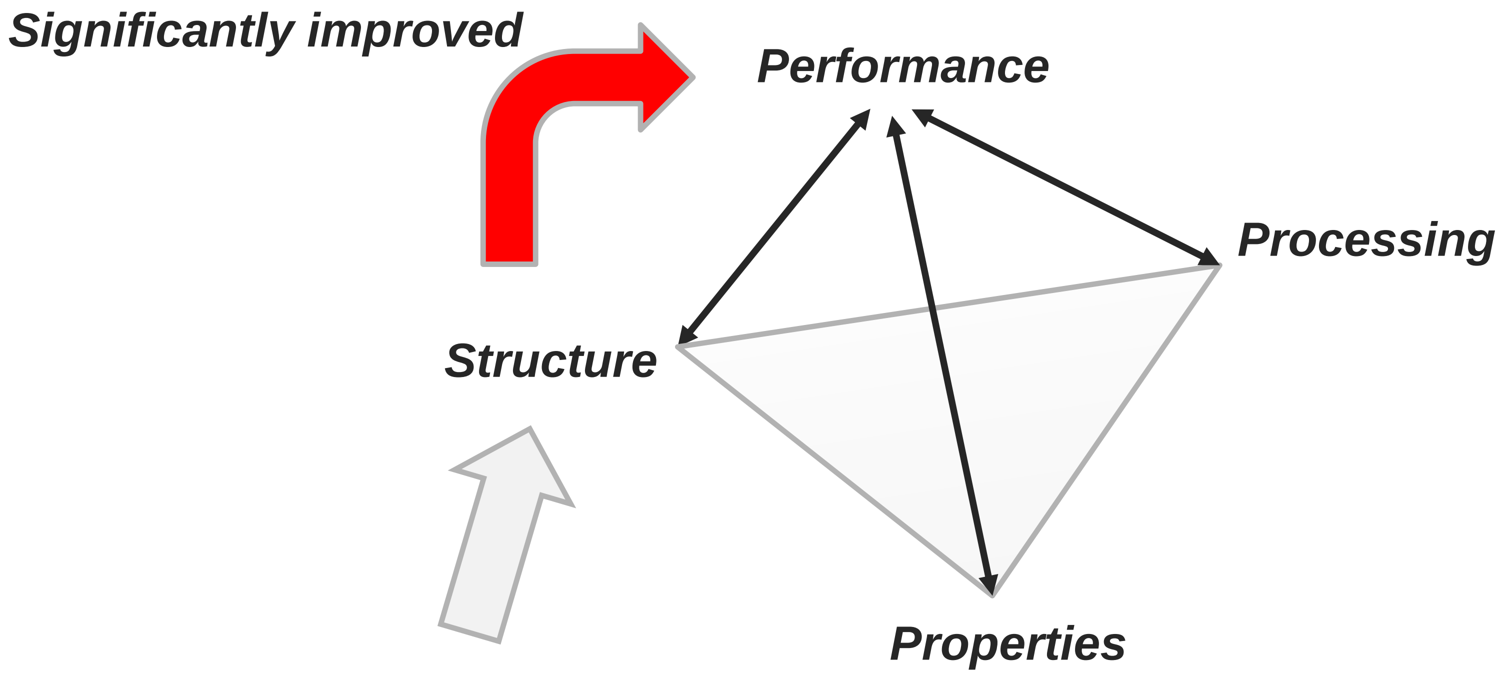

Additive manufacturing is perfectly suited for direct <u>microstructure manipulation</u>

- ***Grain size & shape***
- ***Anisotropy/ texture***

Agenda

1. Stainless steel 316L

2. Ni-based alloy IN 718

3. High-Mn Fe-based alloys

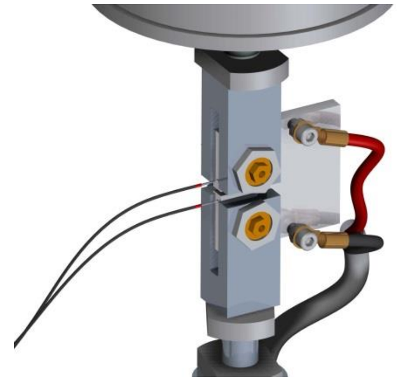

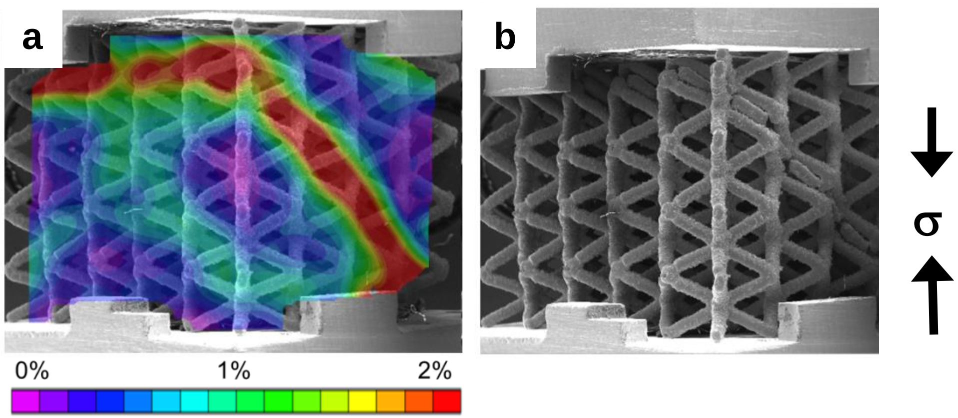

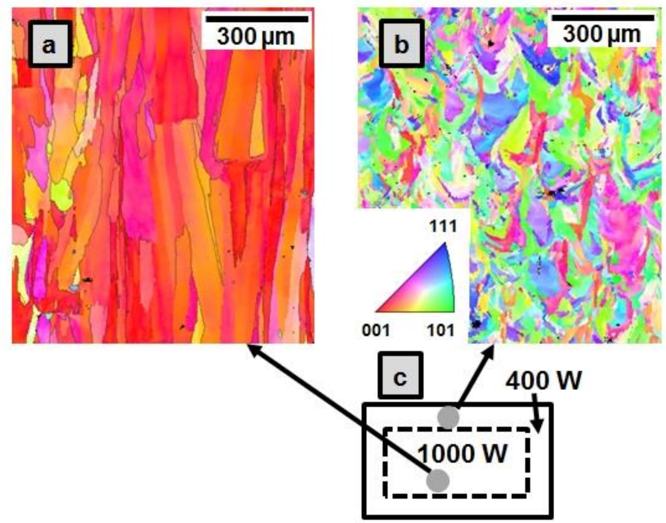

	Cast & Wrought	SLM

Process

Cast & Wrought:

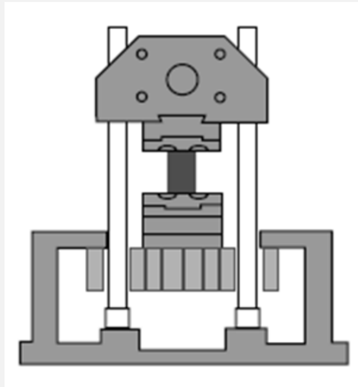

SLM:

Material

Cast & Wrought:

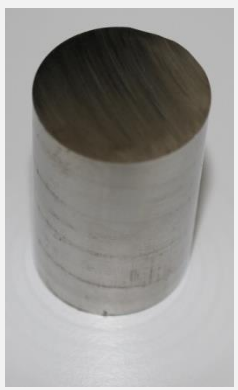

SLM:

Building Direction

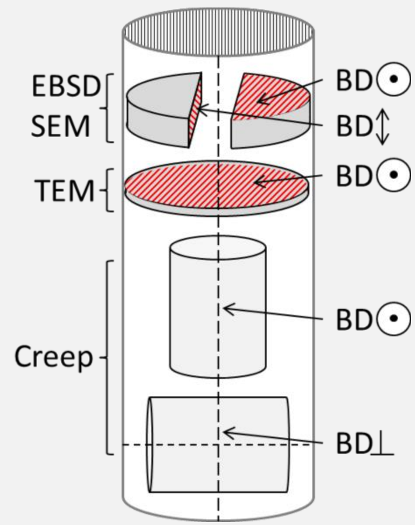

Element	Ni	Cr	Fe	Nb	Al	Ti	Mo	C
wt %	Bal.	19.0	18.5	5.1	0.5	0.9	3.0	0.04

δ-phase (Ni_3Nb)
Orthorhombic ($D0_a$)

γ″-phase (Ni_3Nb)
Tetragonal bcc ($D0_{22}$)

γ′-phase (Ni_3Al)
Cubic ($L1_2$)

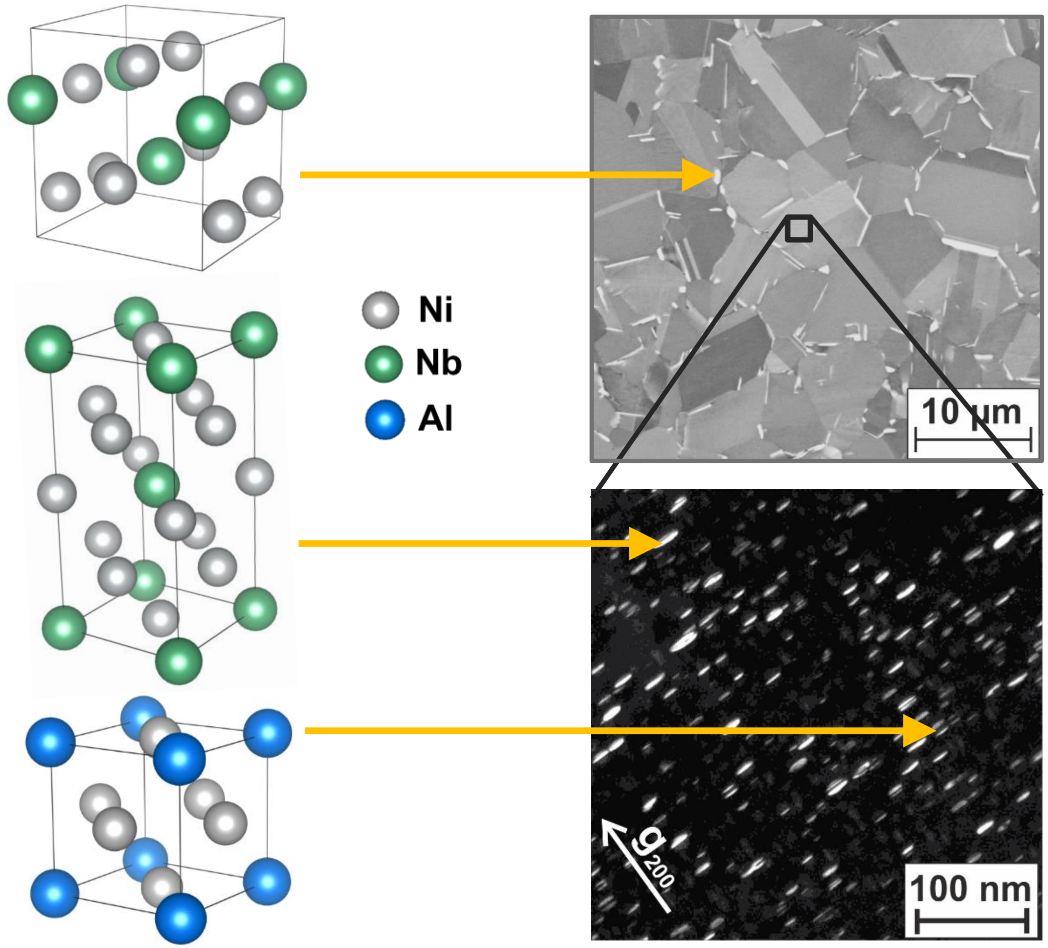

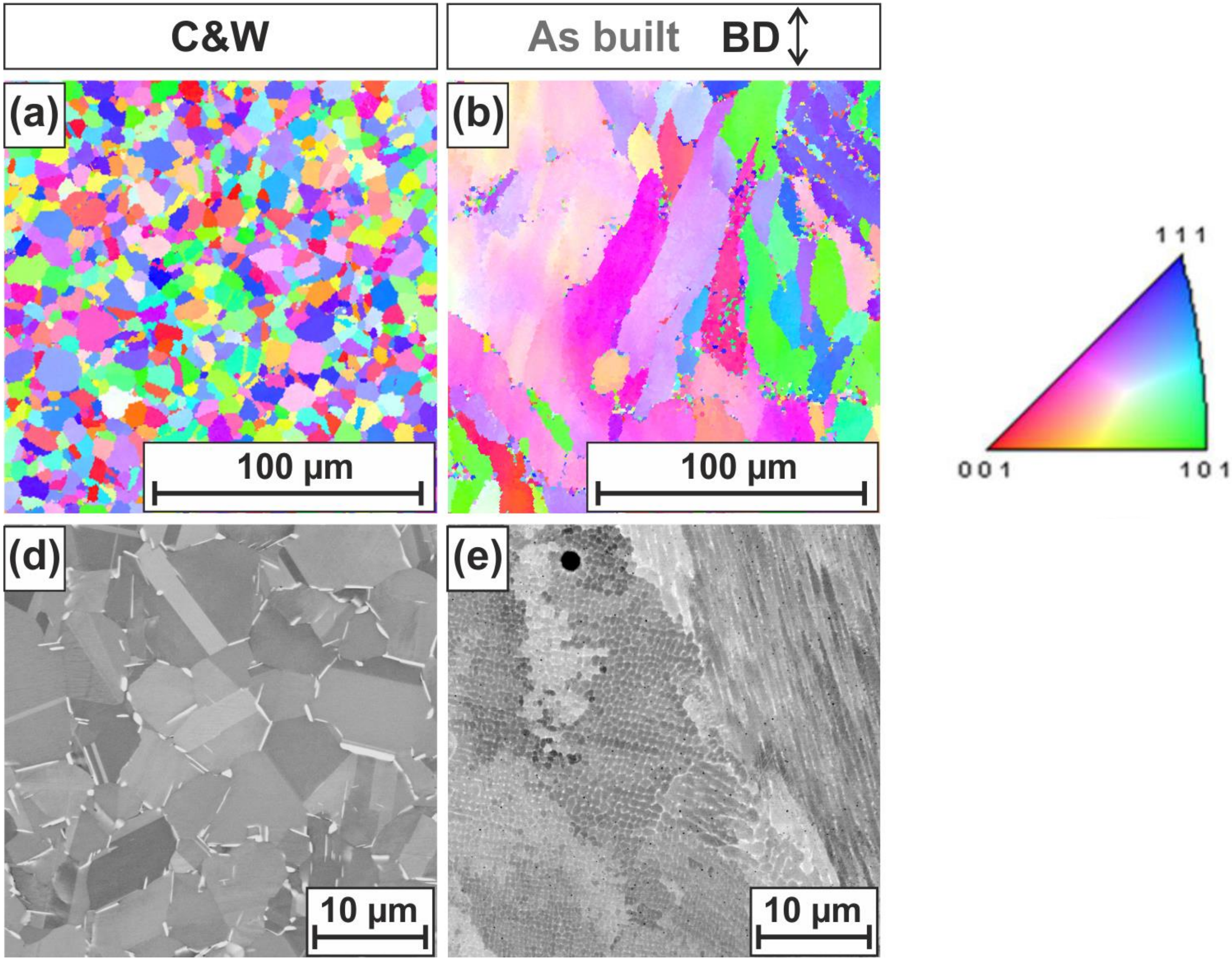

M. Pröbstle et al., Mater. Sci. Eng. A, 2016, *submitted*.

SEM-BSE

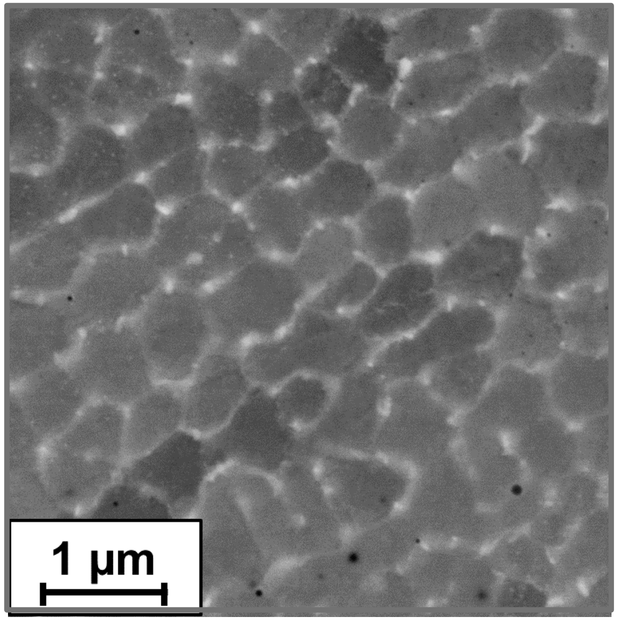

TEM-BF

TEM-DF

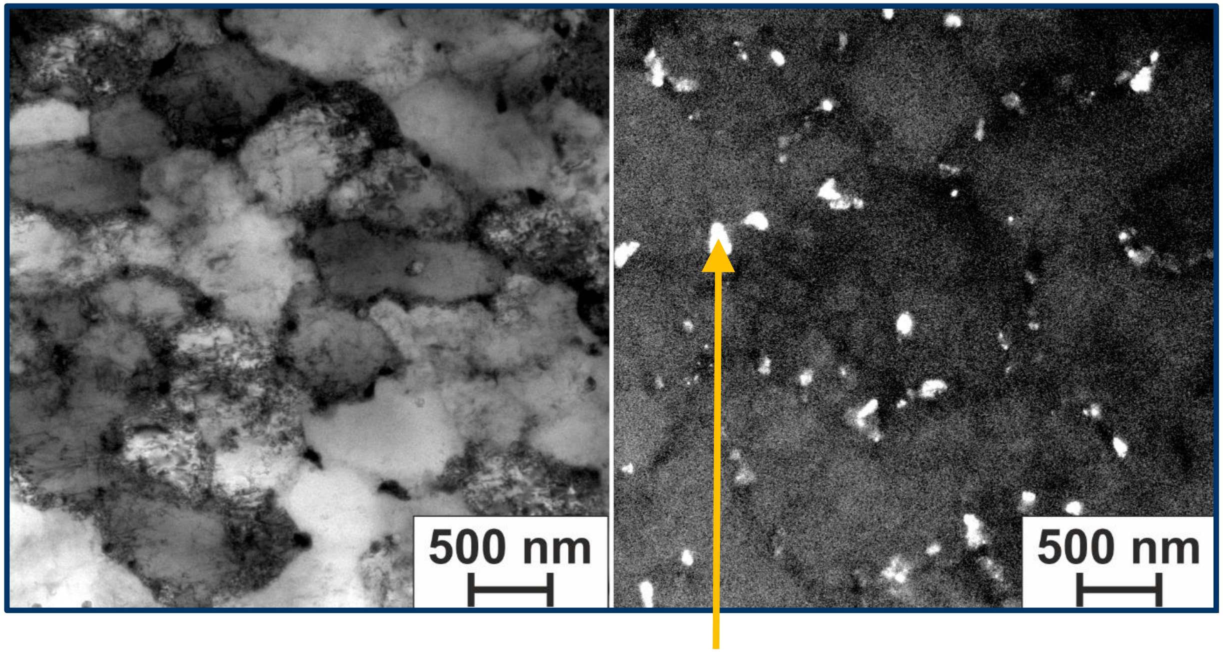

- Substructures in as-built condition
- Bright contrast in SEM => enrichment in Nb
- Laves phase particles

C14

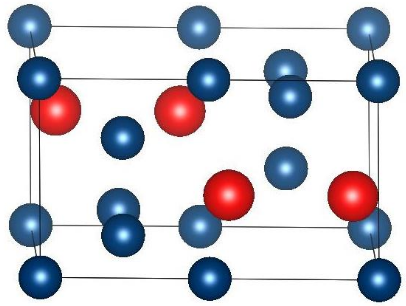

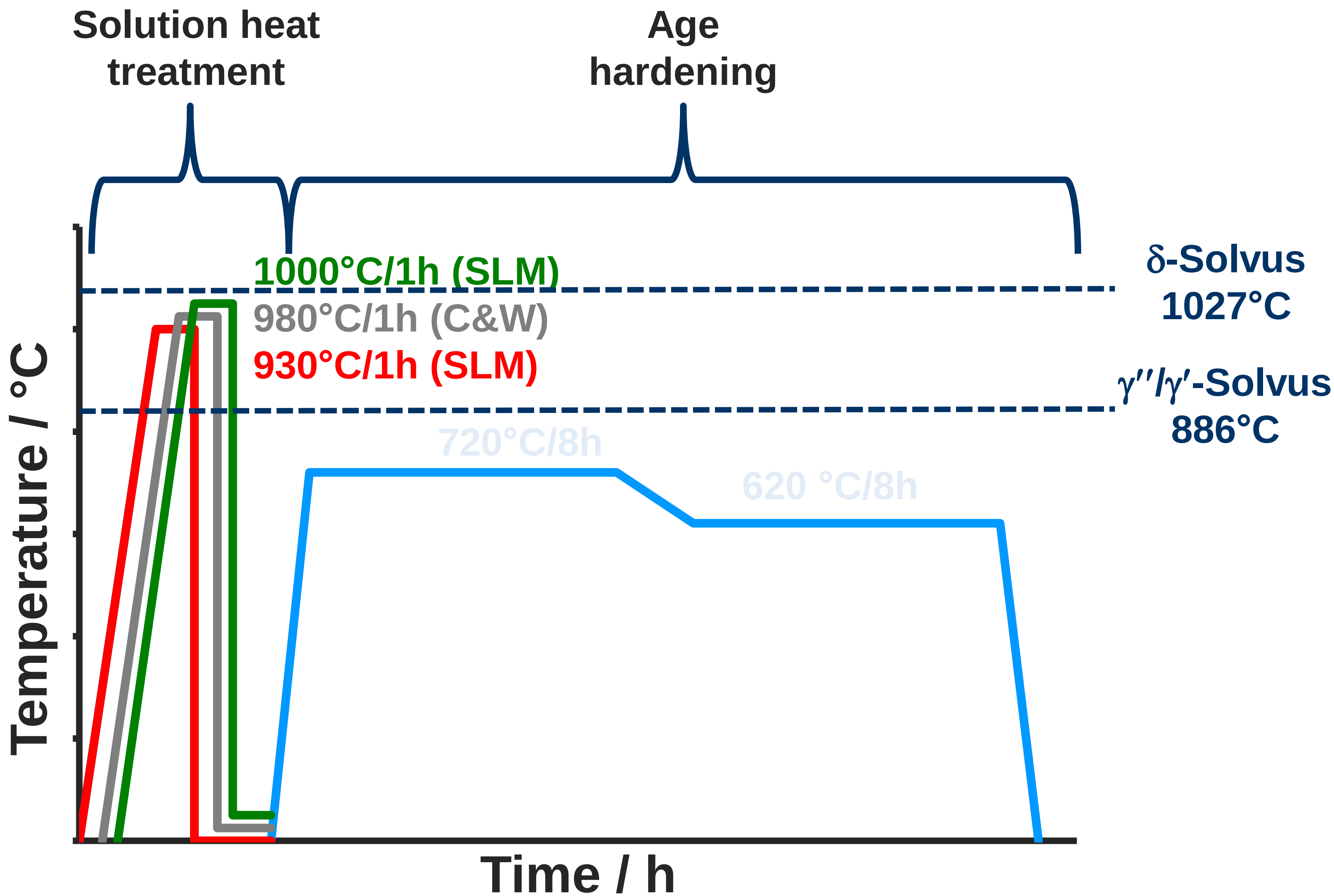
Solution heat treatment
Age hardening
1000°C/1h (SLM)
980°C/1h (C&W)
930°C/1h (SLM)
δ-Solvus 1027°C
γ''/γ'-Solvus 886°C
720°C/8h
620 °C/8h
Temperature / °C
Time / h

	Solution heat treatment	Aging heat treatment	
C&W	980°C / 1.5h	720°C / 8h	620°C / 8h
SLM – as built	-	-	-
SLM – DA	-	720°C / 8h	620°C / 8h
SLM – 930°C	930°C / 1h	720°C / 8h	620°C / 8h
SLM – 1000°C	1000°C / 1h	720°C / 8h	620°C / 8h

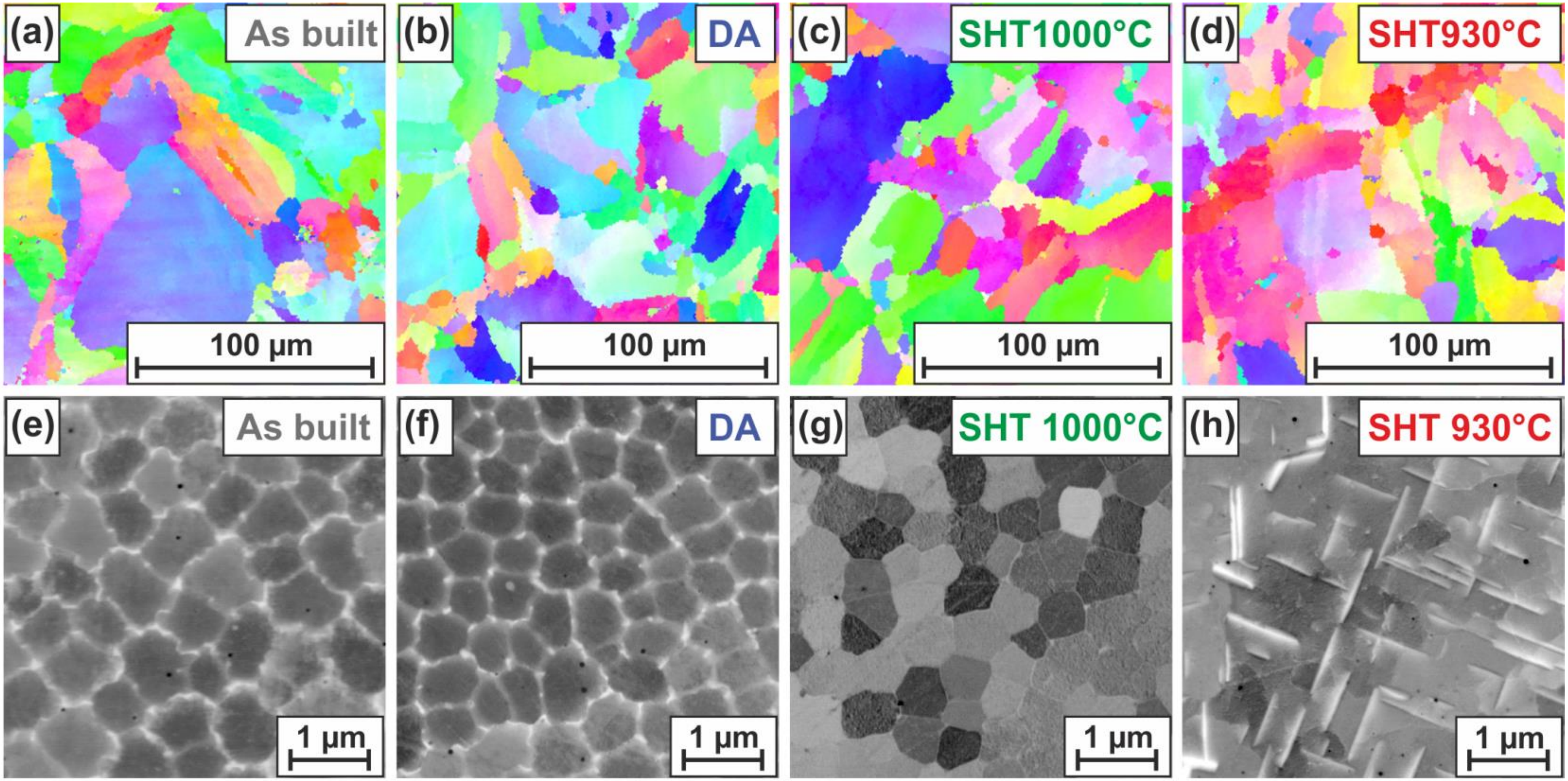

- Substructures are thermally stable
- Solutionizing eliminates segregations

 M. Pröbstle et al., Mater. Sci. Eng. A, 2016, *submitted*.

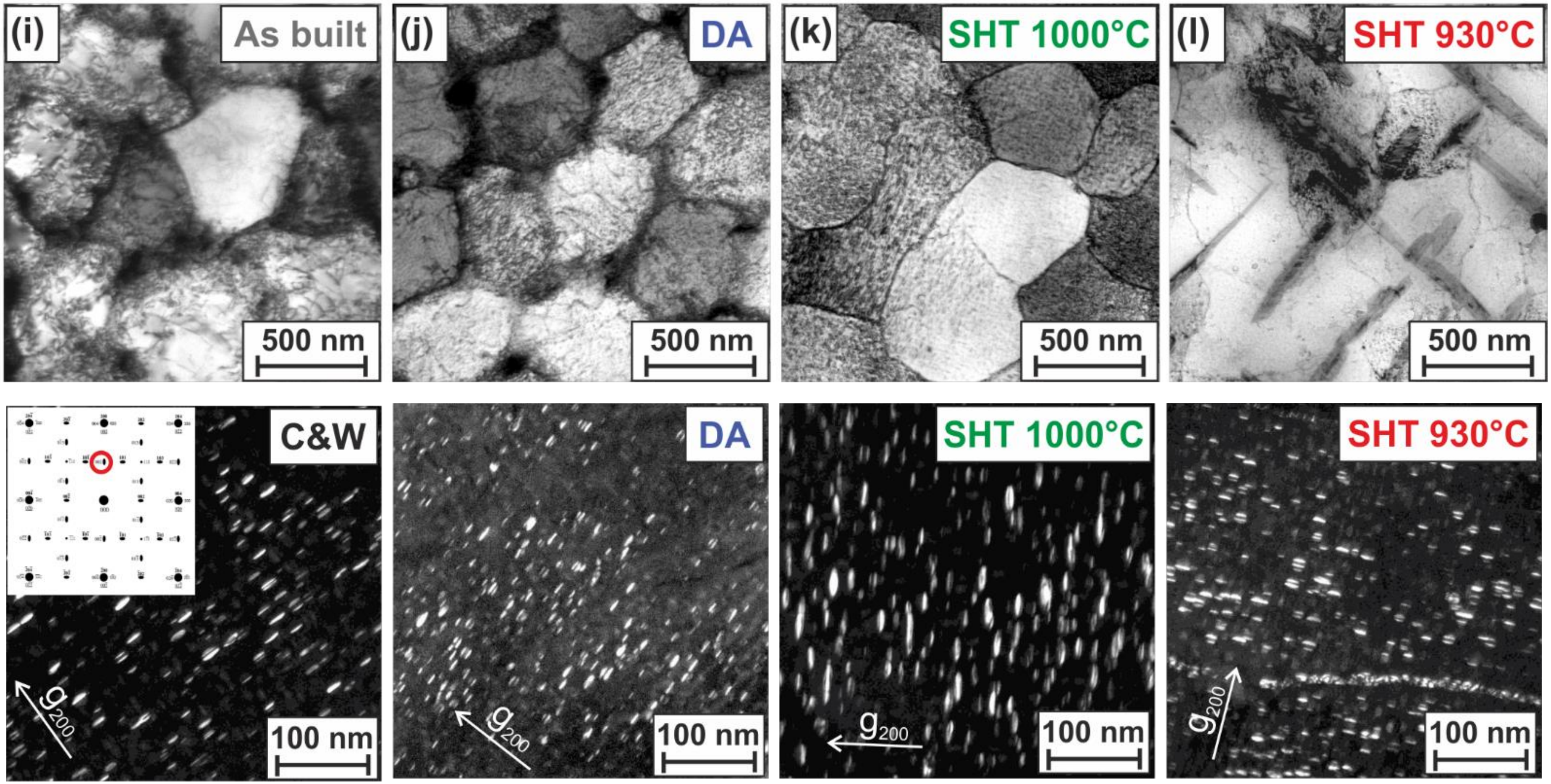

- Substructures are thermally stable
- γ''-phase evolves upon ageing

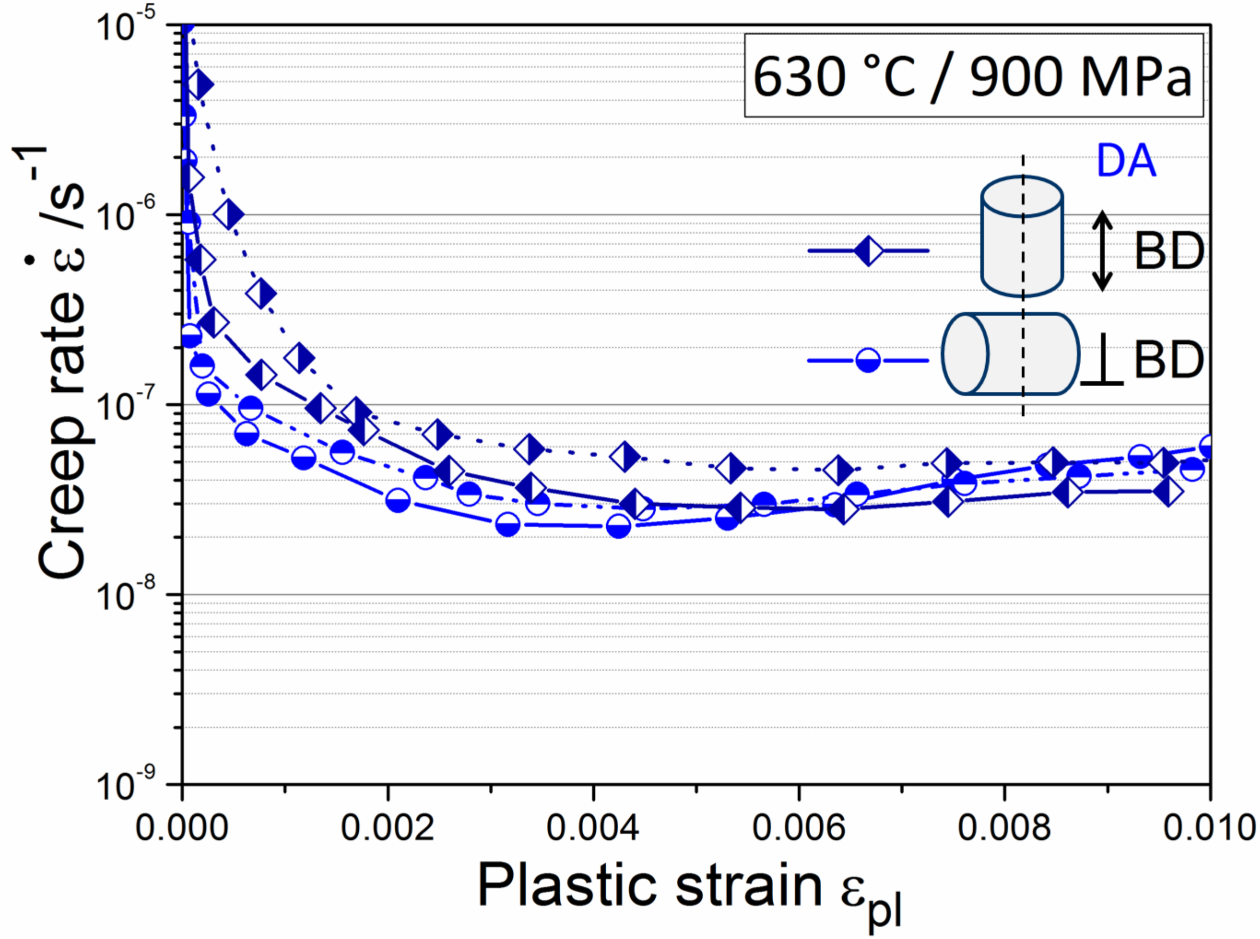

- No significant difference between different orientations

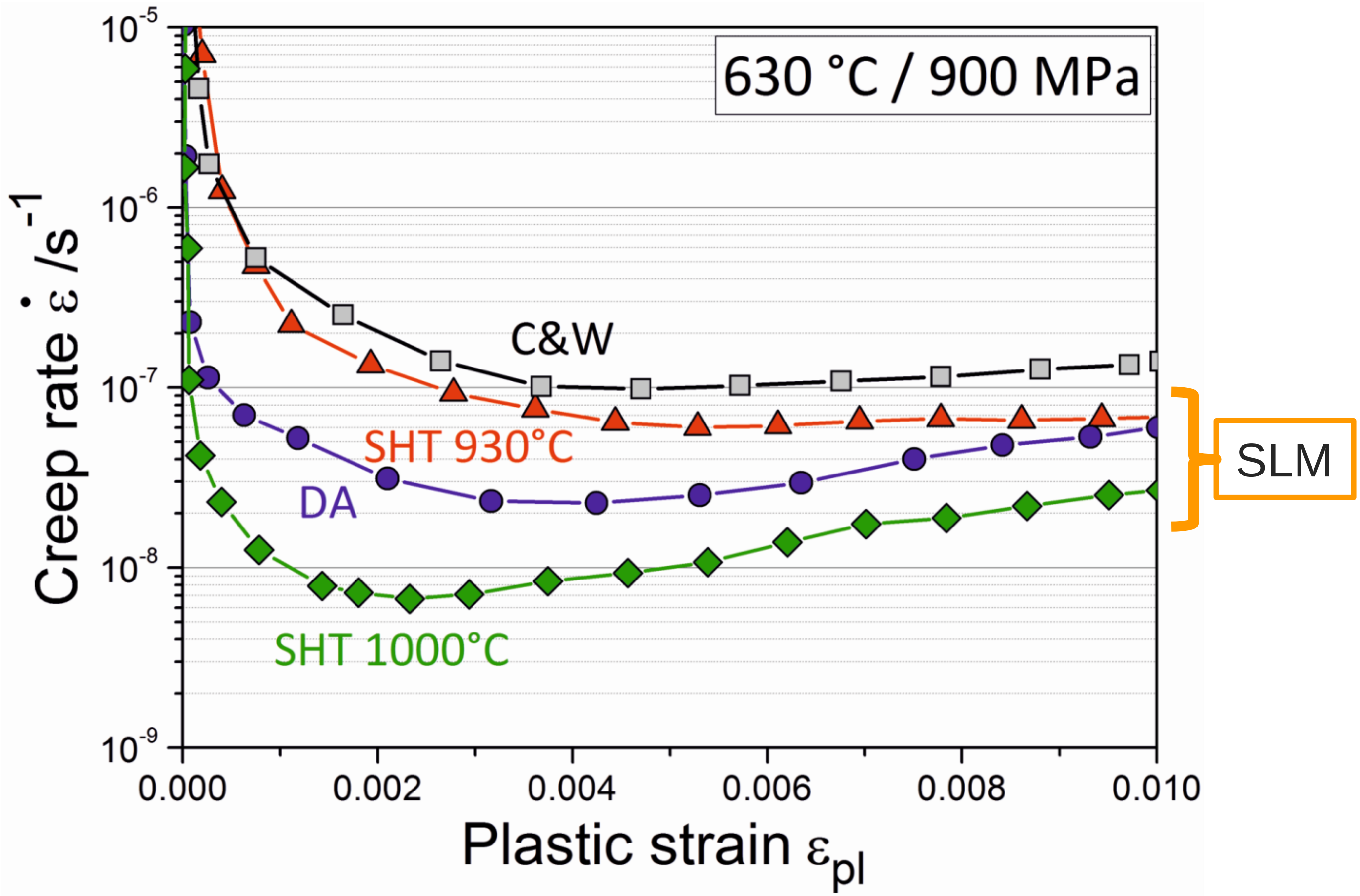

- SLM material → superior creep strength

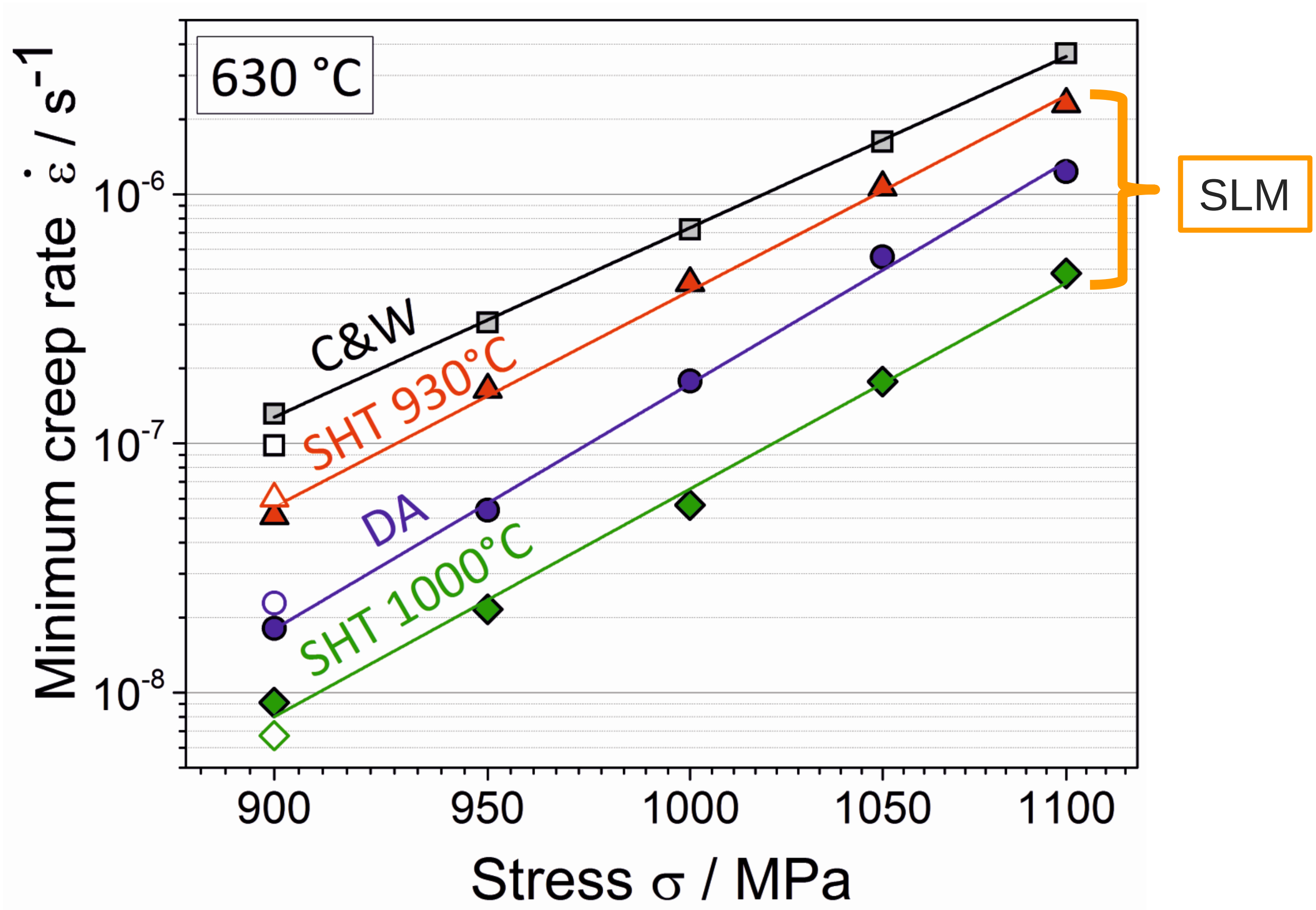

Norton plot

- SLM material → superior creep strength

Compression creep

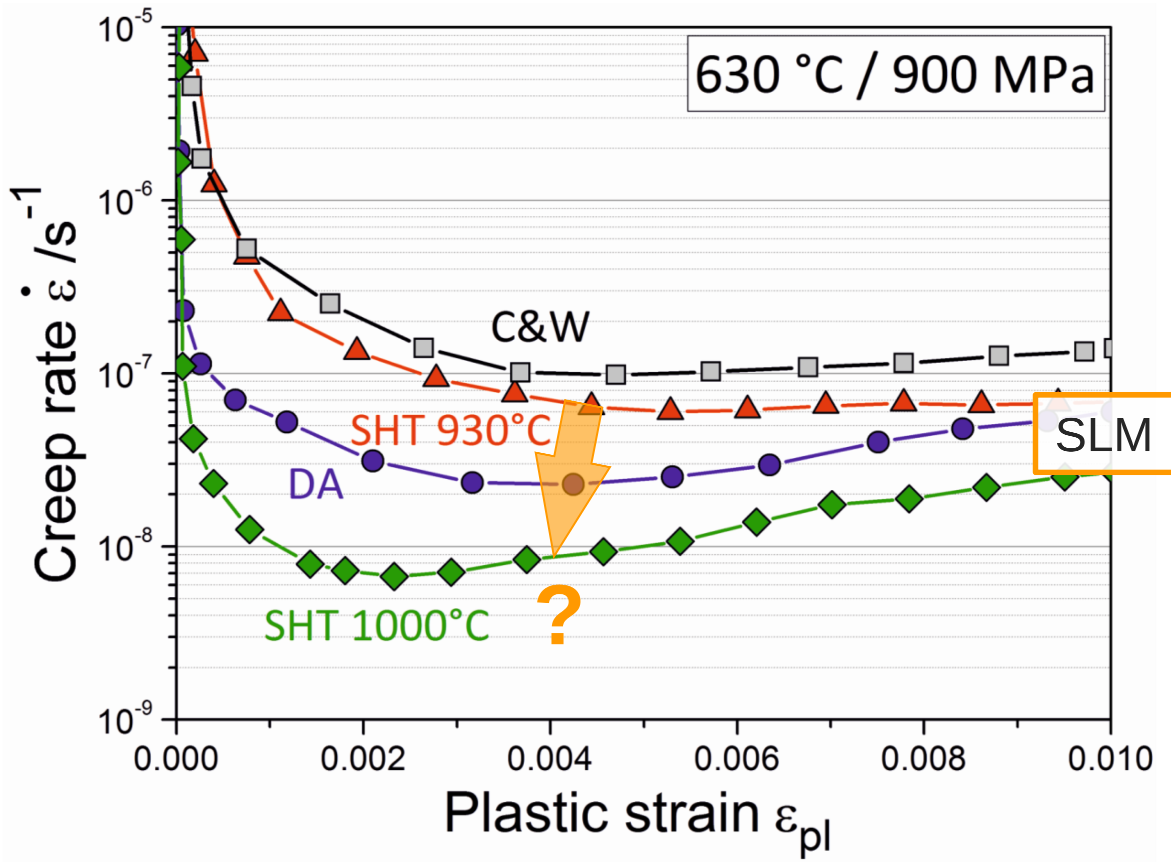

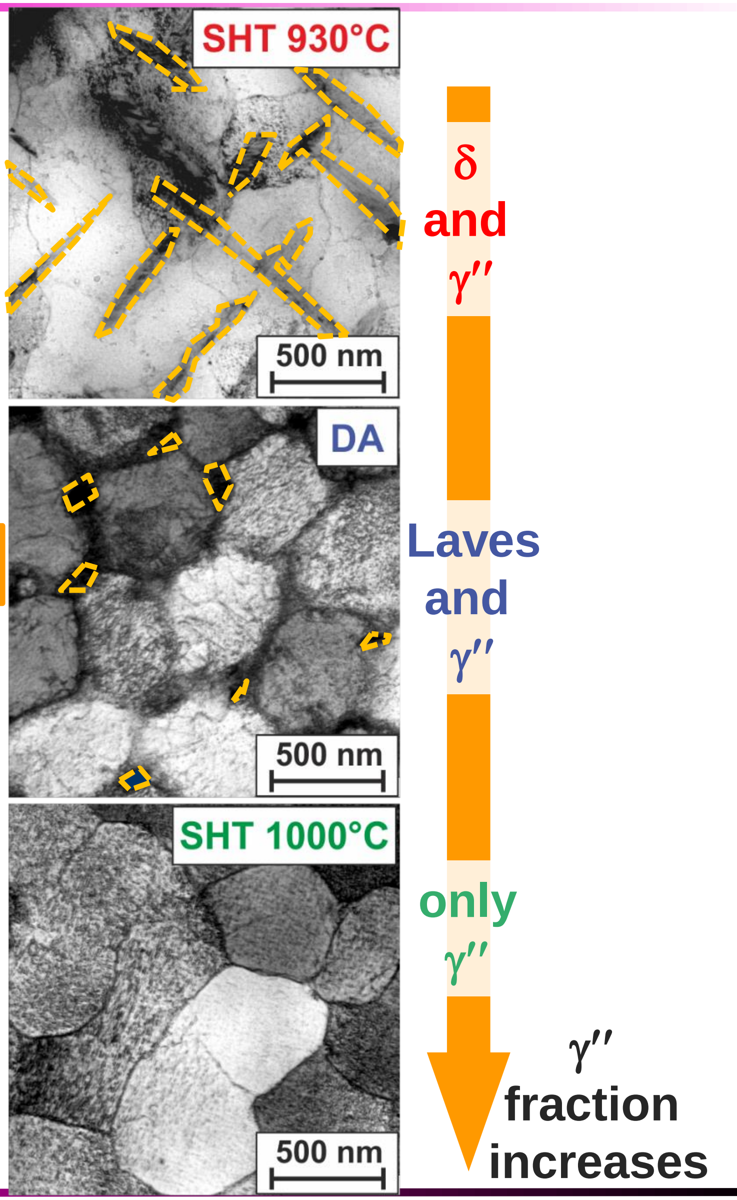

UNI KASSEL VERSITÄT

Compression creep

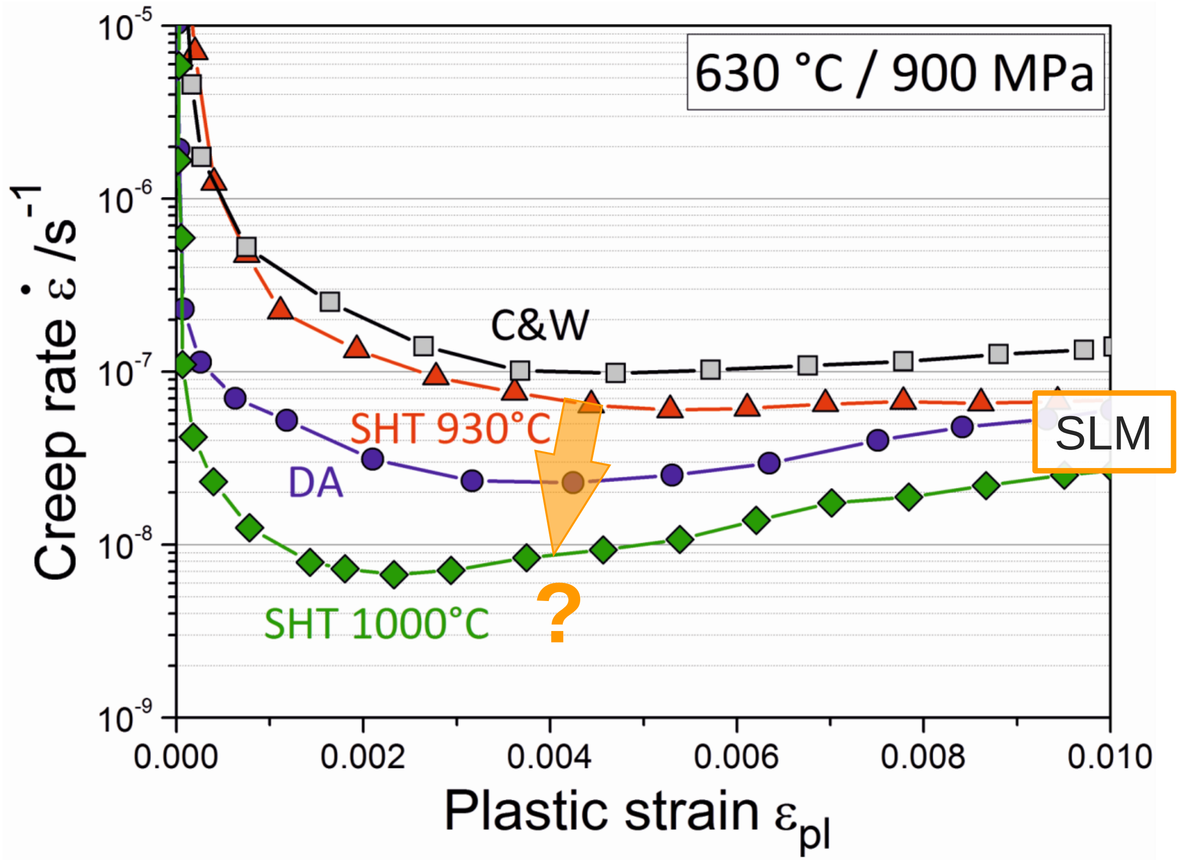

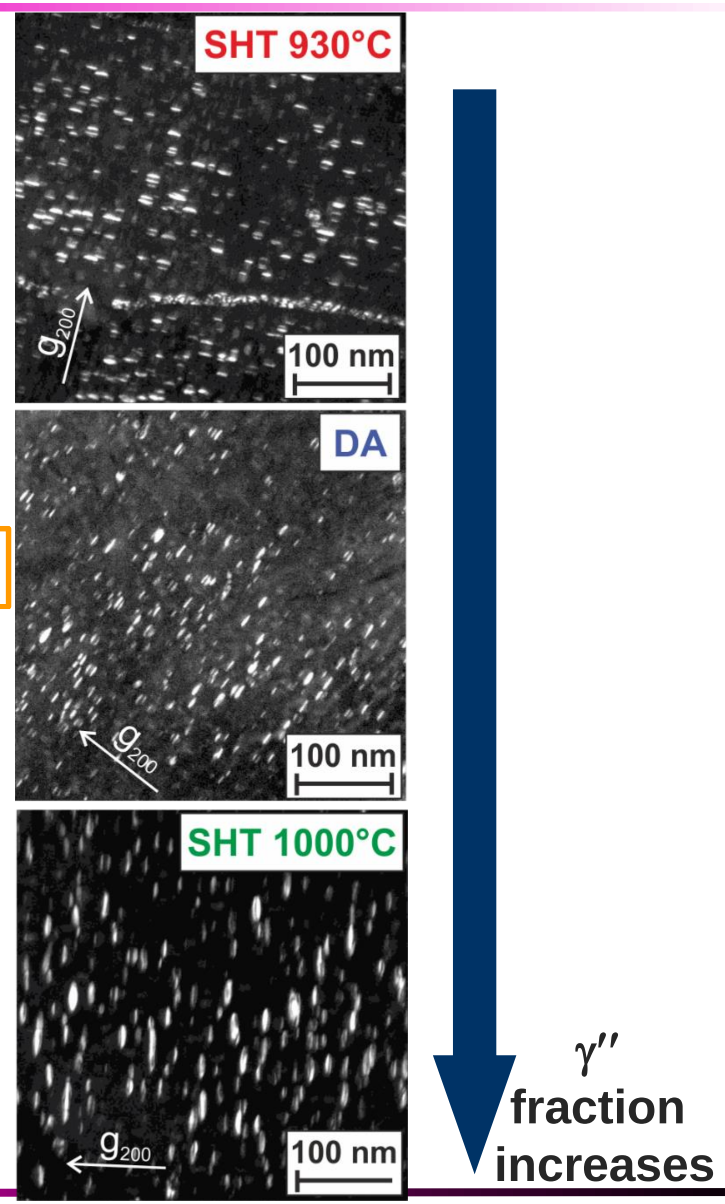

Compression creep

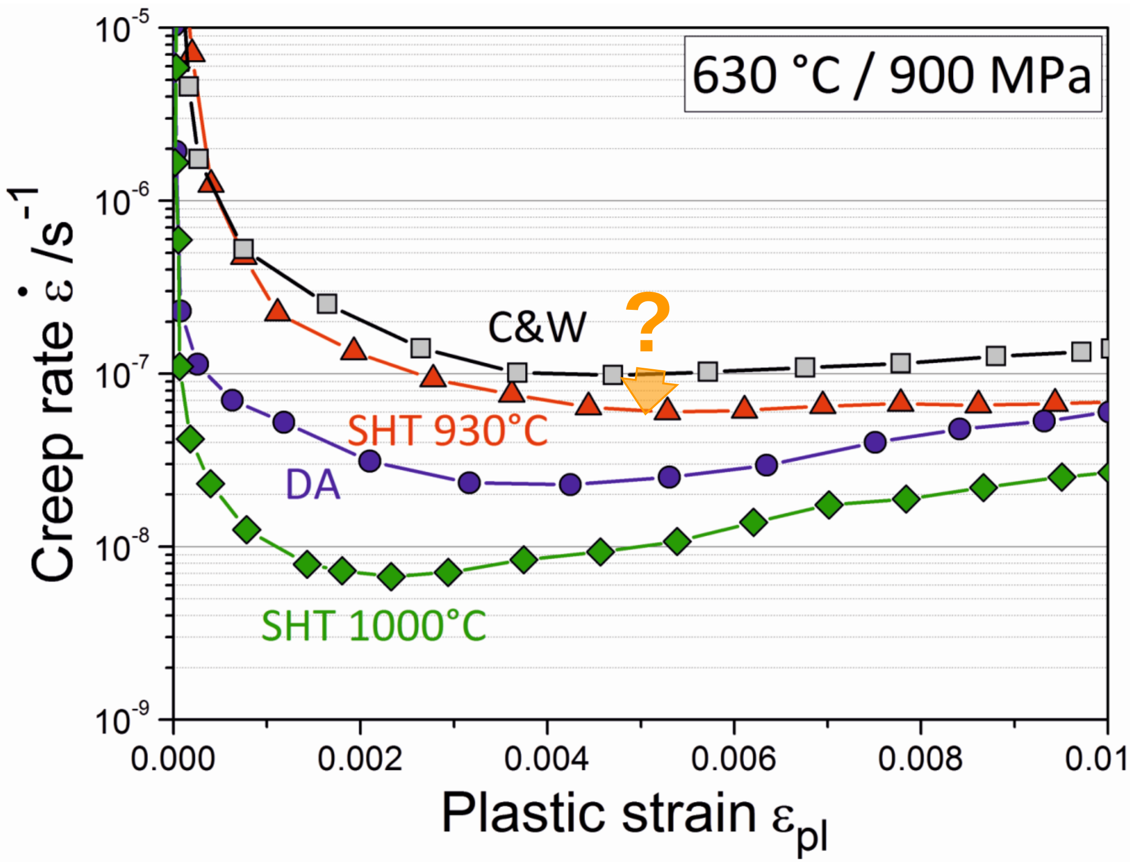

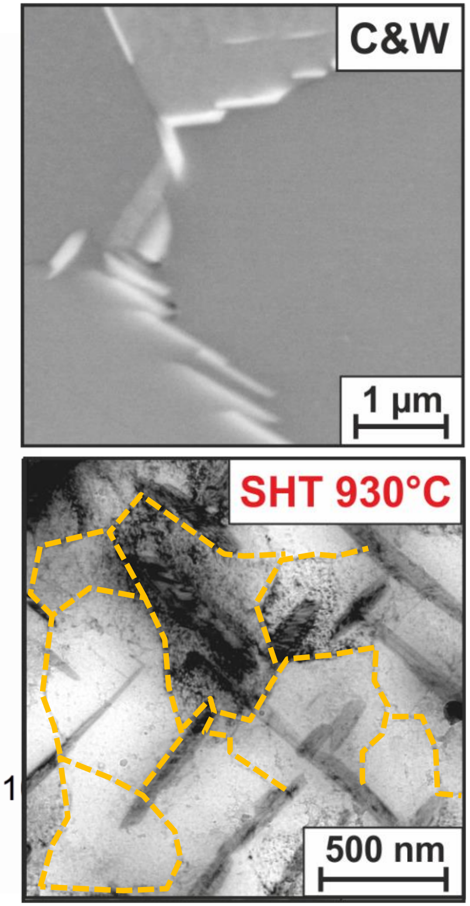

3.5 % δ

5.8 % δ but
- **finer**
- **subgrains**

Compression creep

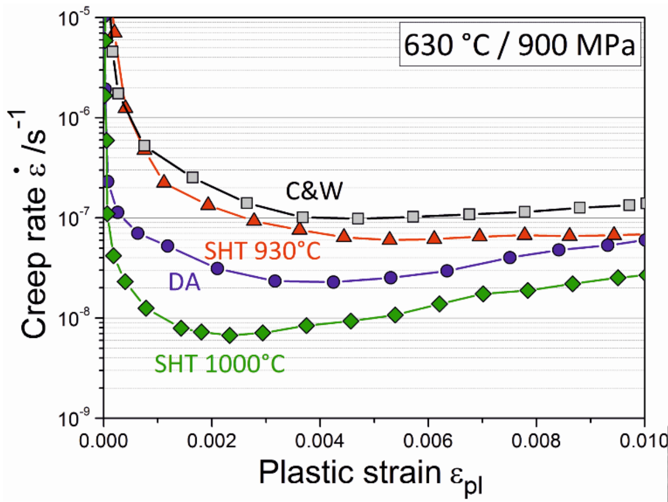

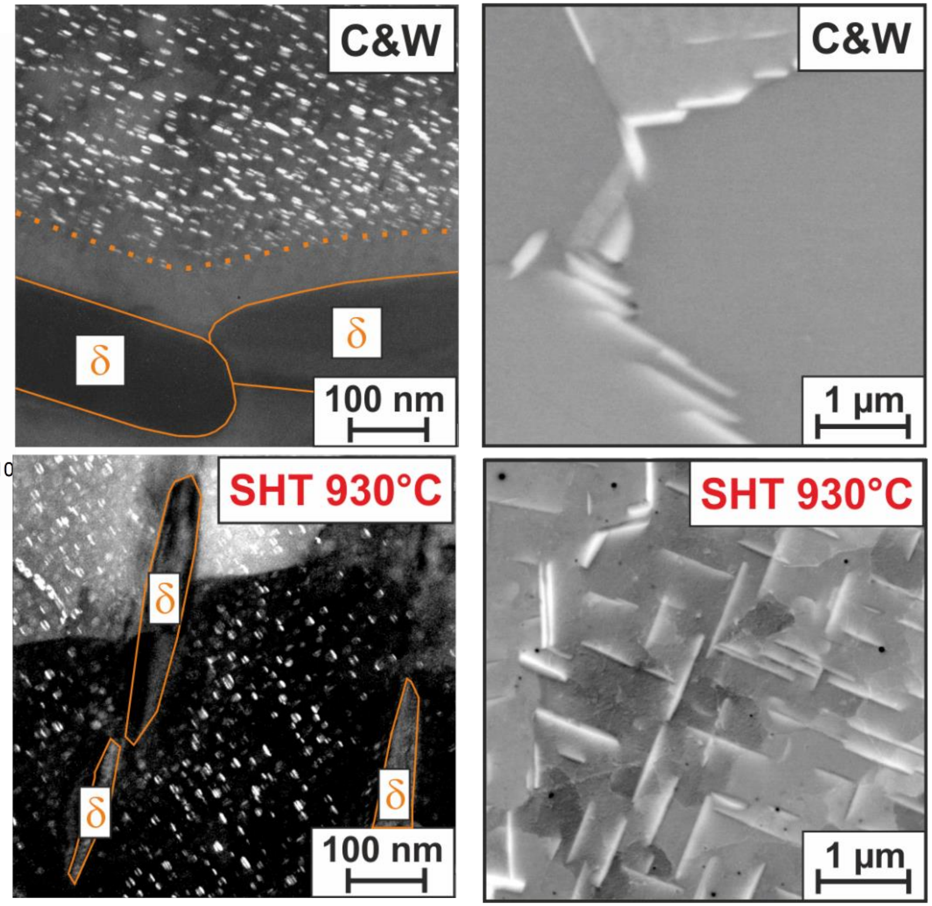

3.5 % δ

5.8 % δ but
- **finer δ**
- **subgrains**
- **smaller γ″ depleted zone**

Conventional **C&W** material:

- δ phase is necessary to pin the grain boundaries during RX
- Less Nb is available for the precipitation strengthening phase γ''

SLM material:

- δ phase is not necessary
  $\rightarrow$ heat treatments can be adjusted
- More Nb is available for solid solution hardening and the formation of strengthening γ'' precipitates

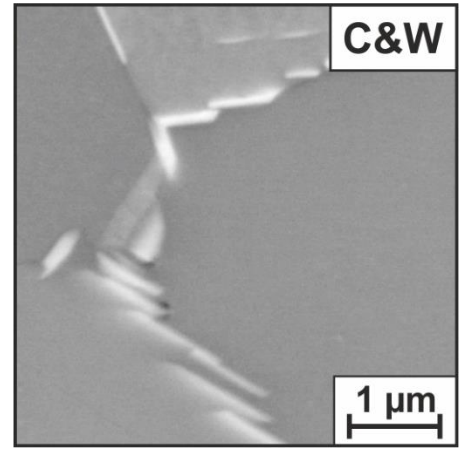

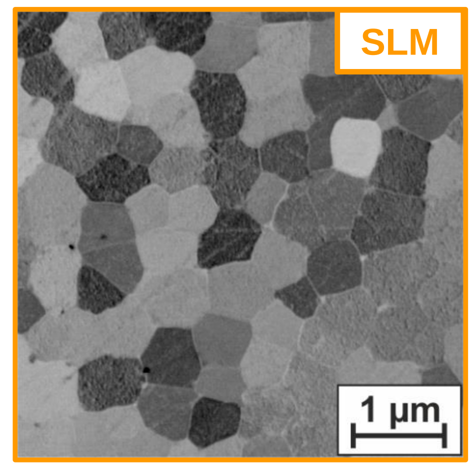

➡ **Higher creep strength of SLM IN718**

Single laser 400 W

Microstructure

➔ EBSD IPF

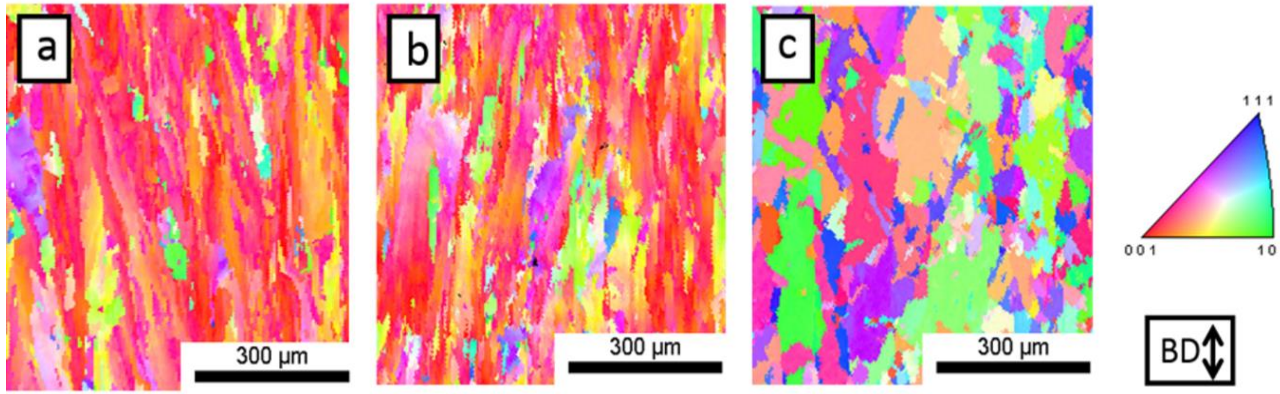

as-built solutionized HIP

Similar to 316L

UNIKASSEL VERSITÄT

Post-treated conditions

Nomenclature	Condition	Details
S	Solution annealed	1000 °C/1 h/Air Cooling (AC)
H	Hot isostatically pressed (HIPed)	1150 °C/1000 bar/4 h/Furnace Cooling (FC)
S+A	Solution annealed +aged	1000 °C/1 h/AC + 720 °C/8 h /FC at 50 °C/h to 621 °C + 621 °C/8 h /AC
H+A	HIPed+Aged	HIPed + 720 °C/8 h/FC at 50 °C/h to 621 °C + 621 °C/8 h/AC
P+H	Arc-PVD+HIPed	1000 °C/1 h/AC + Arc-PVD(Ni-20Cr) + HIPed
P+H+A	Arc-PVD+HIPed+Aged	1000 °C/1 h/AC + Arc-PVD(Ni-20Cr) + HIPed + 720°C/8 h/FC at 50 °C/h to 621 °C + 621 °C/8 h/AC

Optical microscopy

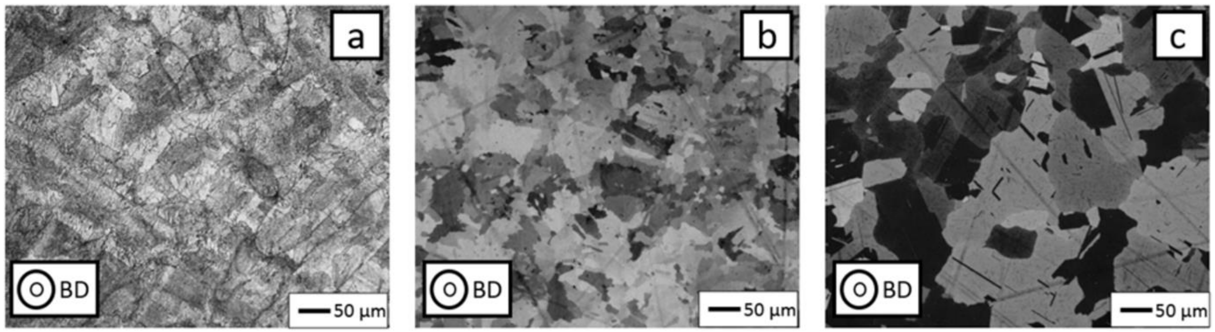

as-built solutionized HIP

Recovery

Recrystallization

Microstructure details?

as-built

Computer tomography (CT)

Resolution limit: 8 µm

HIP

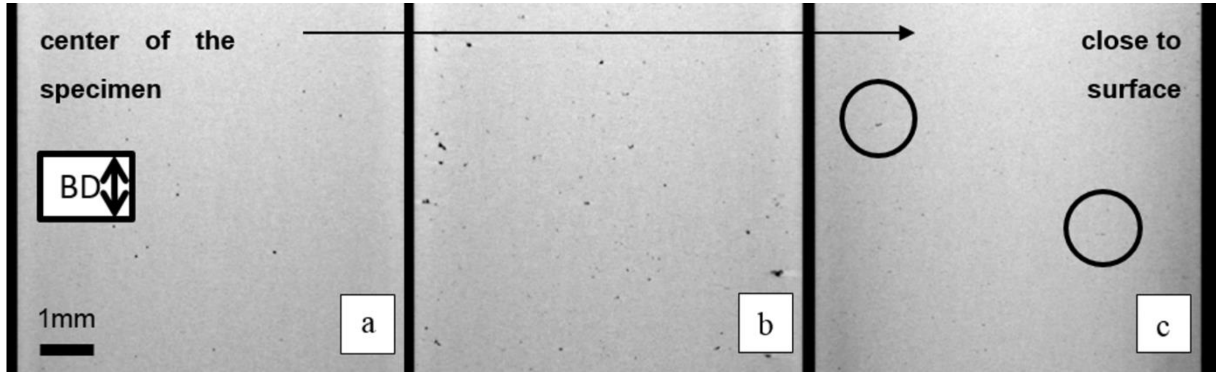

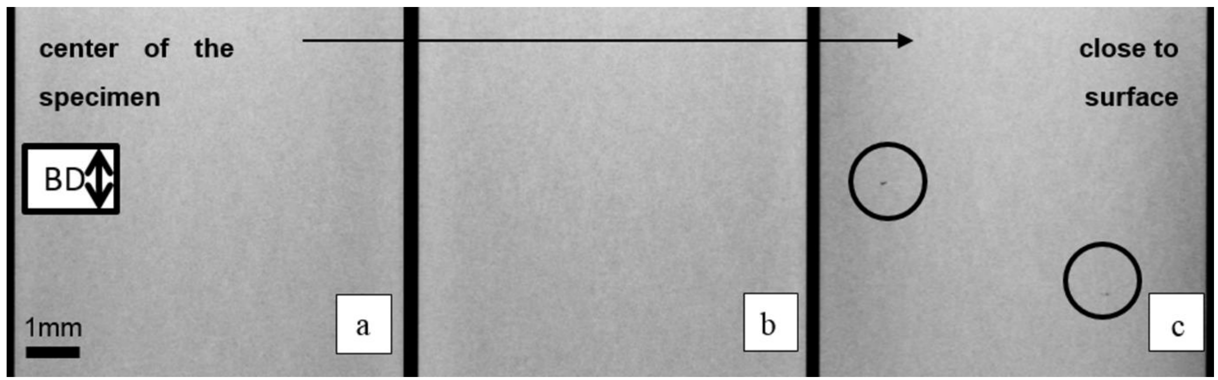

Low degree of porosity ➔ BUT: local differences

➔ Most critical: porosity close to the surface cannot be eliminated by HIP

 M.E. Aydinöz et al., Mater. Sci. Eng. A669, 2016, 246-258.

UNIKASSEL VERSITÄT

Tensile tests

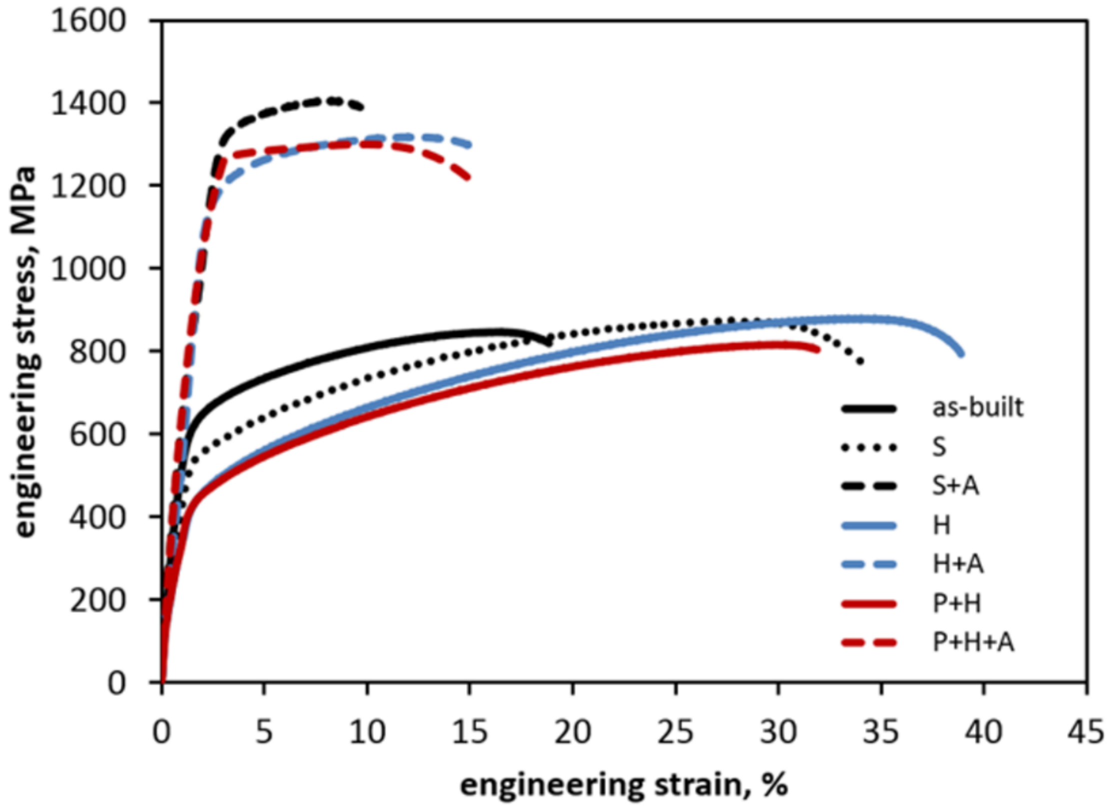

 M.E. Aydinöz et al., Mater. Sci. Eng. A669, 2016, 246-258.

IN 718 –Fatigue

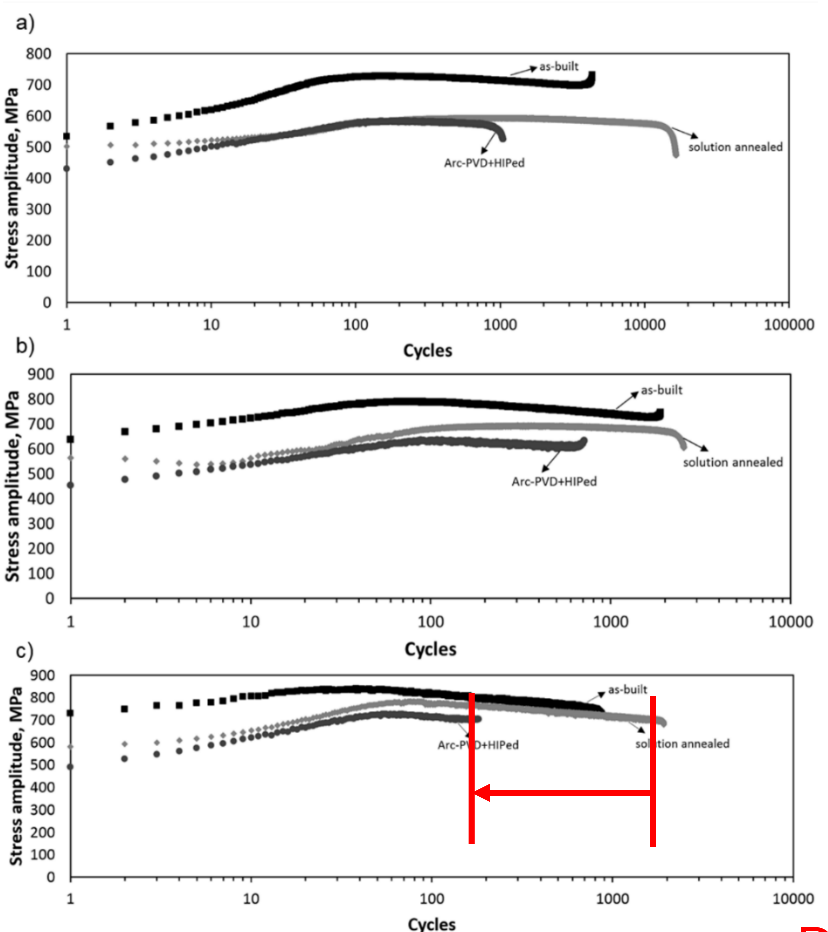

0.35 %

0.5 %

0.8 %

LCF- strain controlled
Stress response

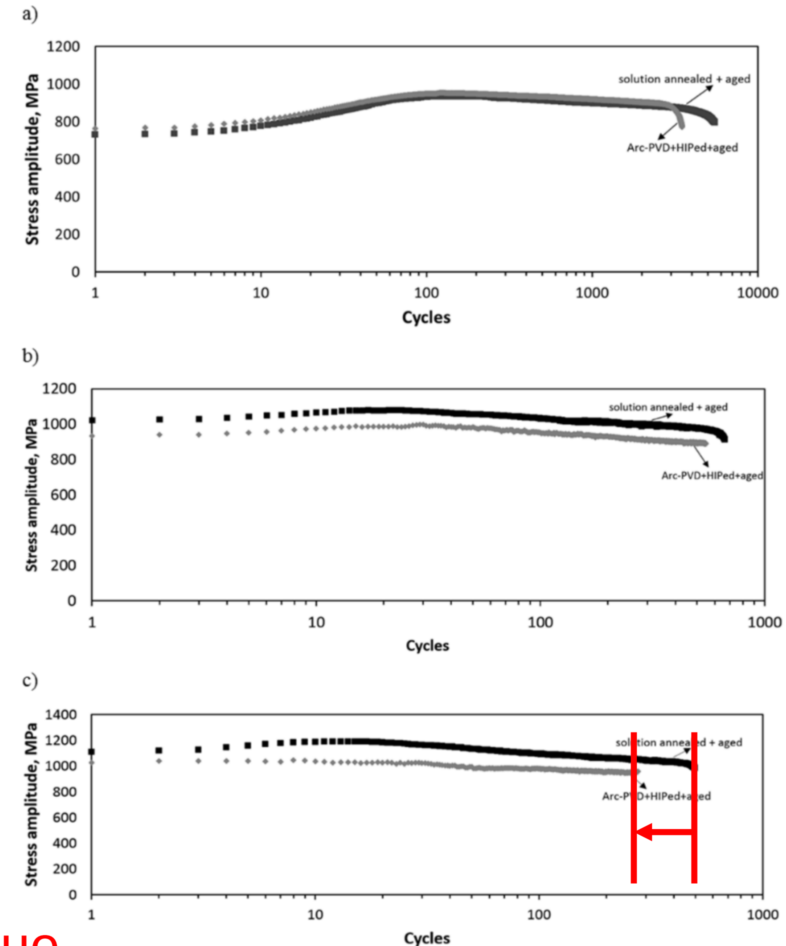

Decrease of fatigue lives upon HIP

As-built, solutionized, HIP; Non-aged

Aged conditions

LCF- strain controlled
Half-life hysteresis

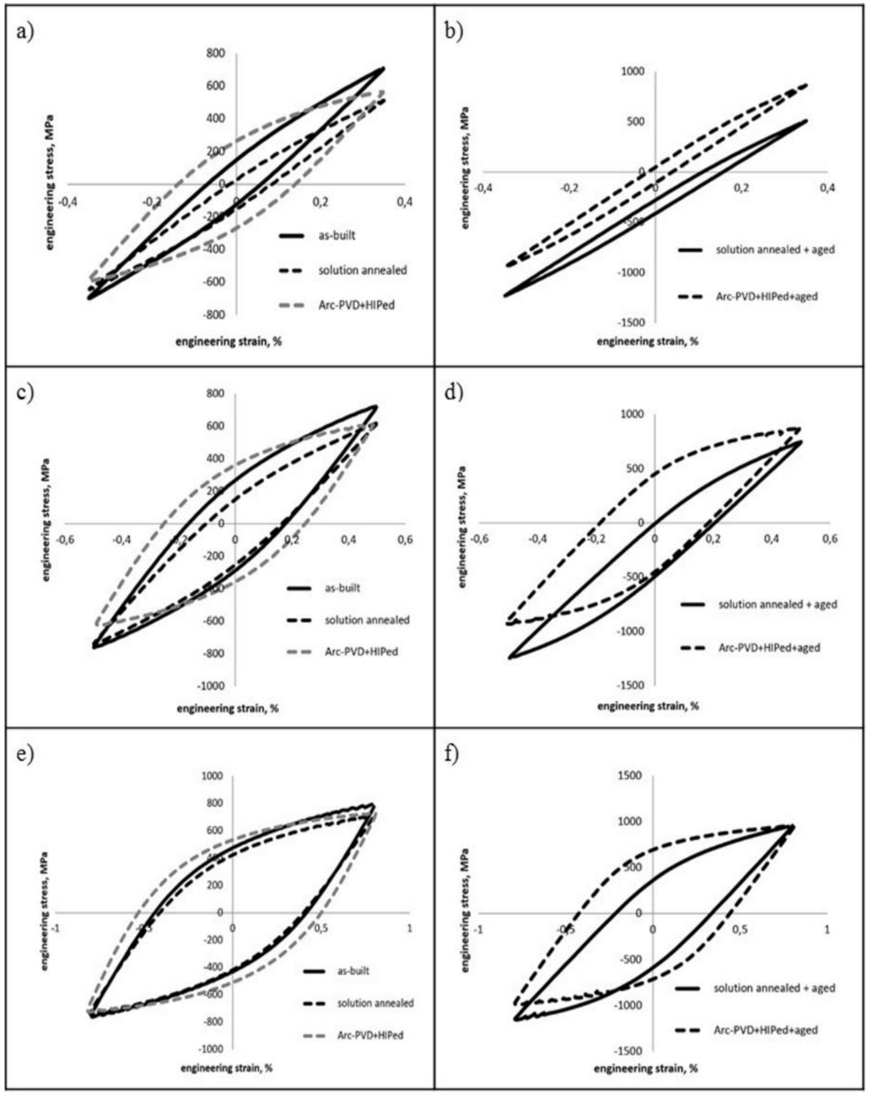

Key parameter:

- Plastic strain
- Mean stress

Energy dissipation per cycle strongly increases upon HIP

 M.E. Aydinöz et al., Mater. Sci. Eng. A669, 2016, 246-258.

Microstructure design in Ni-based alloys

➔ Thermal stability during solutionizing?

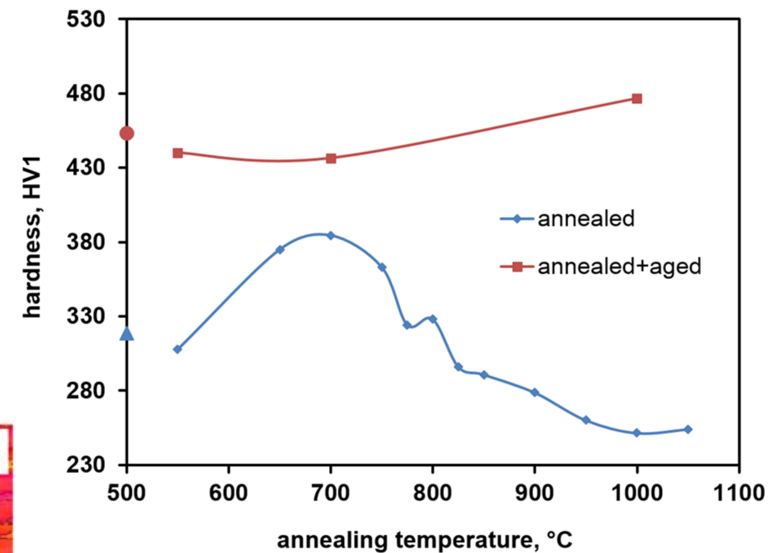

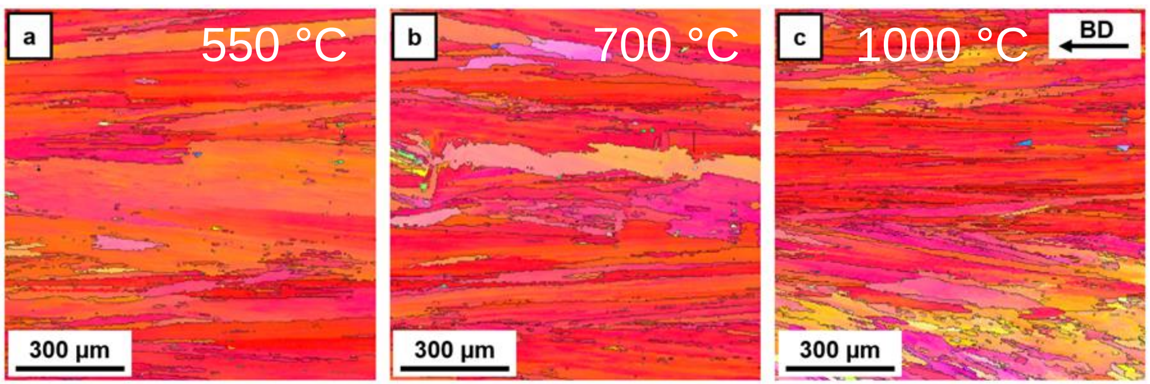

➔ EBSD: Hardly any change in microstructure up to 1000 °C
➔ BUT: Significant changes in hardness

Microstructure on different length scales

- ➔ Sub-structures
- ➔ Laves-Phase
    - ➔ Partially dissolved upon solutionizing at 1000 °C

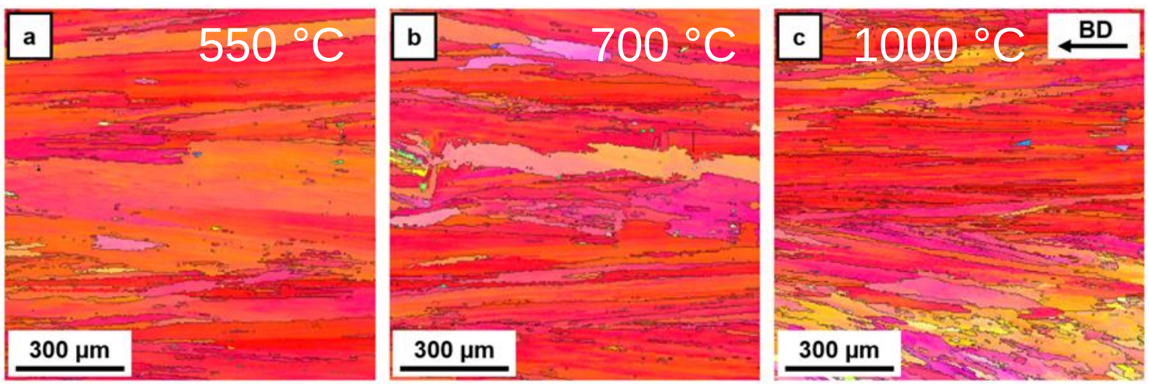

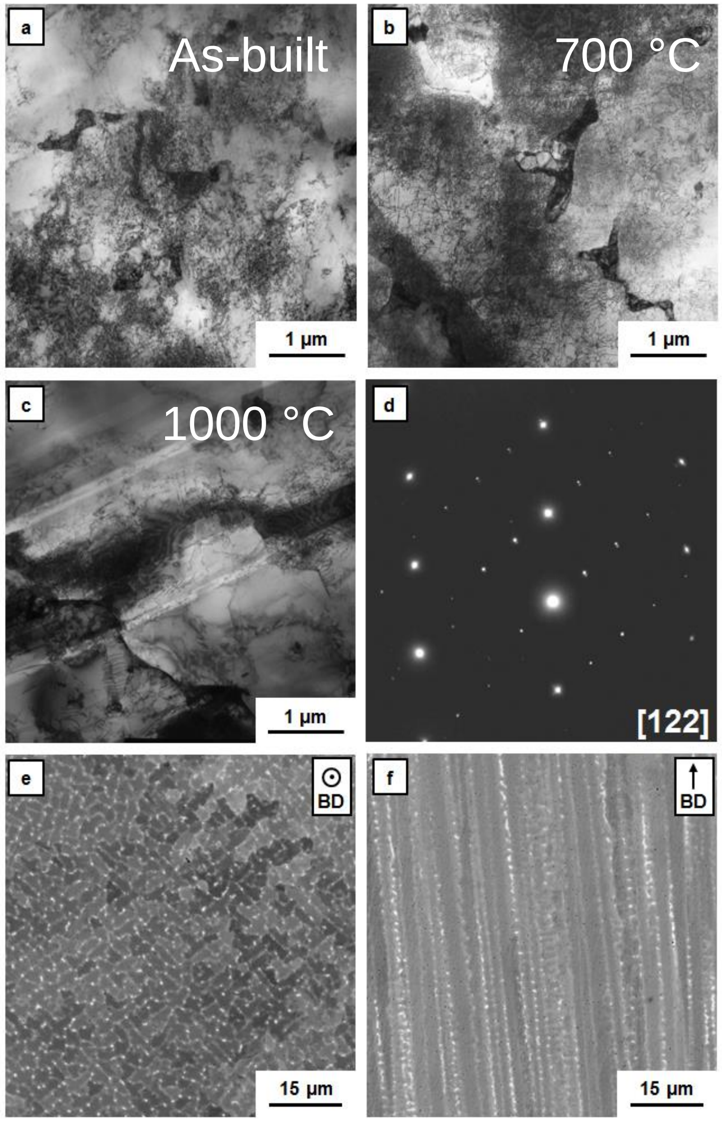

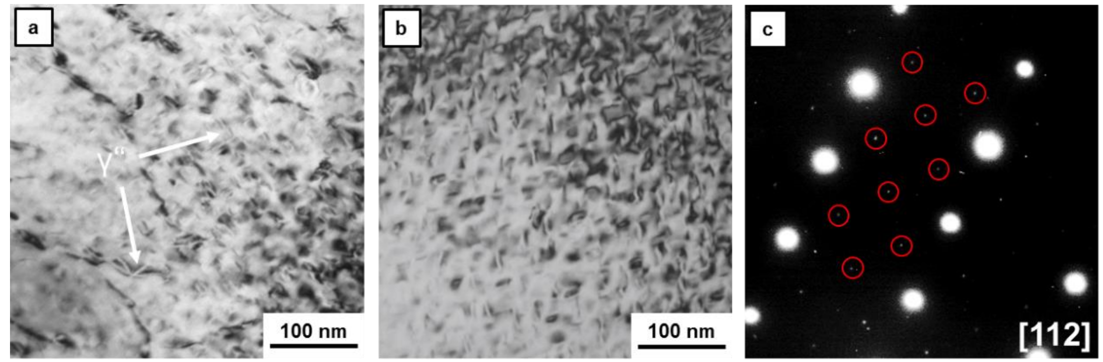

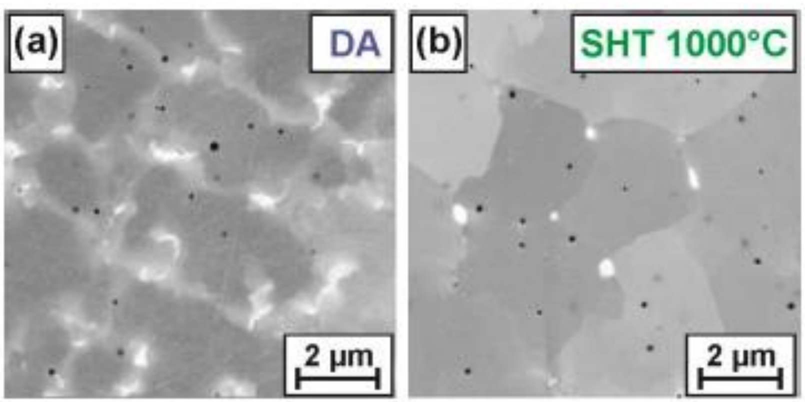

Microstructure on different length scales

- ➔ Sub-structures
- ➔ Laves-Phase
  - ➔ Partially dissolved upon solutionizing at 1000 °C
- ➔ γ ”-phase evolves upon aging

 F. Brenne et al., Progr. Additive Manufacturing, 2016, *in press*.

Tensile tests:
In good agreement with hardness evolution

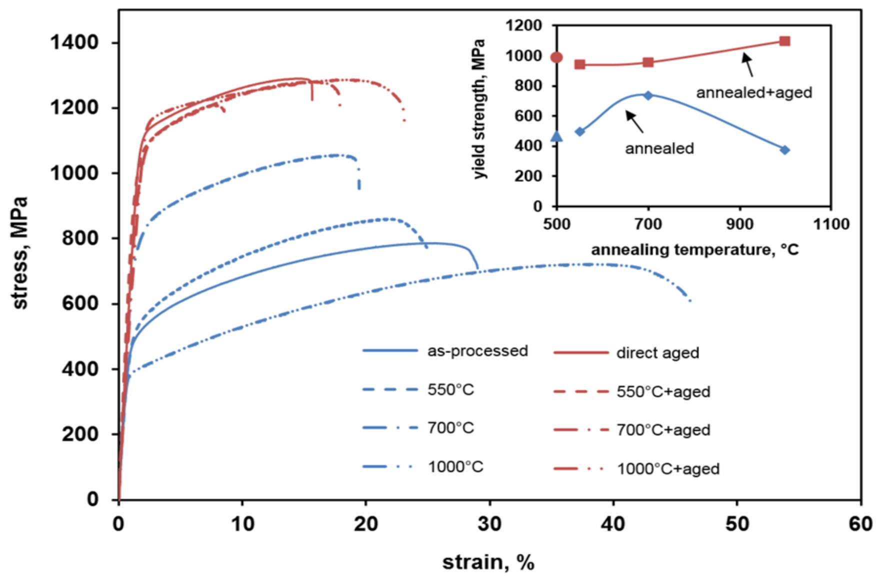

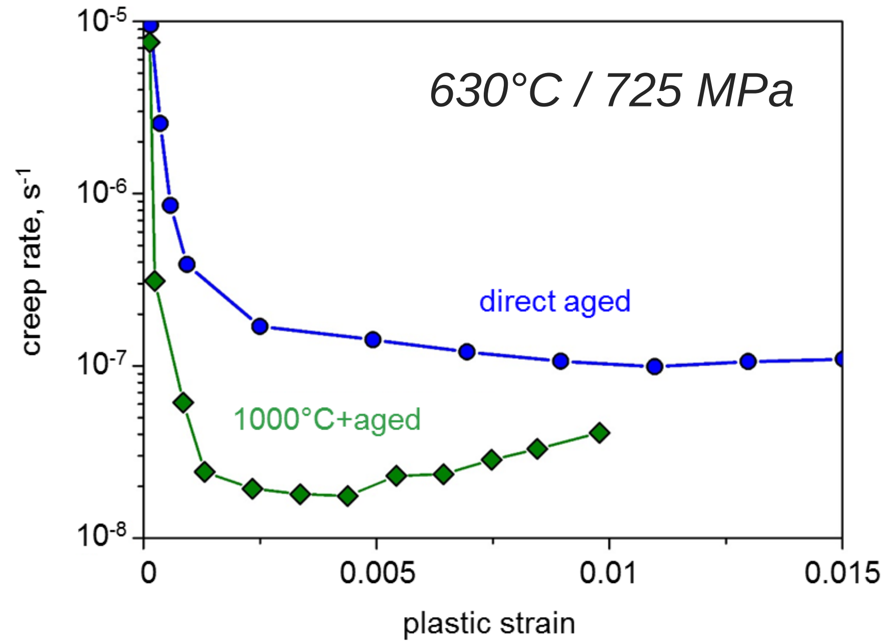

Compression creep:

➔ Laves-Phase detrimentally affects creep rate

➔ Inferior to the fine grained condition

1. Stainless steel 316L

2. Ni-based alloy IN 718

3. High-Mn Fe-based alloys

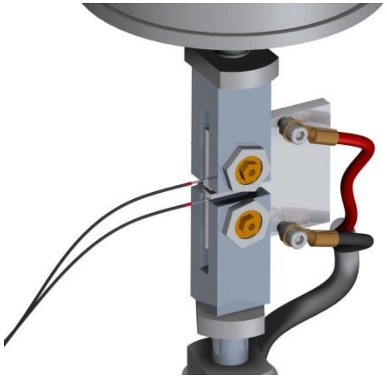

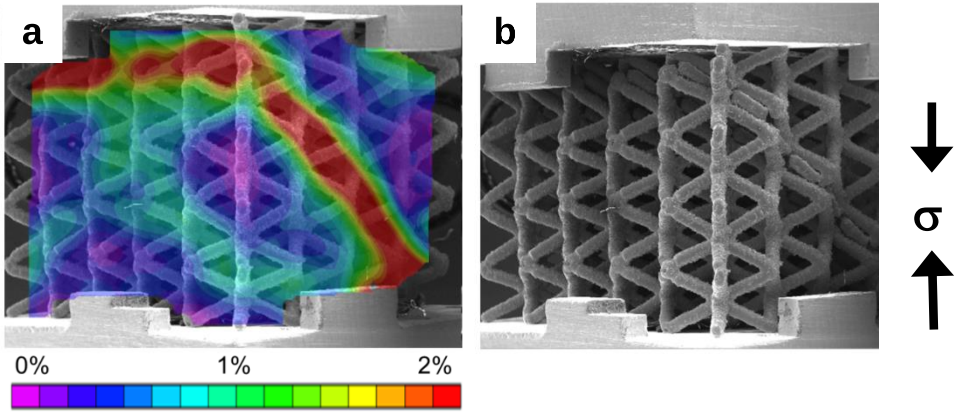

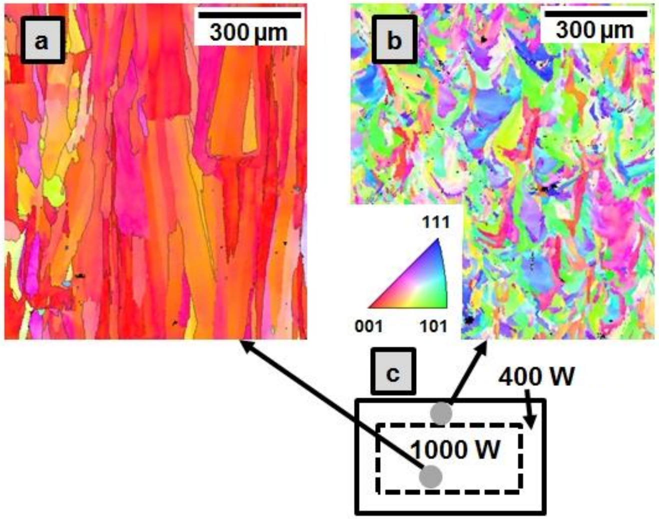

New Materials processed by Additive Manufacturing

- Fe-based alloys

- TWIP steel
  ➔ delayed necking due to twinning
  ➔ extreme ductility
  ➔ high hardening capability

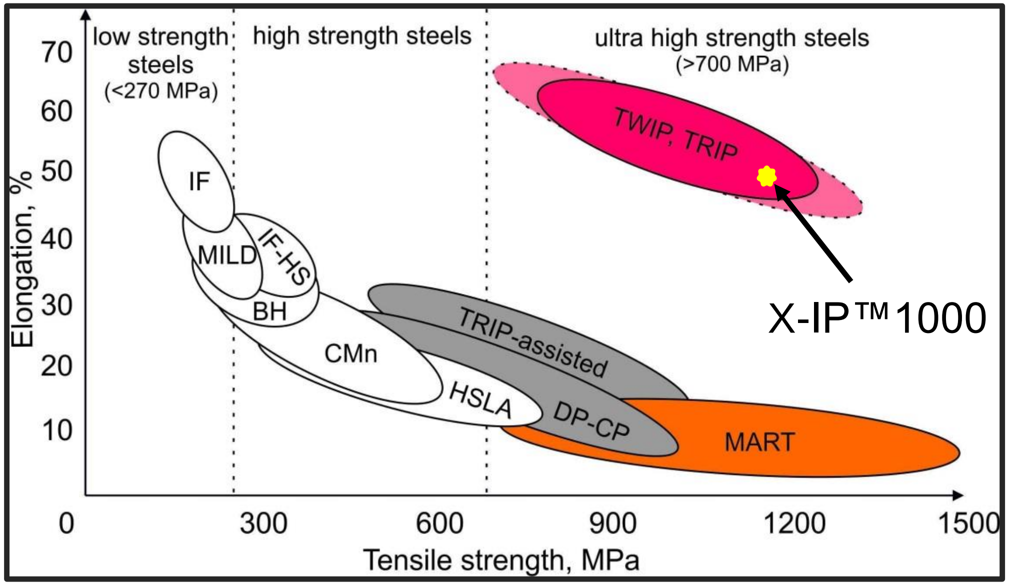

Main goals

- Determination of mechanical performance and microstructural characteristics
  - after SLM
  - after heat treatment

→ Comparison to thermo-mechanically processed blanks

Powder processing

➔ TLS Technik, Bitterfeld

Process parameters

➔ Same as for 316L stainless steel

Heat treatment
(aiming in recrystallization)

- In vacuum atmosphere
- 1h, 1050°C

Specimen geometry

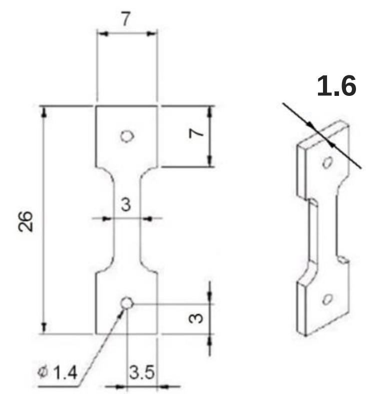

Bulk material

Microstructure – Scanning electron microscopy

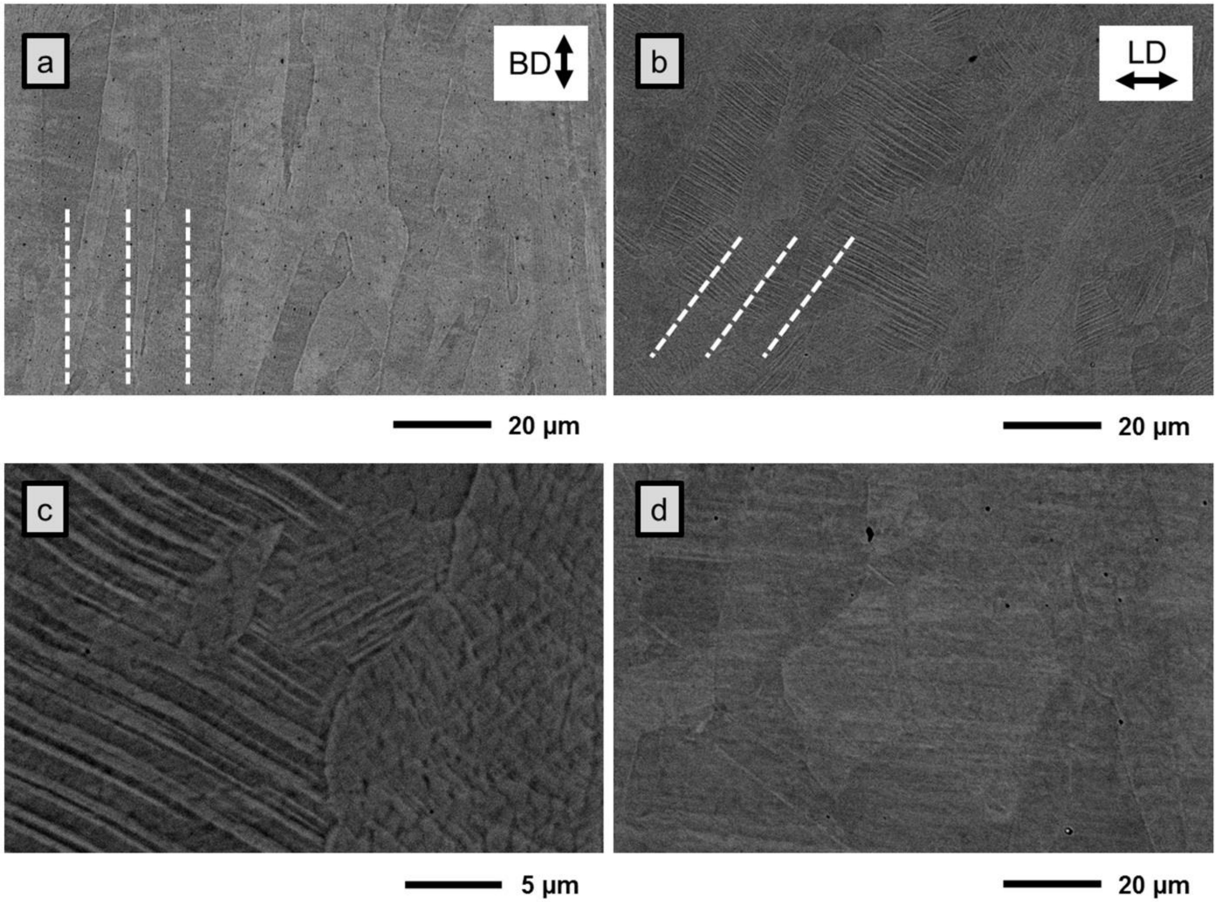

- Fairly large grains (Reference material from blank: 2-5 µm)
- Grains elongated parallel to BD
- Parallel features following deformation in numerous grains ➔ Twins?
- Dislocation cells in several grains
  ➔ submicron-scale
- Following heat treatment
  ➔ large equiaxed grains

 T. Niendorf et al., Mater. Character. 85, 2013, 57-63.

Microstructure – Scanning electron microscopy - EBSD

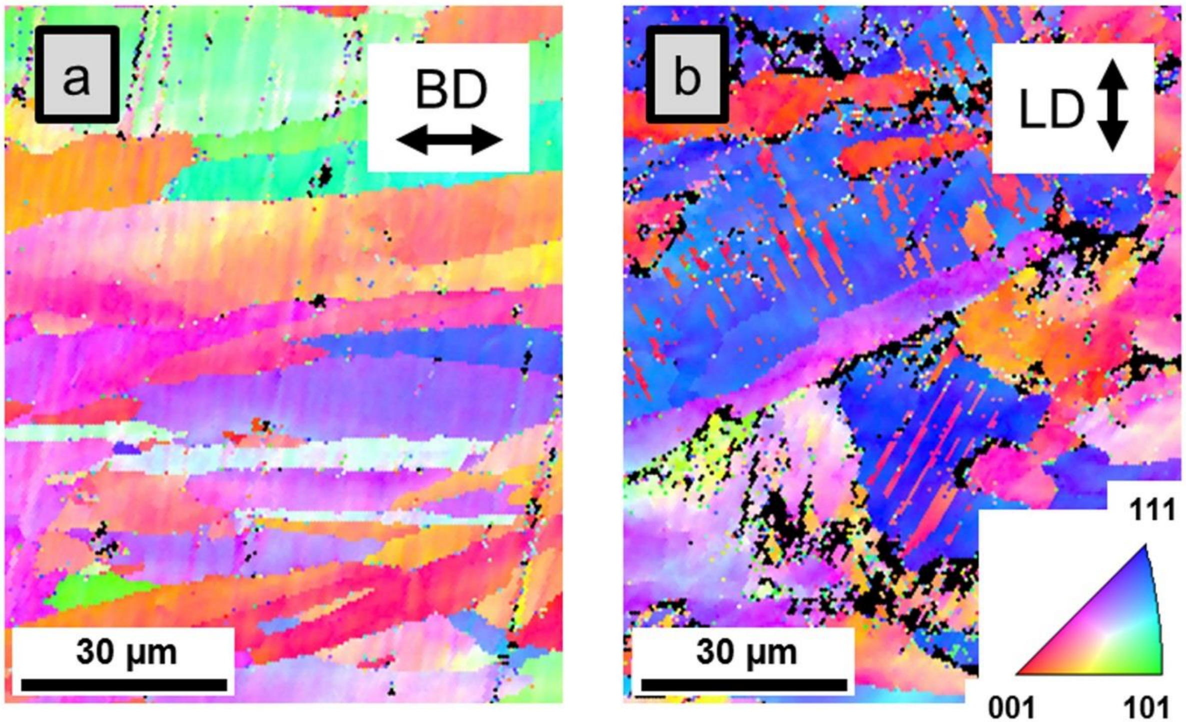

- Orientations plotted for LD
- Weak local texture for As-built
- Following deformation
  ➔ <111> <001> texture
- Slip and twinning

  ➔ TWIP effect

Microstructure – X-ray diffraction

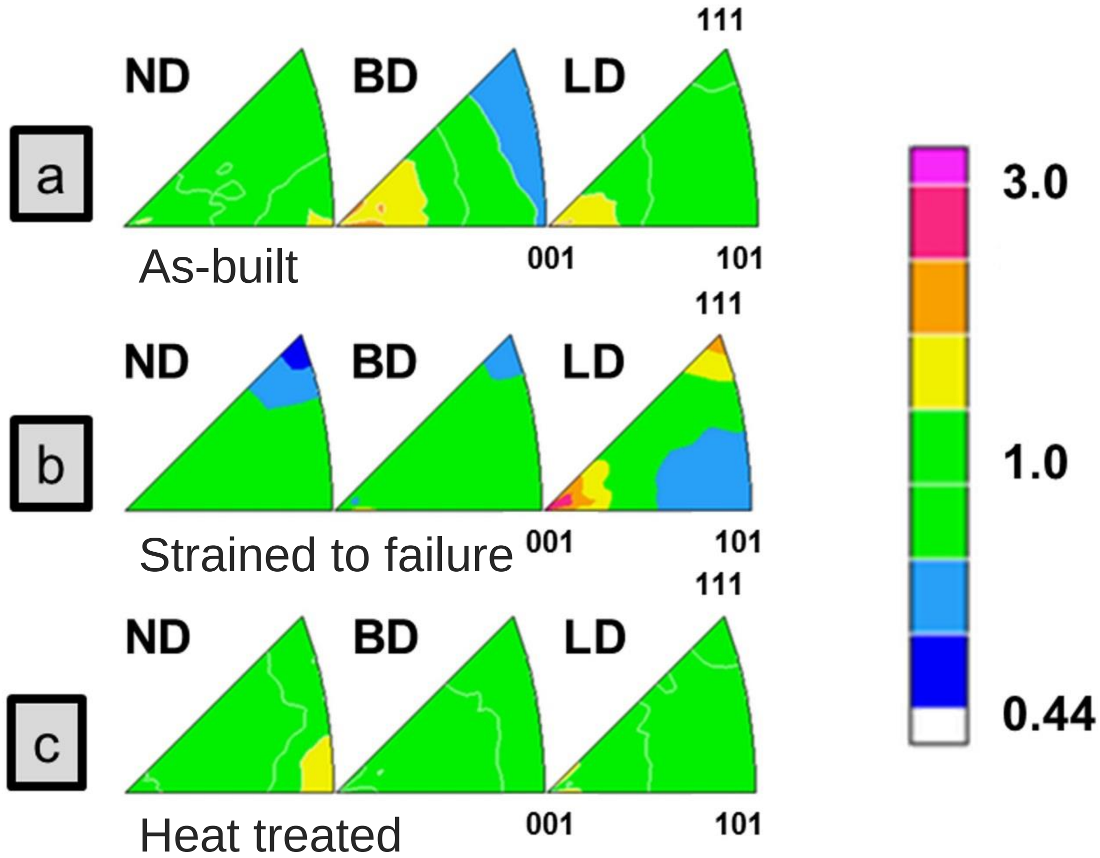

- BD dominated by <001> in as-built
- <001> <111> in LD following deformation
  ➔ Slip and twinning ➔ TWIP
- Randomization following heat treatment

Mechanical properties

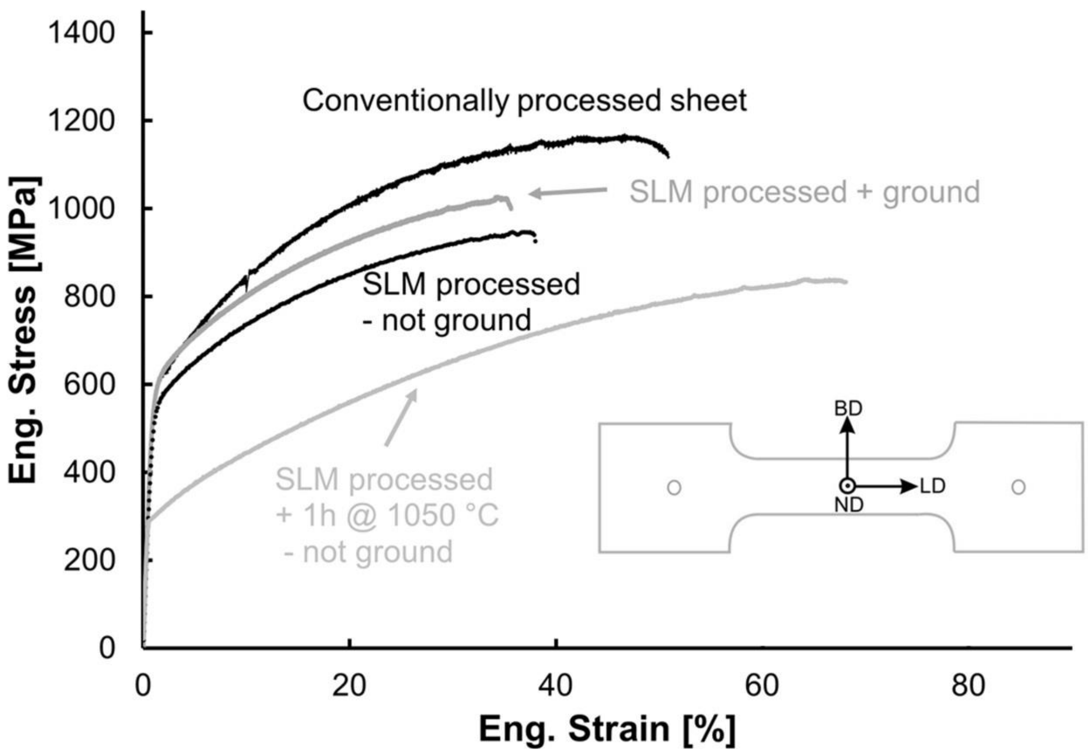

- Reference: Conventionally processed sheet; UTS: 1160 MPa Elongation to failure: ~50 %
- Not ground SLM processed TWIP steel ➔ slightly lower values
- SLM processed + ground ➔ almost equal
- Further increase of ductility following heat treatment

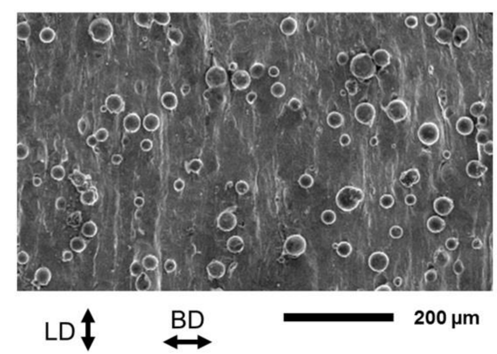

SLM TWIP steel does not suffer from surface quality

Incorrect cross-section area measured by use of caliper gauge

 T. Niendorf et al., Mater. Character. 85, 2013, 57-63.

Mechanical properties

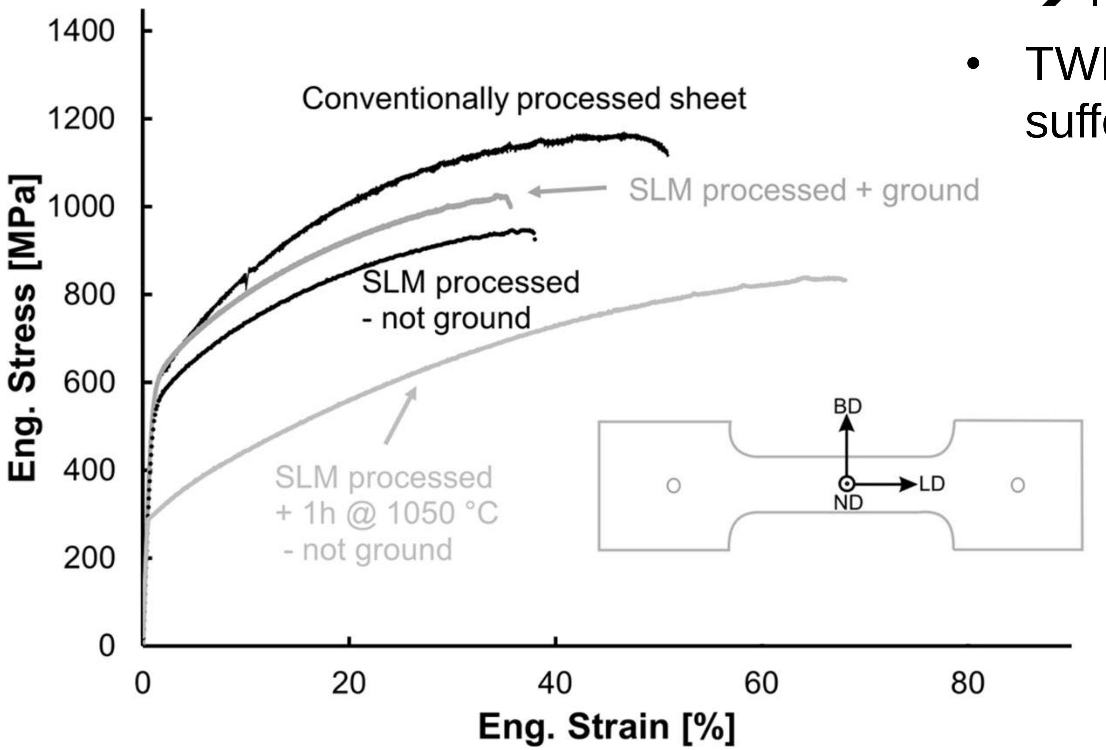

- Dimple like fracture
  ➔ high ductility
- TWIP steel does not severely suffer pores

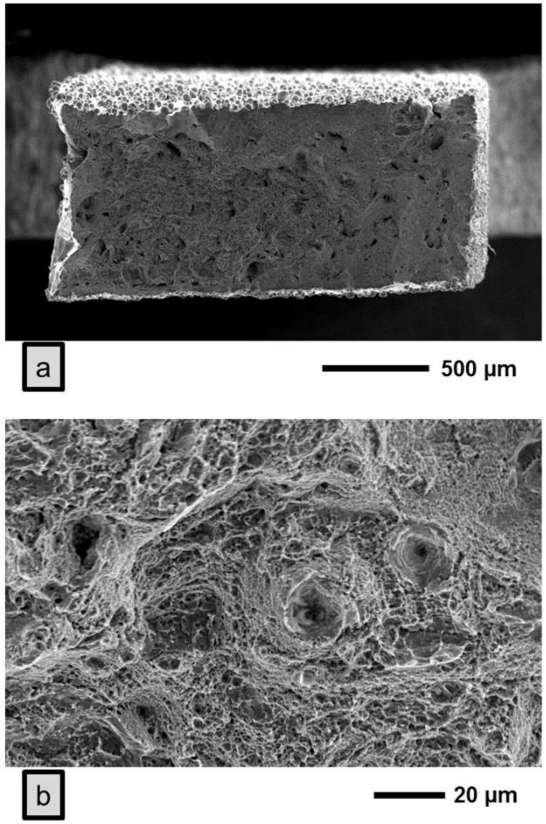

TWIP steel

Microstructure:

→ **elongated grain morphology**

→ **micro-scaled substructures**

→ **<001> texture for BD**

Mechanical performance:

→ **High strength and ductility** already in the as-built condition

→ TWIP effect

Compared to thermo-mechanically processed material:
→ Similar properties

Well suited base material for future work

 T. Niendorf et al., Mater. Character. 85, 2013, 57-63.

SLM TWIP steel as base for a new alloy solely processable by AM

⇓

TWIP-Ag

⇓

Bioresorbable implants

 T. Niendorf et al. Metall. Mater. Trans. A 46, 2015, 2829-2833.

Microstructure –SEM

➔ Ag is fairly homogeneously distributed within the TWIP matrix

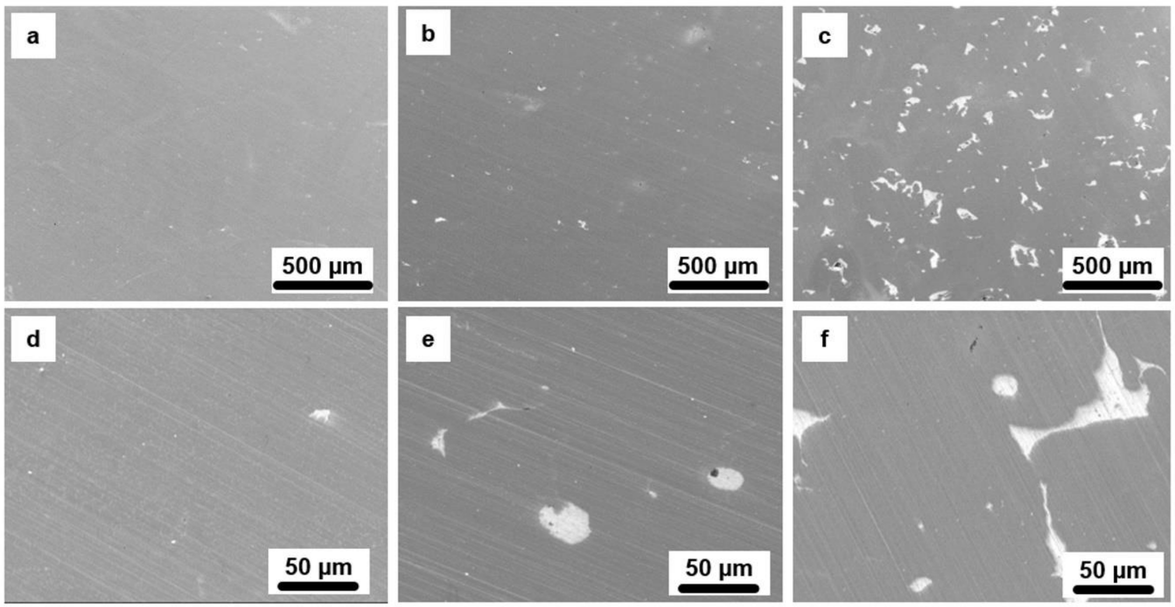

TWIP-1Ag TWIP-2Ag TWIP-5Ag

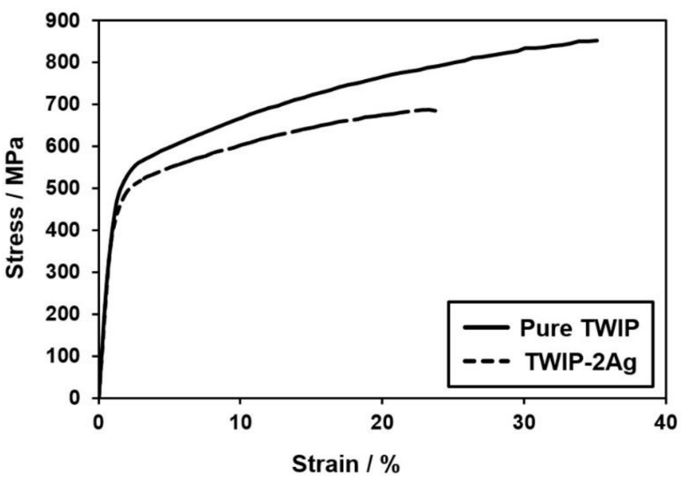

Tensile tests
➔ Good performance

 T. Niendorf et al. Metall. Mater. Trans. A 46, 2015, 2829-2833.

New materials

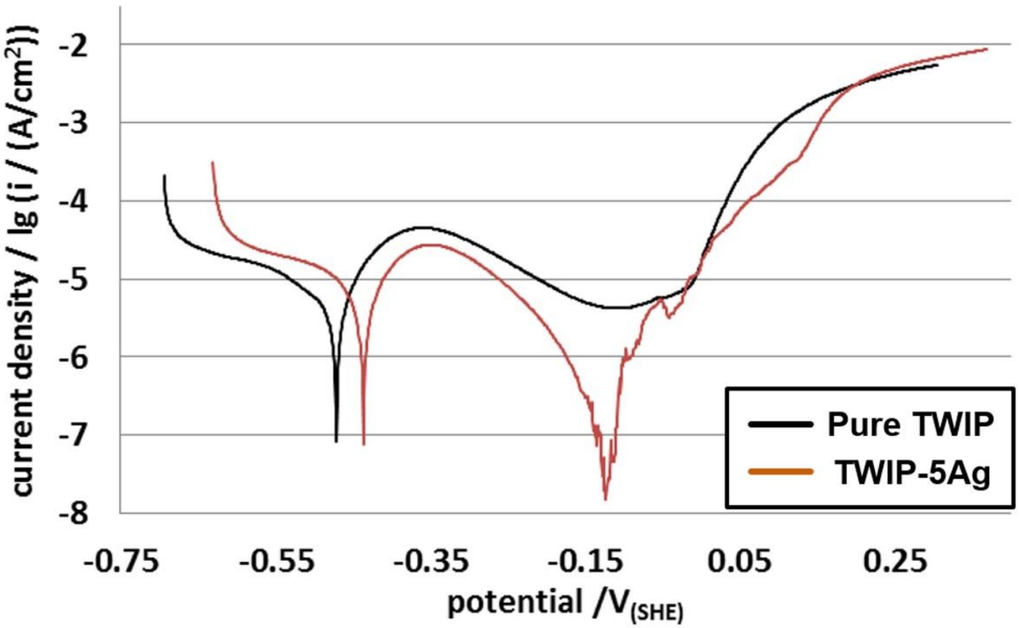

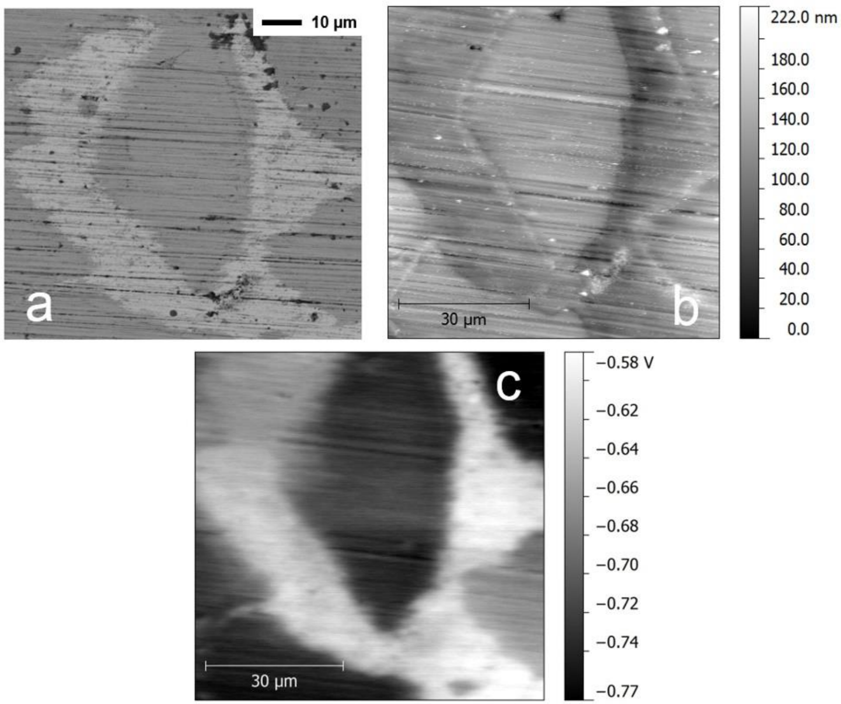

➔ Impact on the global and local corrosion behavior are evident

➔ Degradation rates in the human body should be increased

Conventionally processed Fe-Mn-Al-Ni SMAs

- α (BCC) - γ´ (FCC) phase transformation
- Max. transformation strain 12 % ([123] oriented single crystal)
- Theoretical transformation strains:
  - 26.5 % (Tension, [001])

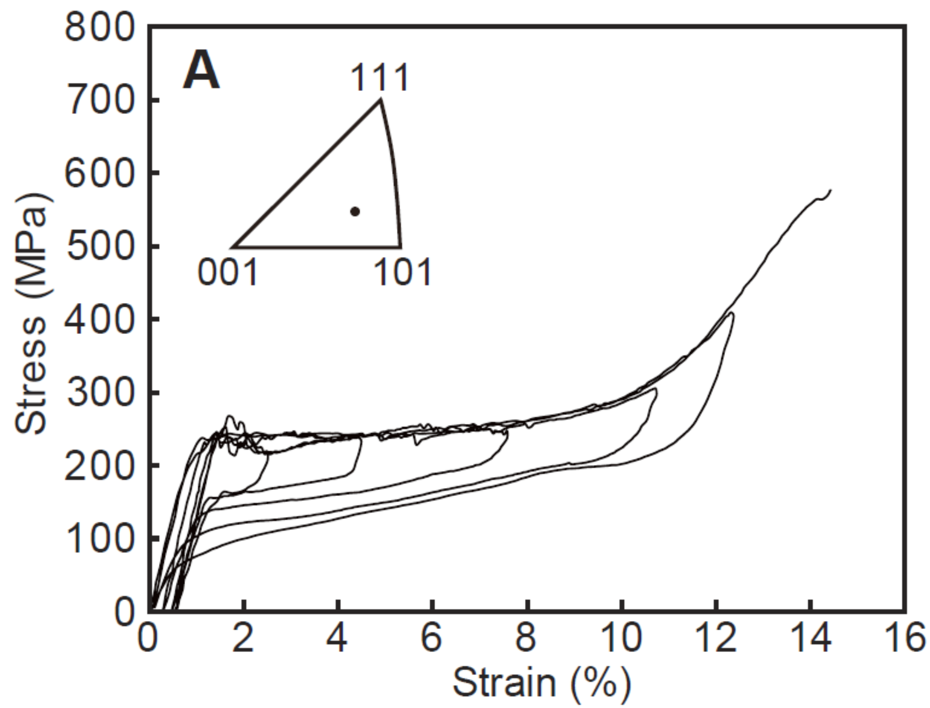

PE-Hystereses, Strain-Increase Test, Fe-Mn-Al-Ni, single crystal

Ref.: Omori et al., Science 2011

Fe-based shape memory alloys

Conventionally processed Fe-Mn-Al-Ni SMAs

β-precipitate: B2 (NiAl)

- Precipitation of β-phase particles induced by ageing at 200°C
  ⇨ *Pre-requisite for thermo-elastic martensitic transformation*

- α (BCC) - γ´ (FCC) phase transformation

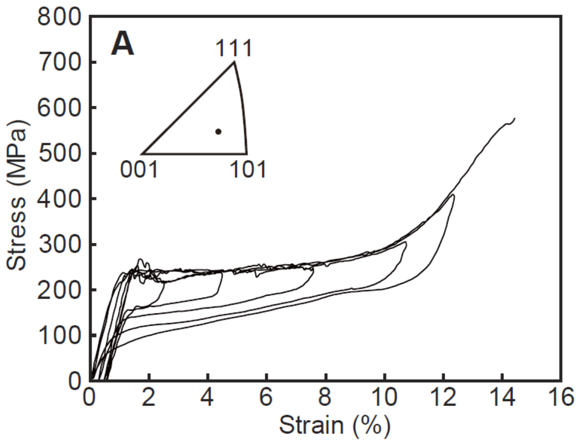

Ref.: Omori et al., APL 2012

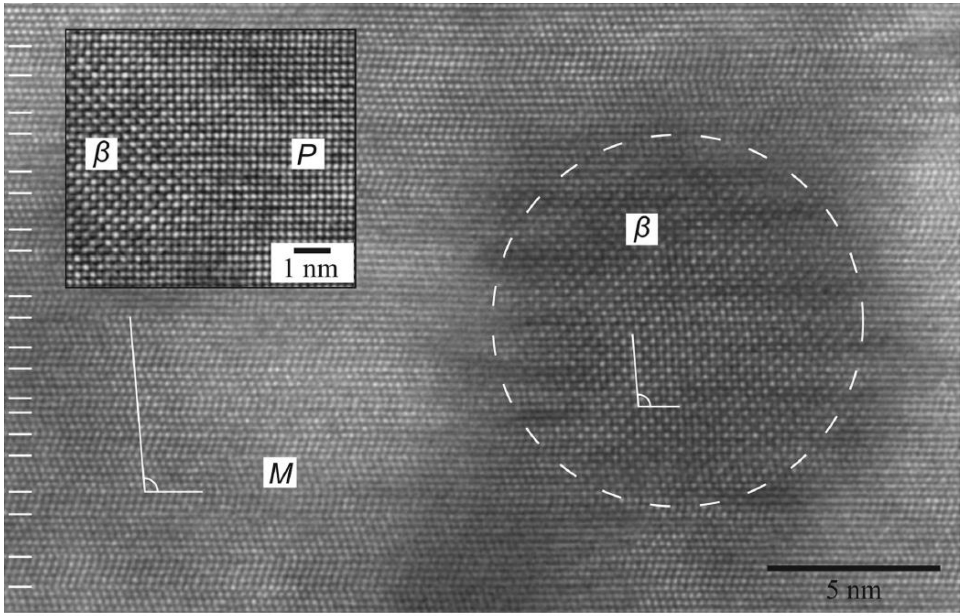

HR-TEM: Nano-scaled β-phase precipitates

Conventionally processed Fe-Mn-Al-Ni SMAs

- Low CC-slope (Increase of transformation stress at increasing temperature)
- Pseudoelastic temperature window 350 K

⇒ Numerous fields for application

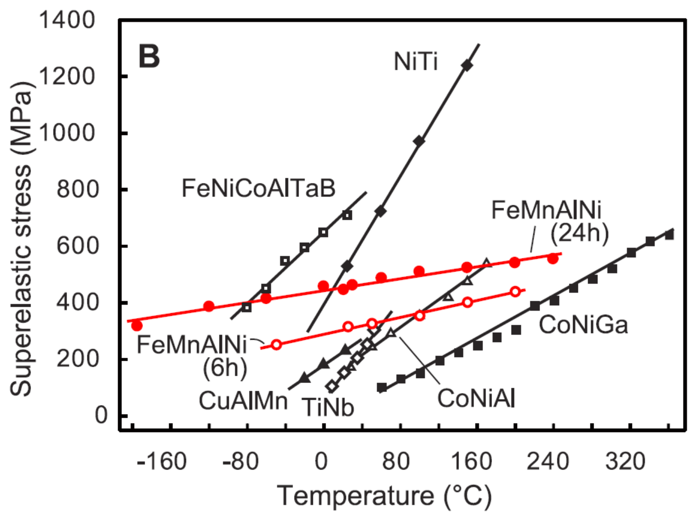

Critical transformation stresses for PE-response as a function of temperature for diverse SMAs

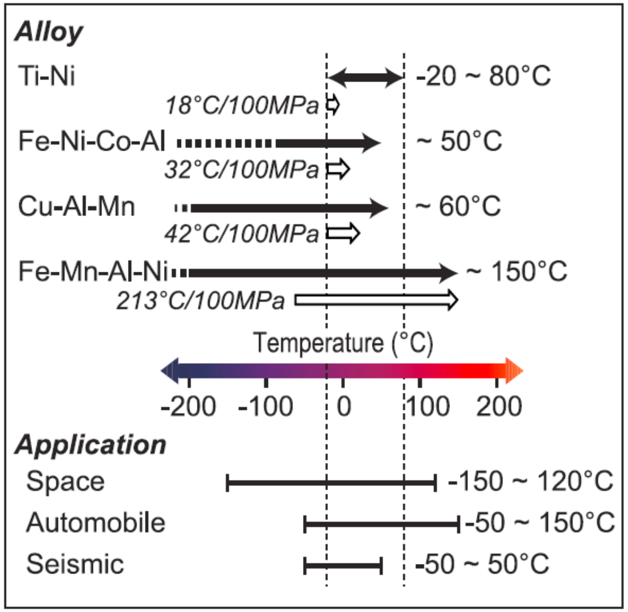

Application temperature ranges of diverse SMAs

Ref.: Omori et al., Science 2011

Conventionally processed Fe-Mn-Al-Ni SMAs

Impact of microstructure

„Bamboo“ structure

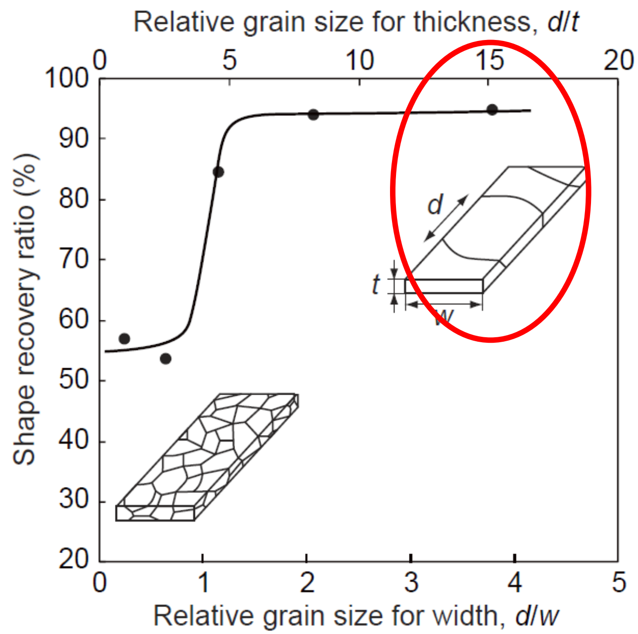

Fe-Mn-Al-Ni, Impact of grain size

Ref.: Omori et al., APL Materials 2013

Pronounced texture and coarse microstructure are needed
➔ Minimization of grain constraints

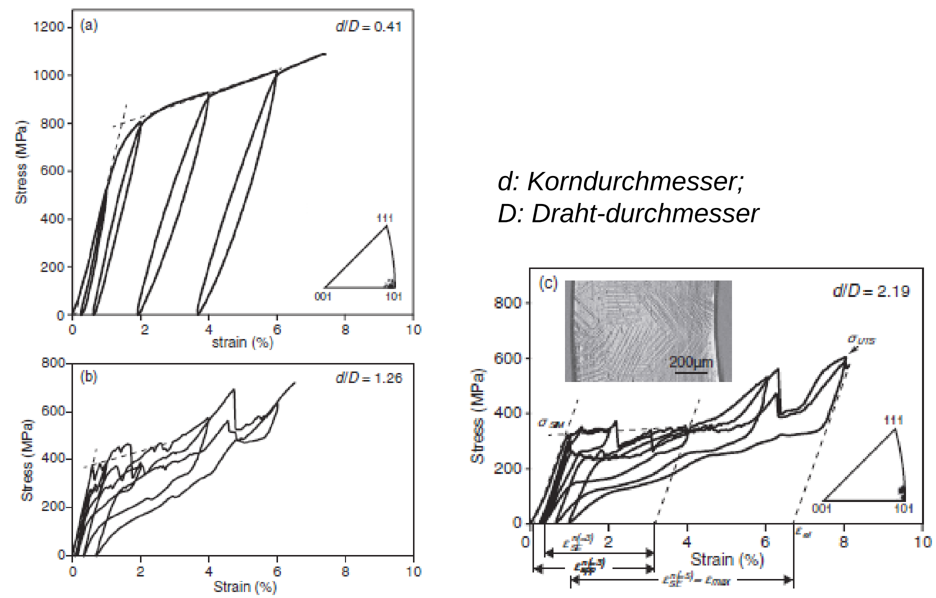

d: Korndurchmesser;
D: Draht-durchmesser

PE response of Fe-Mn-Al-Ni wires in different conditions

Fe-Mn-Al-Ni SMAs processed by SLM

- Solidification in cubic phase (bcc)
- Similar impact of processing parameters and geometry as in case of 316L

⇩

- Direct microstructure design
- BUT: Surface cracking

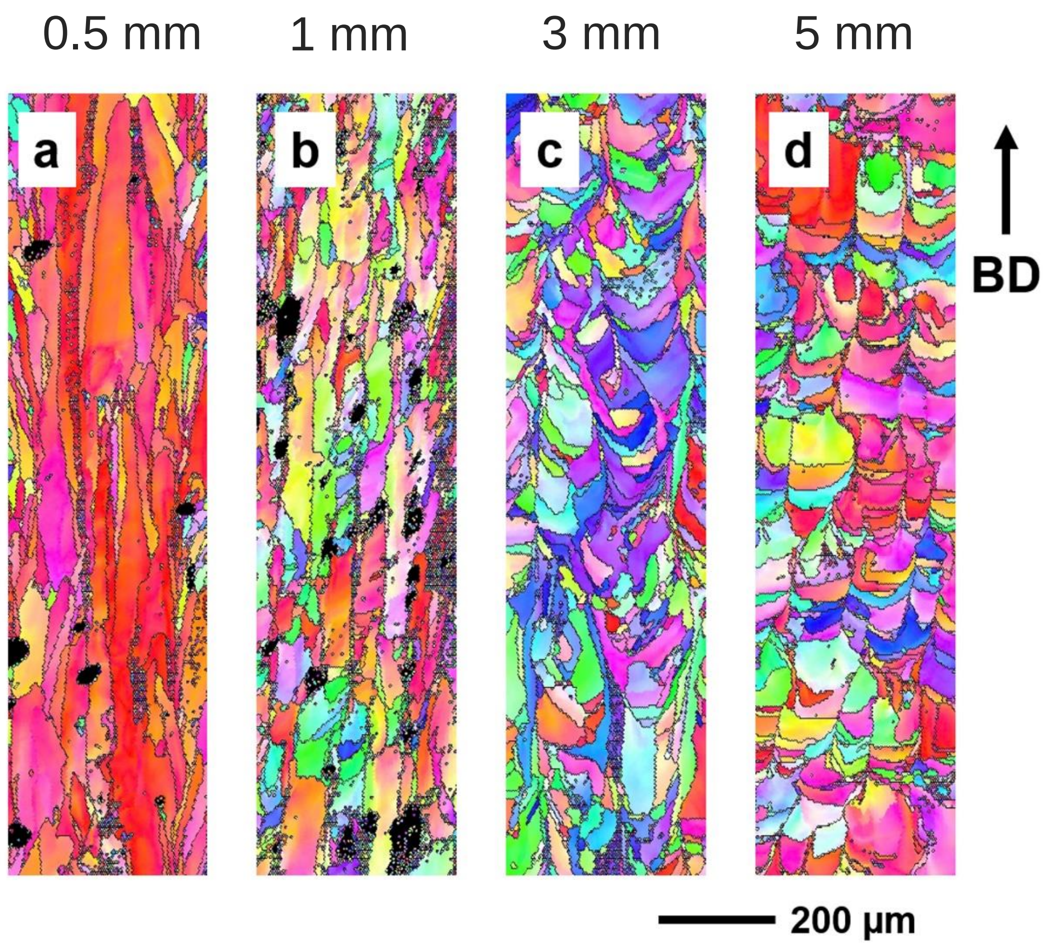

 T. Niendorf, et al. Metall. Mater. Trans. A 47, 2016, 2569-2573.

Fe-Mn-Al-Ni SMAs processed by SLM

- Plattform: 200 °C
- Evolution of β-Phase during SLM processing
- High residual stresses
- Surface cracking
- BUT: High driving force for abnormal grain growth
  ➔ bamboo structures

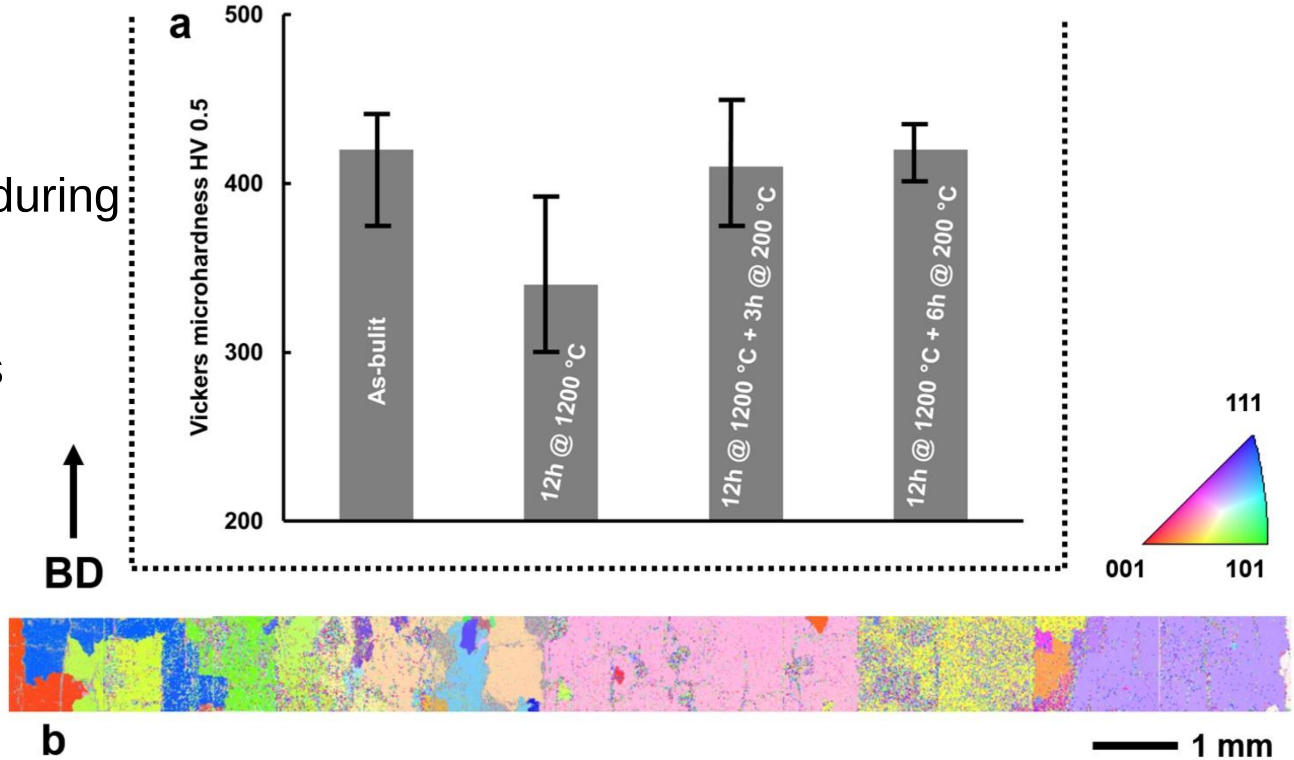

Fe-Mn-Al-Ni SMAs processed by SLM

- Strain increase test under compressive load at -100 °C

- Pseudoelastic response

- Reversible strain up to 7 %

- BUT: Rapid functional degradation

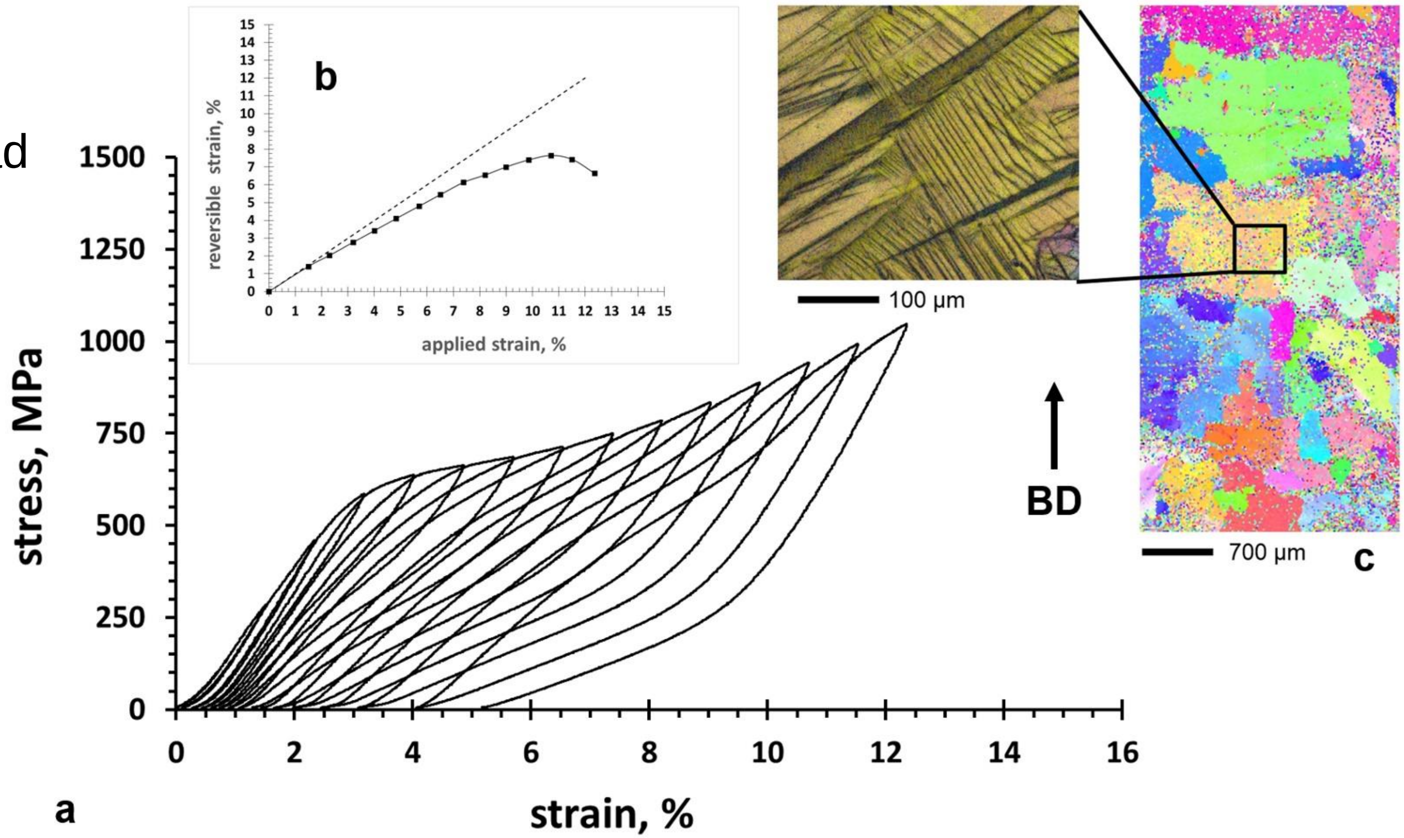

T. Niendorf, et al. Metall. Mater. Trans. A 47, 2016, 2569-2573.

References

- **T. Niendorf**, F. Brenne: *Steel showing twinning-induced plasticity processed by selective laser melting - An additively manufactured high performance material*, Materials Characterization 85, 2013, 57-63.
- **T. Niendorf**, S. Leuders, A. Riemer, H.A. Richard, T. Tröster, D. Schwarze: *Highly anisotropic steel processed by selective laser melting*, Metall. Mater. Trans. B 44, 2013, 794-796.
- P. Kanagarajah, F. Brenne, **T. Niendorf**, H.J. Maier: Inconel 939 processed by Selective Laser Melting: Effect of microstructure and temperature on the mechanical properties under static and cyclic loading, Mater. Sci. Eng. A 588, 2013, 188-195.
- A. Riemer, S. Leuders, M. Thöne, H.A. Richard, T. Troester, **T. Niendorf**: *On the fatigue crack growth behavior in 316L stainless steel manufactured by selective laser melting*, Eng. Fract. Mech. 120, 2014, 15-25.
- S. Leuders, T. Lieneke, S. Lammers, T. Tröster, **T. Niendorf**: *On the fatigue properties of metals manufactured by Selective Laser Melting – The role of material ductility*, J. Mater. Res. 29, 2014, 1911-1919.
- **T. Niendorf**, S. Leuders, A. Riemer, F. Brenne, T. Tröster, H.A. Richard, D. Schwarze: Functionally graded alloys obtained by additive manufacturing, Adv. Eng. Mater. 16, 2014, 857-861.
- **T. Niendorf**, F. Brenne, P. Hoyer, D. Schwarze, M. Schaper, R. Grothe, M. Wiesener, G. Grundmeier, H.J. Maier: *Processing of new alloys by additive manufacturing – Iron-based alloys containing silver for biomedical applications*, Metall. Mater. Trans. A 46, 2015, 2829-2833.
- **T. Niendorf**, F. Brenne, P. Krooß, M. Vollmer, J. Günther, D. Schwarze, H. Biermann: *Microstructure evolution and functional properties of Fe-Mn-Al-Ni shape memory alloy processed by selective laser melting*, Metall. Mater. Trans. A 47, 2016, 2569-2573.
- M.E. Aydinöz , F. Brenne, M. Schaper, C. Schaak, W. Tillmann, J. Nellesen, **T. Niendorf**: *On the microstructural and mechanical properties of additively manufactured Inconel 718 superalloy under quasi-static and cyclic loading*, Mater. Sci. Eng. A669, 2016, 246-258.
- F. Brenne, A. Taube, M. Pröbstle, S. Neumeier, D. Schwarze, M. Schaper, **T. Niendorf**: *Microstructural design of Ni-base alloys for high temperature applications – Impact of heat treatment on microstructure and mechanical properties after Selective Laser Melting*, Progress in Additive Manufacturing, 2016, *in press*.
- M. Pröbstle, S. Neumeier, J. Hopfenmüller, L.P. Freund, **T. Niendorf**, D. Schwarze, M. Göken: *Superior creep strength of Inconel 718 produced by selective laser melting*, Mater. Sci. Eng. A, 2016, *submitted*.

Acknowledgements:

- DFG and DMRC for funding
- Dr. D. Schwarze (SLM Solutions)
- E. Aydinöz, F. Brenne, P. Kanagarajah, Dr. S. Leuders, A. Riemer (University of Paderborn, DMRC)
- Dr. S. Neumeier, M. Pröbstle (Materials Science & Engineering, Institute I, FAU)

Questions?

Inconel 939

- Ni-based superalloy
- Typical material for high-temperature applications

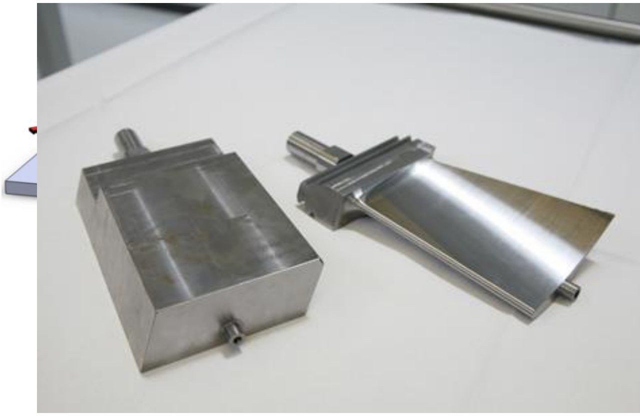

Source: www.schleifblog.de

Main goals

- Determination of microstructural characteristics
  - after SLM
  - after solution-annealing
  - after ageing
- Examination of mechanical properties
  - cyclic / montonic
  - room temperature / 750°C
  - horizontally / vertically manufactured specimens

→ Comparison to conventionally fabricated Inconel 939

Experimental procedure

Process parameters

	volume contour	volume area
hatch distance, mm	0.15	0.12
laser power, J s^{-1}	100	175
laser speed, mm s^{-1}	540	620
layer thickness, µm	30	30

Heat treatment
(standard for land-based turbine blades)

- In vacuum atmosphere
- Solution annealing: 4h, 1160°C
- Single stage ageing: 16h, 850°C

Specimen geometry

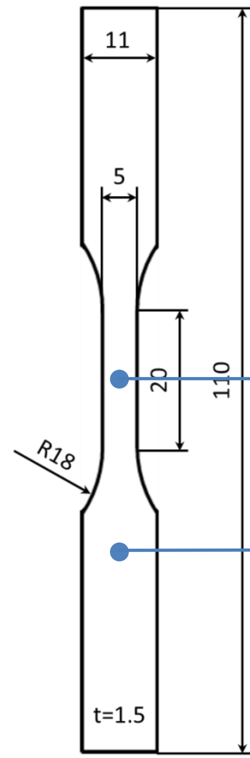

EBSD
- Grain orientation
- Grain size
- Grain boundary characteristics

TEM
- Dislocation characteristics
- Precipitates
- Local chemical compositions

Microstructure, as-built – optical microscopy

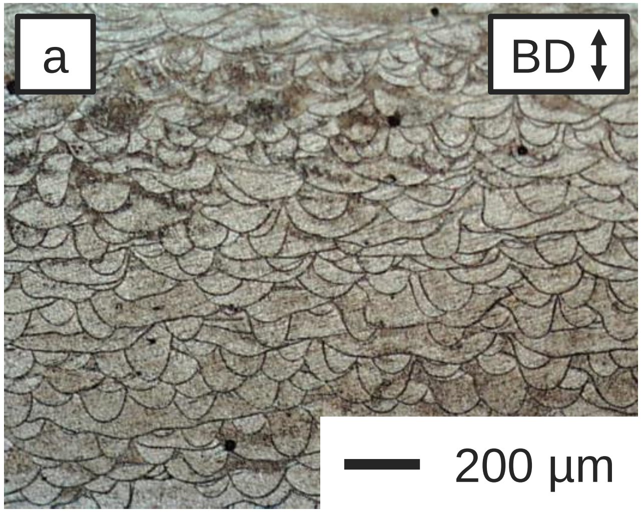

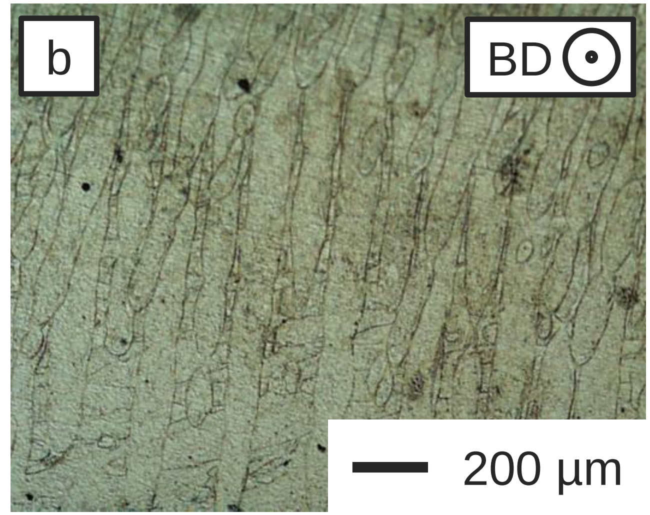

Parralel to building direction:
→ Arch-shaped lines resulting from melt pool

Perpendicular to building direction
→ Elongated structure due to laser movement

Microstructure, as-built – electron backscatter diffraction

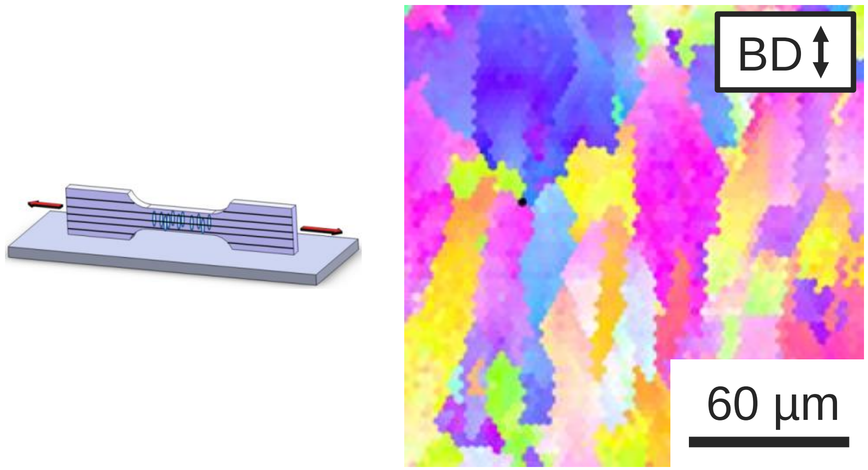

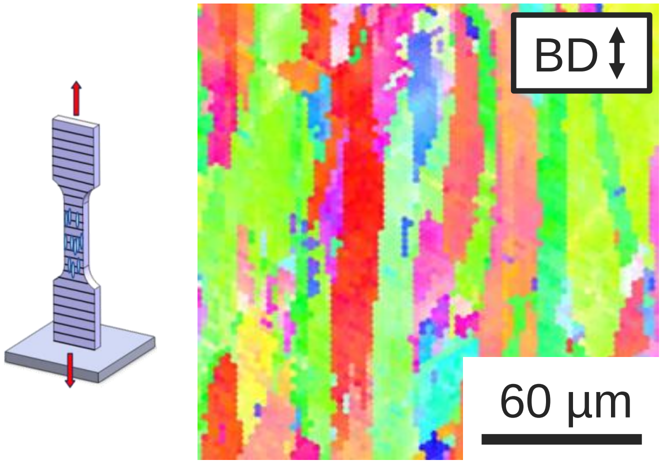

- Columnar grains alongside the building direction
- Grains grow across several layers (>30µm)
- Thicker and shorter grains in case of vertically manufactured sample due to additional heat flux towards grip sections

→ No relation between the features as visible by optical microscopy and the grain orientation and morphology

 P. Kanagarajah et al., Mater. Sci. Eng. A 588, 2013, 188-195.

Microstructure, aged – electron backscatter diffraction

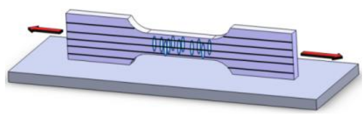

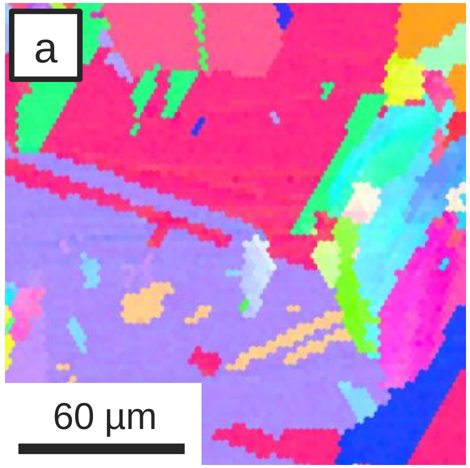

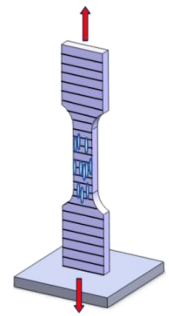

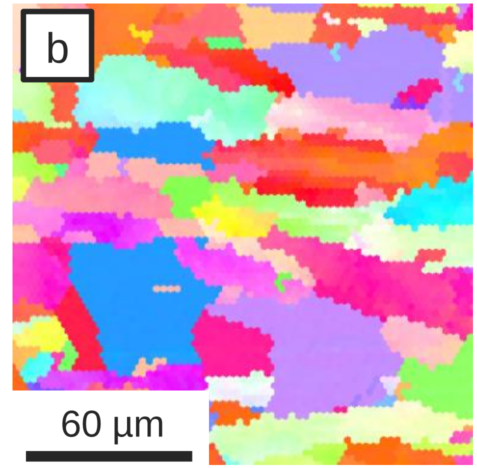

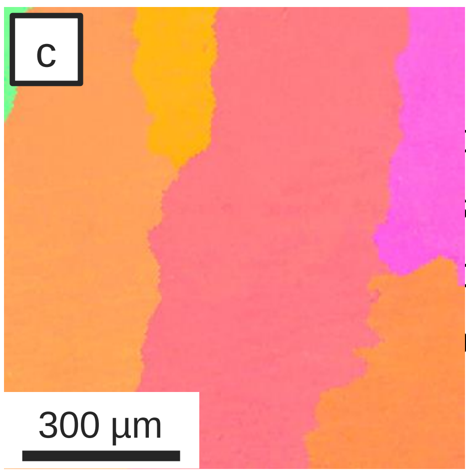

due to high annealing temperatures, high residual stresses)

ening

→ In comparison to cast material still small grain sizes!

ctly columnar morphology

f vertically manufactured sample (average grain diameter 35 µm vs. 70 µm)

Microstructure – X-ray diffraction

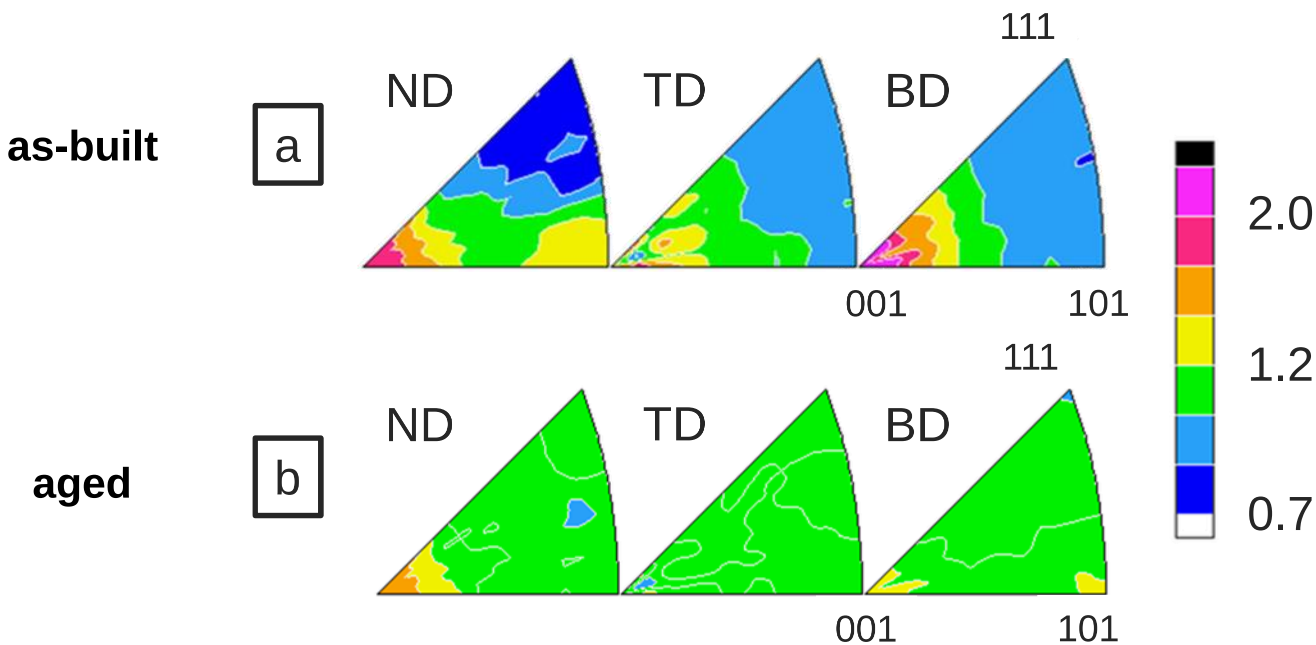

- Preferred orientation of the [001] fibre alongside BD → optimally suited for high temperature creep
  → Grain orientation highly dependent on heat flux during processing
- Much weaker texture after ageing due to recrystallization

As-built microstructure – transmission electron microscopy

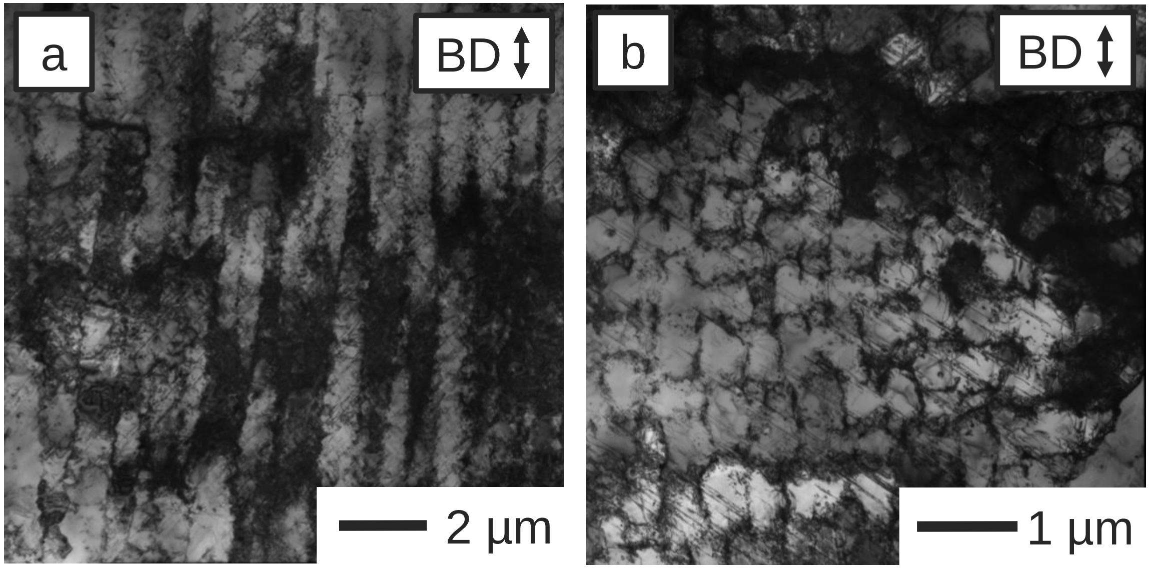

- Elongated structures on very small scale parrallel to the building direction
- Likewise cell-shaped strucutures were found

→ Formation and distribution still is unclear

→ Effect on the mechanical properties…?!

Microstructure, aged – transmission electron microscopy

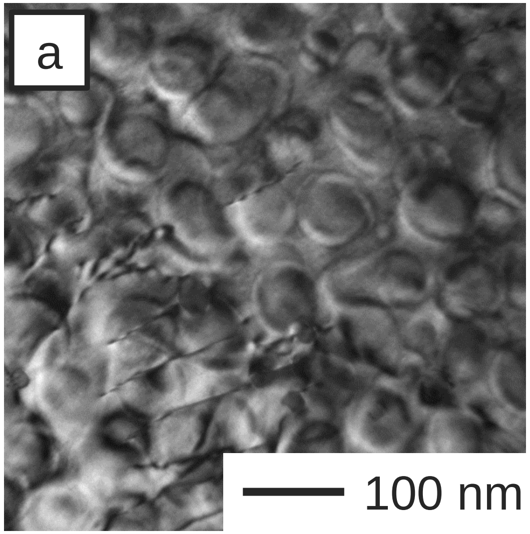

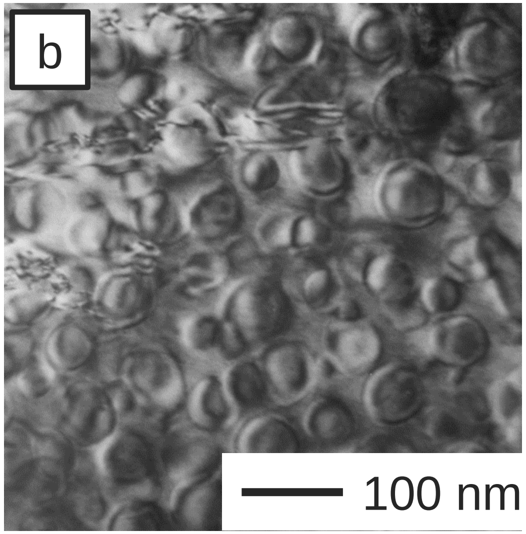

- γ'-precipitates $(Ni\ldots)_3(Al,Ti,\ldots)$ in both after SLM and casting
  - → Hardening effect
  - → Resistance against high temperature creep
- γ'-precipitates are larger in case of SLMed material → reason?

Microstructure – transmission electron microscopy

aged

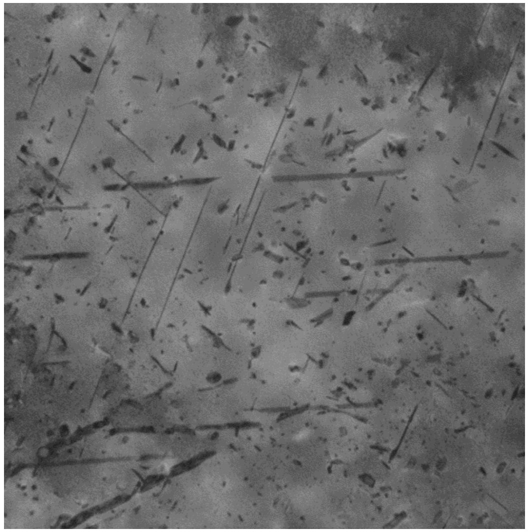

solution annealed

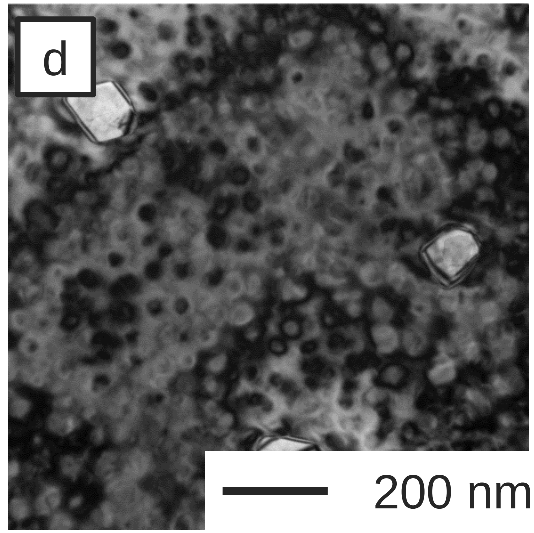

- In addition to γ'-precipitates brittle phases are present already after ageing (normally after long time operation)
- Smaller γ'-precipitates already in the solution annealed condition (normally first during ageing)

→ Formation kinetics much faster than in cast material

→ Nuclei for precipitations are formed during SLM

Influence of building direction

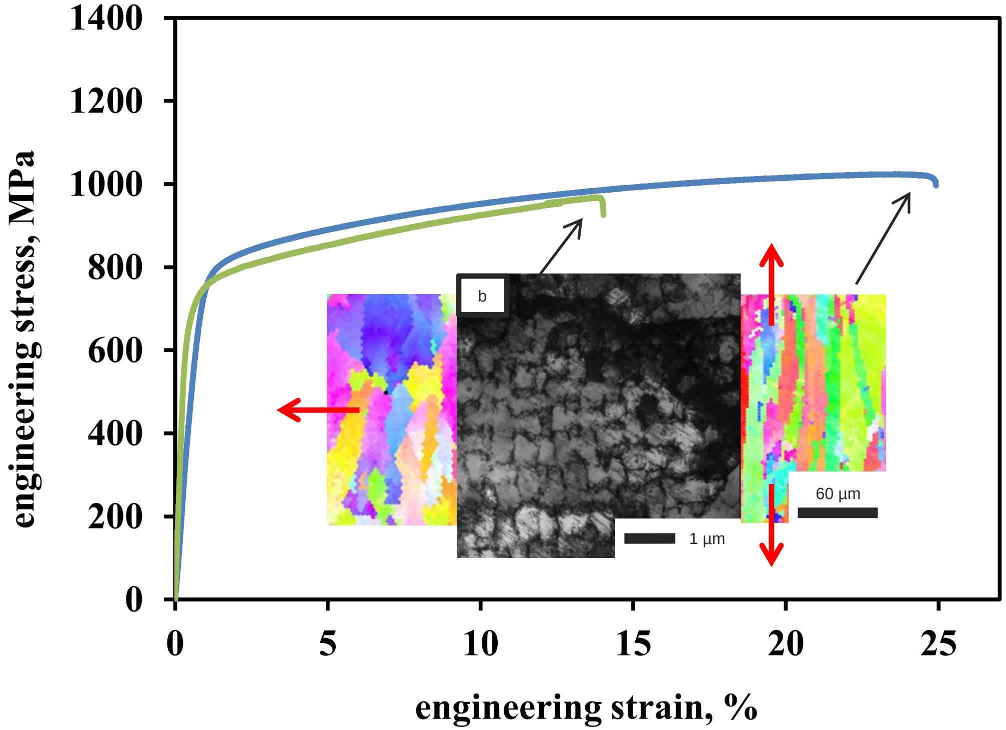

Loading axis alongside building direction:

- Higher ductility
- Yield strength almost equal

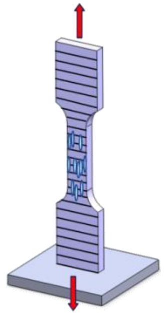

Microstructural reasons:

- Cell-shaped substructures act as barriers for dislocation movement → similar σ_y
- Elongated grains alongside BD → higher ductility

Monotonic mechanical properties – impact of heat treatment

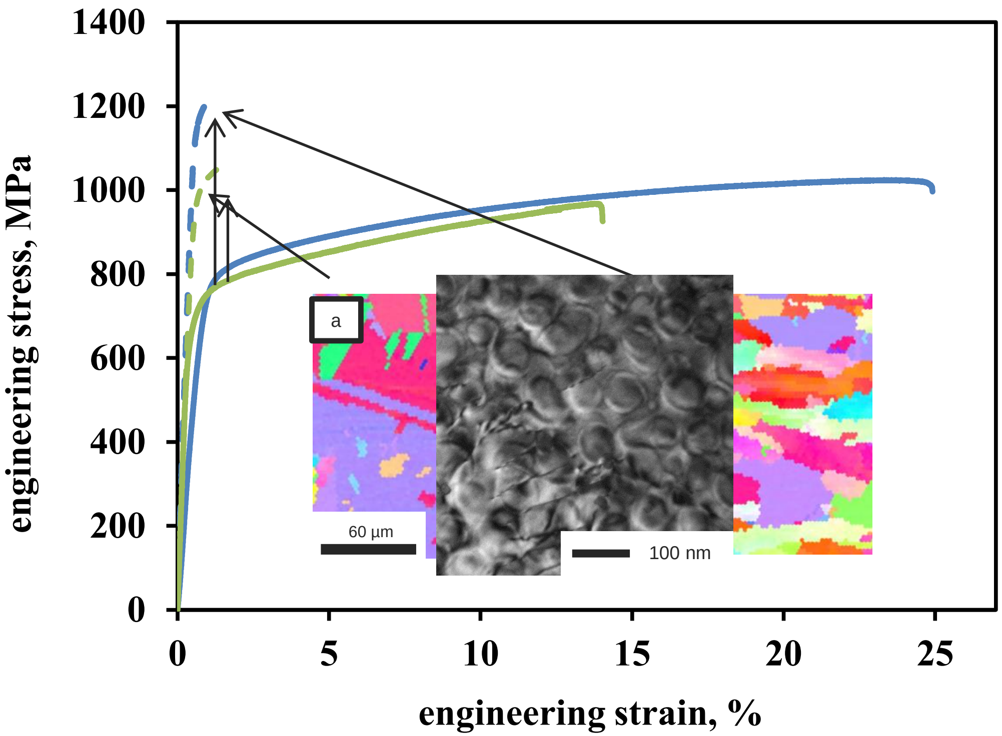

→ Overall increase of yield strength

Microstructural reason:

Formation of precipitates → overall increase of σ_y

Loading axis alongside building direction:

- Higher yield strenght
- Ductility equal

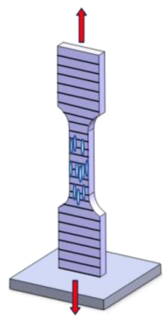

Microstructural reason:

Substructures get dissolved, yield strength dominated by grain size → higher σ_y

Monotonic mechanical properties – influence of temperature

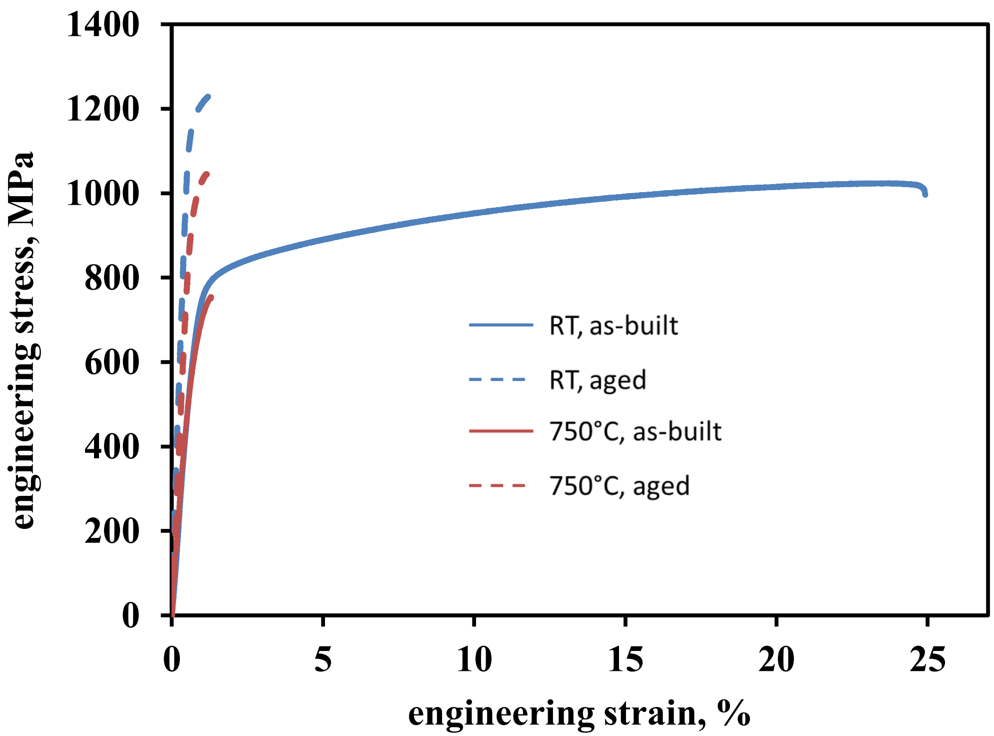

Clearly decreased ductility of as-built condition

→ Fast formation of precipitates + embrittlement

 P. Kanagarajah et al., Mater. Sci. Eng. A 588, 2013, 188-195.

Monotonic mechanical properties – comparison to cast material

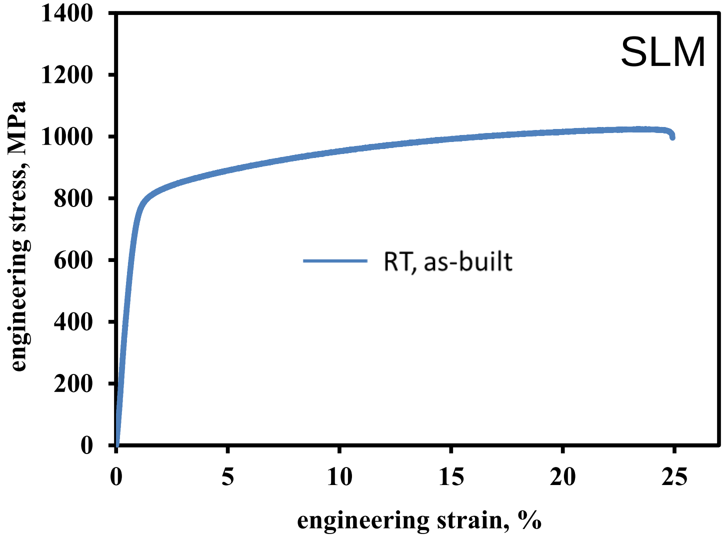

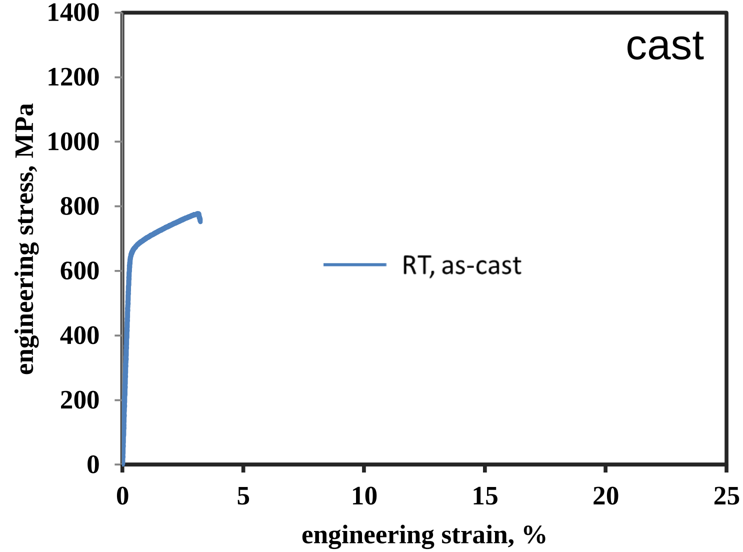

$\sigma_{y,SLM}$= 750 MPa – 950 Mpa

$\sigma_{y,cast}$= 500 MPa – 800 Mpa

as-built / as-cast - RT:

→ Higher yield strength

→ Significantly higher ductility in case of as-built SLM

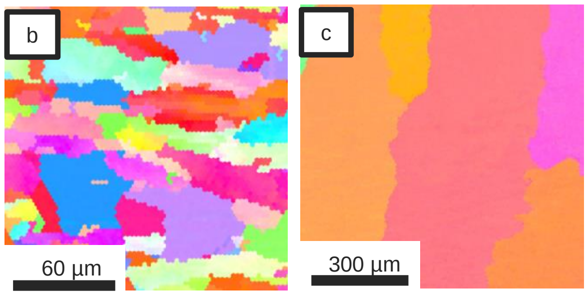

Temperature influence – as-built / as-cast conditions

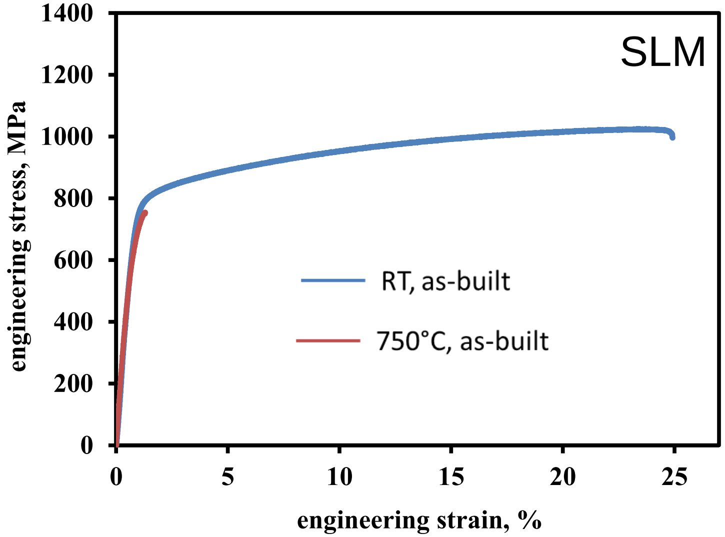

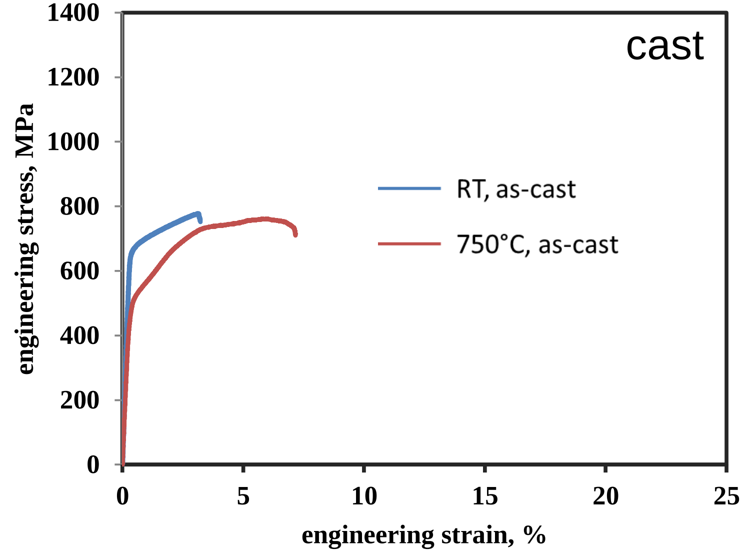

$\sigma_{y,SLM}$= 750 MPa – 950 Mpa

$\sigma_{y,cast}$= 500 MPa – 800 Mpa

SLMed material shows
→ Higher yield strength
→ Lower ductility
due to fast formation of precipitates

solution annealed

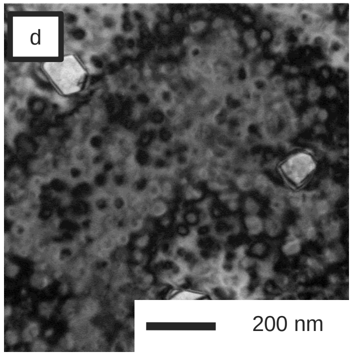

Temperature influence – aged condition

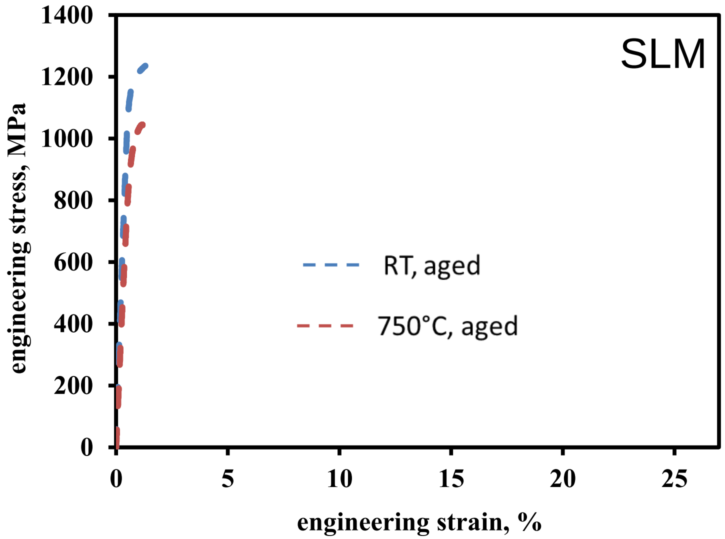

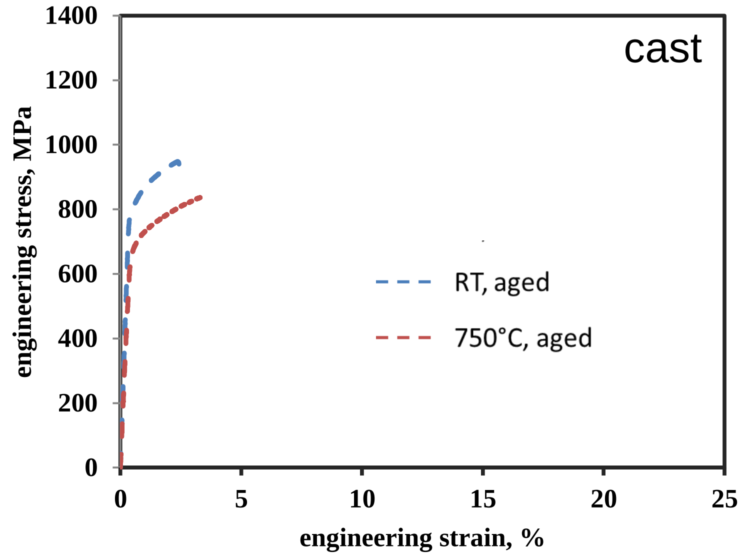

$\sigma_{y,SLM}$= 750 MPa – 950 Mpa

$\sigma_{y,cast}$= 500 MPa – 800 Mpa

aged

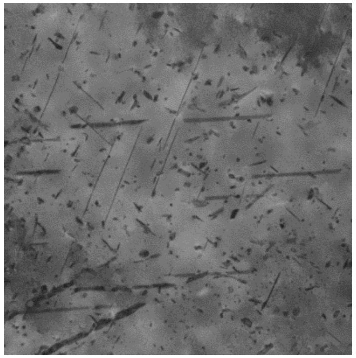

aged – RT / 750°C:

→ Higher yield strength

→ Lower ductility

due to fast formation of brittle phases

Fatigue lifes – as-built / as-cast condition

condition	SLMed, as-built	SLMed, aged	cast, as-cast	cast, aged
N_f, RT	4702	1598	313	2677
N_f, 750 °C	209	73	230	272

→ At RT higher fatigue life for as-built SLMed material (although not polished)

Reason:

Strain amplitude of 0.5 % leads to relatively high stresses

→ Yield strength of cast material is exceeded

→ Loading of SLMed material is mere elastic

At lower strain amplitudes (0.35 %) similar fatigue lifes were reached for both SLM and cast material

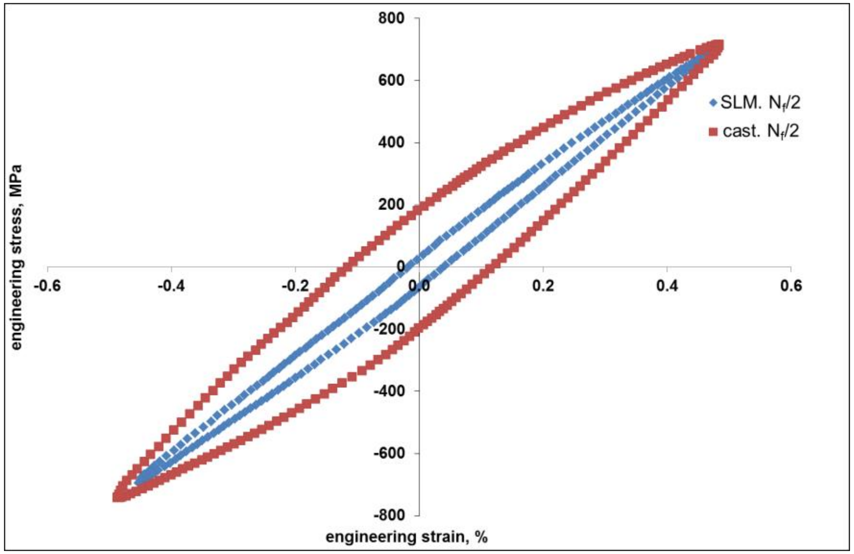

Fatigue lifes – aged conditions

condition	SLMed, as-built	SLMed, aged	cast, as-cast	cast, aged
N_f, RT	4702	1598	313	2677
N_f, 750 °C	209	73	230	272

→ Lower fatigue life for aged SLMed material (even if polished)

Reason:

SLM: Formation of brittle phases and process induced defects (pores)

→ Higher sensitivity to crack initiation and growth

aged

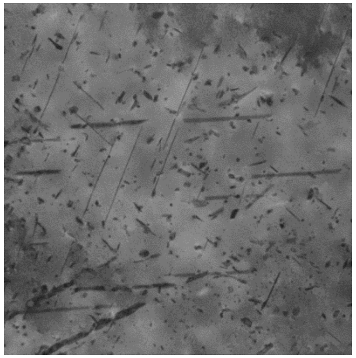

Cast: Increase of yield strength due to precipitates

→ Lower plastic strain amplitude

Fatigue lifes – temperature influence

condition	SLMed, as-built	SLMed, aged	cast, as-cast	cast, aged
N_f, RT	4702	1598	313	2677
N_f, 750 °C	209	73	230	272

→ General reduction of fatigue life in comparison to RT

Reason:

Enhanced dislocation mobility, typically occurring at high temperatures

Restricitions:

Only few tests were conducted → scatter?

Conclusions

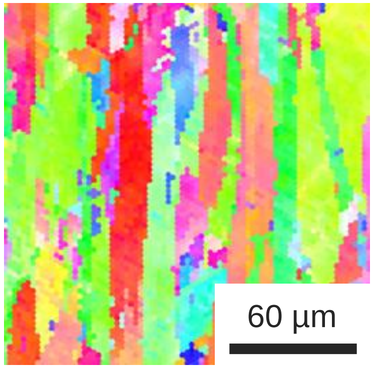

Microstructure:

→ **fine columnar grains**

→ **micro-scaled substructures**

Two-stage heat treatment:

→ **recrystallization**

→ still **grain sizes significantly** lower than in the cast alloy

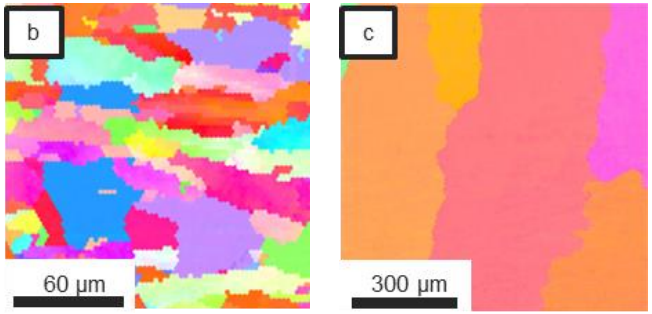

Monotonic load:

→ **High ductility** of the as-built condition

→ **Increase of yield strength and embrittlement by ageing**

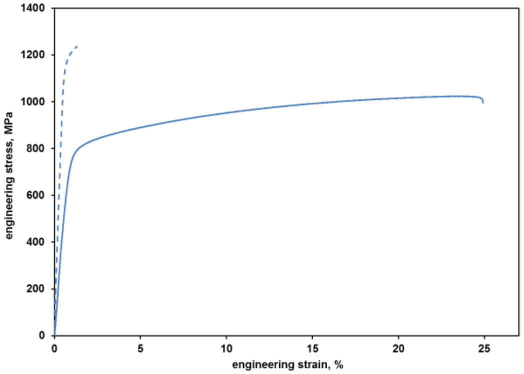

Compared to cast material:
→ **always higher yield strength** in case of SLMed material

Conclusions

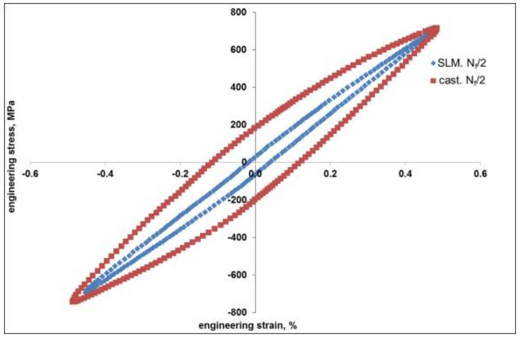

Cyclic loading at RT:

→ **Better performance of the as-built SLM-processed condition**

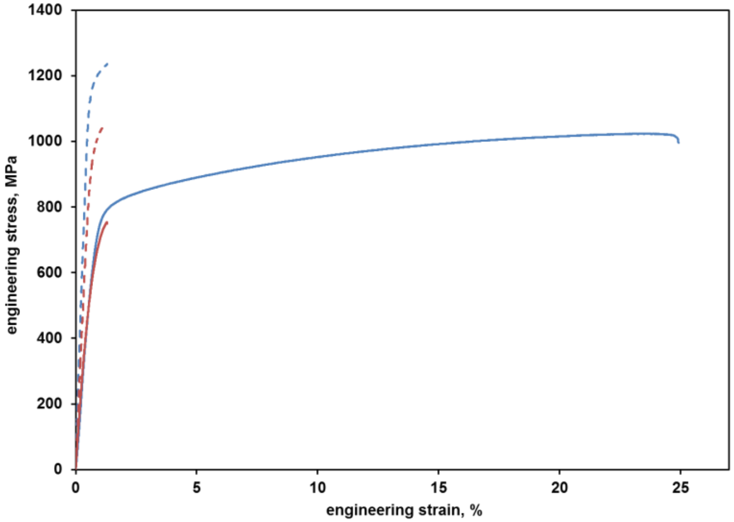

Testing at high temperatures:

→ fast formation of precipitates
→ embrittlement of the SLM-processed as-built condition

→ **Reduction of ductility and fatigue lives**

 P. Kanagarajah et al., Mater. Sci. Eng. A 588, 2013, 188-195.